UNIVERSITÀ DEGLI STUDI DI FIRENZE
Dipartimento di Fisica e Astronomia

Scuola di dottorato in Scienze

Dottorato di ricerca in

FISICA - CICLO XXIV

S.S.D. FIS/02 (fisica teorica)

Quantum information transmission in quantum many-body systems

Leonardo Banchi

Gennaio 2012

Supervisori: Dott.ssa Paola Verrucchi
Prof. Alessandro Cuccoli
Coordinatore: Prof. Alessandro Cuccoli

Anno Accademico 2011/2012

Contents

Overview **1**

1 Theory of composite quantum systems **5**
1.1 Digest on quantum mechanics 5
1.1.1 Qubit: the simplest quantum system 7
1.1.2 Entanglement 8
1.2 Quantum subsystems 10
1.2.1 Measurement: POVM 13
1.2.2 Time evolution: Kraus operators 14
1.3 Quantum channels 16
1.3.1 One qubit maps 19
1.3.2 Symmetries 20

2 Quantum information transmission **23**
2.1 Teleportation 24
2.2 State transmission 28
2.2.1 Fidelity of teleportation 31
2.3 Entanglement as a resource 32
2.4 Explicit formulas for two-qubits channels 34
2.4.1 Minimum fidelity 34
2.4.2 Concurrence 35

3 Quantum communication through spin chains dynamics **39**
3.1 Quantum communication with unmodulated chain 42
3.2 Quasi-free Hamiltonians 45
3.3 Interacting Systems 52
3.3.1 XXZ Hamiltonian 53
3.4 Concluding remarks 56

4 Routes to perfection and near perfection **57**
4.1 Perfect mirroring 58
4.1.1 Generalization to XY models 60
4.1.2 Perfect transmission without mirroring 61
4.2 Wave packet encoding 61
4.3 Qubits weakly coupled to the bus 63
4.4 Coherent ballistic dynamics 64

5 Optimal dynamics with the XX model **67**
5.1 Dynamical evolution . . . 68
5.2 Optimal dynamics . . . 70
5.2.1 Transfer regimes . . . 71
5.2.2 Ballistic regime and optimal values . . . 73
5.3 Information transmission exploiting optimal dynamics . . . 75
5.4 Concluding remarks . . . 80

6 Optimal dynamics with the XY model **83**
6.1 Optimal transfer . . . 85
6.1.1 Ising case . . . 86
6.2 Concluding remarks . . . 87

7 Entangling gates between distant qubits **89**
7.1 Introducing the model . . . 90
7.2 Application . . . 93
7.2.1 Time scale . . . 94
7.2.2 Imperfections . . . 95
7.3 Concluding remarks . . . 96

Prospects **97**

A Some mathematical results **99**
A.1 The Weyl-Schur duality . . . 99
A.1.1 The *twirling* superoperator . . . 99
A.2 Theorems on tridiagonal matrices . . . 100

B Quadratic Hamiltonians for Fermions **103**
B.1 Canonical transformation . . . 103
B.2 Diagonalization . . . 106
B.2.1 Ground state . . . 106
B.2.2 Time evolution . . . 107
B.2.3 Expectation values . . . 108
B.3 Particular cases . . . 109
B.3.1 Conserved number of particles . . . 109
B.3.2 Reflection symmetry (Mirror symmetry) . . . 110

C Some explicit formulas **111**
C.1 Quasi-uniform tridiagonal matrices . . . 111
C.1.1 Mirror symmetric quasi-uniform matrix . . . 113
C.1.2 More elements on the edges . . . 115

C.2 Analytical evaluation of $U_{N+1,0}(t)$ in the uniform XX model 116
C.3 Large-N limit of the amplitude in the ballistic XX model 117
C.4 Evolution of the boundary spins: algorithms 118

Bibliography **123**

Journal publications

Parts of this thesis are based on material published in the following papers:

- **Optimal dynamics for quantum-state and entanglement transfer through homogeneous quantum systems**,
  L. Banchi, T. J. G. Apollaro, A. Cuccoli, R. Vaia, and P Verrucchi,
  Phys. Rev. A, vol. 82, no. 5, p. 052321, 2010.
  (Chapter 5 and 6)

- **Nonperturbative entangling gates between distant qubits using uniform cold atom chains**,
  L. Banchi, A. Bayat, P. Verrucchi, and S. Bose,
  Phys. Rev. Lett., vol. 106, p. 140501, Apr 2011.
  (Chapter 7)

- **Initializing an unmodulated spin chain to operate as a high-quality quantum data bus**,
  A. Bayat, L. Banchi, S. Bose, and P Verrucchi,
  Phys. Rev. A, vol. 83, p. 062328, Jun 2011.
  (Chapter 3)

- **Long quantum channels for high-quality entanglement transfer**,
  L. Banchi, T. Apollaro, A. Cuccoli, R. Vaia, and P Verrucchi,
  New Journal of Physics, vol. 13, no. 12, p. 123006, 2011.
  (Chapter 5)

- **Efficient quantum information transfer through a uniform channel**,
  L. Banchi, T. Apollaro, A. Cuccoli, R. Vaia, and P Verrucchi,
  Nanomaterials and Nanotechnology, vol. 1, no. 1, pp. 24–28, 2011.
  (Chapter 6)

Other papers not covered in this thesis to which the author contributed:

- **When finite-size corrections vanish: the $S = \frac{1}{2}$ XXZ model and the Razumov-Stroganov state**,
  L. Banchi, F. Colomo, P. Verrucchi,
  Phys. Rev. A 80, p. 022341, 2009.

- **Propagation of non-classical correlations across a quantum spin chain**,
  S. Campbell, T. J. G. Apollaro, C. Di Franco, L. Banchi, A. Cuccoli, R. Vaia, F. Plastina, M. Paternostro,
  Phys. Rev. A 84, p. 052316, 2011.

Acknowledgements

I wish to express my gratitude to all the people who contributed to my research work during these years.

First of all, I would like to thank my supervisors, Paola Verrucchi and Alessandro Cuccoli for motivation and support in all the time. Special thanks also to Ruggero Vaia and Tony J. G. Apollaro both for the good times we spent together and for the scientific support. Without their advices and efforts my work would be much more complicated.

It is also a pleasure to thank Sougato Bose and Abolfazl Bayat for having given me the opportunity to do research at the University College of London in an extraordinary scientific atmosphere.

Furthermore, in these years I enjoyed the collaboration with other scientists as Andrea Fubini, Andreas Osterloh, Francesco Plastina, Mauro Paternostro and in particular Filippo Colomo, the supervisor of my graduation thesis.

Overview

This thesis is devoted to the study of many-body one-dimensional quantum systems as quantum wires, a recent intriguing topic which ranges between several branches of modern physics. A *quantum wire* is a communication channel between two quantum objects which preserves the quantum coherence. The interest in quantum communication channels has raised in recent years as novel experimental techniques permit to access and manipulate single quantum objects with extremely good precision and long coherence times, paving the way for the realization of a *quantum computer*, i.e., a device which exploits peculiar features of quantum mechanics for elaborating and processing information. Quantum entanglement is a fundamental resource, but it is responsible both for the power of quantum computers and for the difficulty of building them, being it very fragile. Therefore, it has become of utmost importance to understand what are the theoretical characteristics that a quantum channel must possess for reliably transfer information between distant parts, preserving all the relevant quantum features, notably entanglement.

Although flying quantum systems, e.g. photons in optical fibers, can be used as quantum information carriers, in this thesis we focus on wires composed of localized quantum systems, statically interacting with their (nearest) neighbours: the transmission occurs by the coherent collective dynamics of the components. This scheme is suitable for short-distance quantum communications, as those occurring between quantum processing units in a quantum computer, since the wire can be fabricated with the same localized objects of the processing units themselves. Many-body quantum wires have a generally rich and complex dynamics with lots of different effects, as the spreading of the wave-function between different sites or the scattering between the elementary excitations. We have analysed several models, with a special emphasis on spin-$\frac{1}{2}$ chains, though our arguments can be applied with little effort to other many-body systems, such as chains of (Majorana) fermions or excitonic systems. Moreover, we have devised a *recipe* for inducing a coherent ballistic dynamics in systems described by Hamiltonians mappable to free-models with some suitable transformation, and we have applied it to different cases and models. Thanks to our recipe the information flows coherently through the one-dimensional wire, allowing a fast high-quality transmission of states and entanglement even in the limit of infinite sites, i.e., in principle, over macroscopic distances. Furthermore, the coherent ballistic information flow entails an effective interaction between distant parts, and can thus be used to dynamically generate long-distance entanglement in a fast and scalable way compared to previous proposals.

The structure of the thesis is the following:

Chapter 1 presents the theory of composite quantum systems and a basic introduction to quantum information concepts. Starting from the postulates of quantum mechanics the description of the state of the components is derived, together with their dy-

namics, and the effect of global measurements are discussed. The formal theory of quantum channels, i.e. mapping between quantum states, is then introduced. Special emphasis is given to quantum channels between qubits (*quantum bits*) which will be used in detail in the subsequent chapters.

Chapter 2 reviews the theory of quantum information transmission. Teleportation is introduced, and some figures of merit of the transmission quality of generic quantum channels are analysed. The role of entanglement is then considered. Finally, explicit expressions of the relevant figures of merit are given for quantum channels between qubits.

Chapter 3 introduces the main motivation for using a spin chain as a quantum wire. We consider a vast class of one-dimensional many-body models which contains some of the most relevant experimental realizations of spin chains. In particular, we consider spin-$\frac{1}{2}$ XY and XXZ model with open boundary conditions. The detailed theory for treating the dynamics is explained, both for XY models, which can be analytically approached thanks to the mapping to quadratic fermionic models, and for the other models where the dynamics is obtained numerically. Uniform interactions are considered and the quality of different wires is analysed depending on the parameters of the model and on the initial state of the wire. Our results show a significant difference between quasi-free fermionic systems (XY) and interacting ones (XXZ), where in the former case initialization can be exploited for improving the entanglement transmission, while in the latter case it also determines the quality of state transmission. In fact, we find that in non interacting systems the interference with the initial state of the chain always has a destructive effect, and we prove that it can be completely removed in the isotropic XX model by initializing the chain in a ferromagnetic state. On the other hand, in interacting systems constructive scattering effects can arise with a proper initialization procedure.

Chapter 4 reviews some proposals for increasing the quality of quantum wires that have mostly inspired our research. Some of them are based on the engineering of the couplings, others on the encoding of the initial state into a wave-packet extended over multiple sites, and still others on connecting the distant parts to the wire with weak couplings. It is then shown how this three approaches merge into our scheme for inducing a coherent ballistic dynamics in systems described by quasi-free models.

Chapter 5 deals with the coherent ballistic dynamics in the XX model, where lots of analytical results are made available for supporting and explaining our idea. It is shown that effective quantum-state and entanglement transfer can be obtained by tuning the coupling between the wire endpoints and the two qubits there attached, to an

optimal value. A general procedure to determine such value is devised, and scaling laws between the optimal coupling and the length of the wire are found. We show that a high-quality entanglement transfer occurs even in the limit of arbitrarily long channels, almost independently of the channel initialization, and that the state transmission fidelity exceeds 90% for any chain length.

Chapter 6 extends the results of Chapter 6 to the XY models, where the induction of a coherent ballistic dynamics is more complicated. Indeed, it is shown that another parameter, the local magnetic field on the external qubits, has to be tuned as well. Some analytical results are obtained for the Ising model.

Chapter 7 considers a fast scalable method for achieving a two-qubit entangling gate between arbitrarily distant qubits in a network by exploiting the coherent ballistic dynamics. As explained in Chapter 5, this is achieved dynamically by switching on a strong interaction between the qubits and the wire formed by a non-engineered XX spin chain. The quality of the gate scales very efficiently with qubit separations. Surprisingly, a sudden switching of the coupling is not necessary and our gate mechanism is not altered by a possibly gradual switching. The wire is also naturally reset to its initial state making complex resetting procedures unnecessary after each application of the gate. Moreover, we propose a possible experimental realization in cold atoms trapped in optical lattices and near field Fresnel trapping potentials, which are both accessible to current technology.

1

Theory of composite quantum systems

1.1 Digest on quantum mechanics

In this section we briefly recall the postulates of quantum mechanics following standard quantum information textbook [1, 2]. We concentrate on the mathematical structure of quantum mechanics without specifying a particular physical system.

The first two postulates define the state space and the observables of a physical system.

Postulate 1. *Associated to any isolated physical system is a Hilbert space $\mathscr{H}$, known as the state space of the system. The system is completely described by a a ray*[1] $|\psi\rangle \in \mathscr{H}$ *in the system's state space.*

Postulate 2. *An observable, namely a property of a physical system that in principle can be measured, is a self-adjoint (Hermitian) operator A on the state space $\mathscr{H}$.*

The third postulate defines how a quantum mechanical system changes in time. In abstract terms:

Postulate 3. *The evolution of a closed quantum system is described by a unitary transformation U, that is $|\psi_2\rangle = U|\psi_1\rangle$, where $|\psi_1\rangle$ and $|\psi_2\rangle$ are the states of the system at a time t_1 and t_2 respectively.*

Every unitary operation can be obtained by composing a certain subset of unitary transformations. These transformations in the quantum computation community [1] are called **universal quantum gates**. However, from a physical viewpoint, the quantum dynamics is described by the Hamiltonian operator H via the Schrödinger equation

$$i\hbar \frac{d}{dt} U = H U, \tag{1.1}$$

[1] A ray is an equivalence class of vectors that differ by a multiplication by a nonzero complex scalar: the states $|\psi\rangle$ and $z\,|\psi\rangle$, with $0 \neq z \in \mathbb{C}$, describe the same physical object. A representative of this class (for any non vanishing vector) is chosen to have a unit norm $\langle\psi|\psi\rangle = 1$.

where U is the resulting unitary evolution operator of Postulate 3. For instance, when H is time-independent, $U(t) = e^{-i\frac{Ht}{\hbar}}$. In this thesis the Planck's constant $\hbar$ is always absorbed into the definition of H or, in other words, $\hbar \equiv 1$. The Schrödinger equation is the quantum analogue of Hamilton's equation in classical mechanics. It can not be justified without making extra assumptions, and has been taken as another postulate, together with Postulate 3.

The fourth postulate deals with the description of composite quantum systems, made up of two (or more) physical objects. It will be very important in this thesis, as it leads to the quantum entanglement and other peculiar features of quantum mechanics.

Postulate 4. *The state space of a composite physical system is the tensor product of the state spaces of the component physical systems*[2].

Indeed, the "classical" Cartesian product is not suitable in quantum realms as it does not preserve the Hilbert space structure of constituents[3], as required by Postulate 1.

The first four postulates deal with the description of a *closed* quantum system, i.e., when there are no interactions with the rest of the world. The interfacing between the quantum realm and the classical reality is still debated, and there are different theories and interpretations. One of the most famous and established is the so-called *quantum decoherence* [3]. The measurement process, which produces a single macroscopic result from the many possible quantum states, can be cast in the framework of quantum decoherence, and derived, with extra assumptions, from the other postulates of quantum mechanics. Here, however, we take a more pragmatic approach and we consider the measurement process as a separate postulate, as in any standard Quantum Mechanics textbook.

Postulate 5. *The outcome of the measurement of an observable A is an eigenvalue of A. Right after the measurement the quantum state of the system lies in an eigenstate of A corresponding to the measured eigenvalue.*

Let $A = \sum_n a_n P_n$ the spectral decomposition of A, where each a_n is an eigenvalue of A and P_n is the corresponding orthogonal projection[4] onto the space of eigenvectors with

[2] Notation:

$$|\psi_1\psi_2\rangle \equiv |\psi_1\rangle \otimes |\psi_2\rangle \,.$$

[3] Indeed, the tensor product naturally arises when we require the following equivalence relations

$$|v_1 + v_2, w\rangle \sim |v_1, w\rangle + |v_2, w\rangle, \qquad |v, w_1 + w_2\rangle \sim |v, w_1\rangle + |v, w_2\rangle, \qquad \alpha|v, w\rangle \sim |\alpha v, w\rangle \sim |v, \alpha w\rangle \,.$$

[4] If a_n are non-degenerate then $P_n = |a_n\rangle\langle a_n|$. In general the P_n's are Hermitian operators satisfying

$$P_n P_m = \delta_{nm} P_m, \quad \sum_m P_m = \mathbb{1} \,.$$

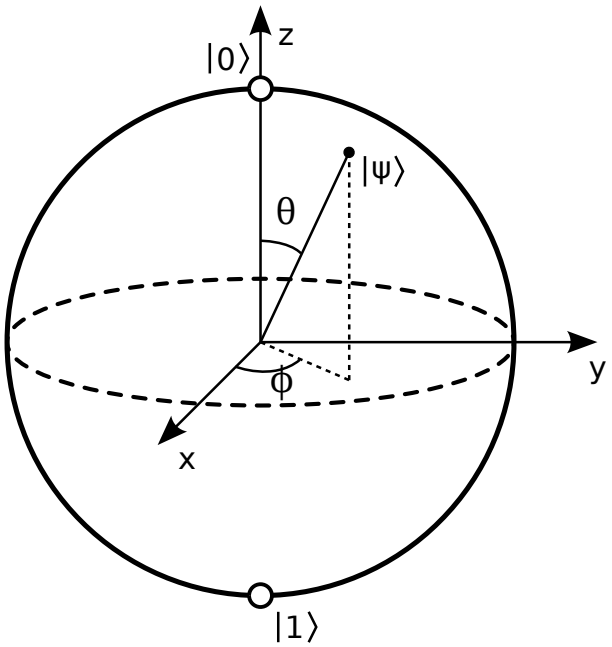

Figure 1.1 – Bloch sphere.

eigenvalue a_n. If $|\psi\rangle$ is the state of the system before the measurement, then the outcome a_n is obtained with probability

$$p(a_n) = ||P_n|\psi\rangle||^2 = \langle\psi|P_n|\psi\rangle \,, \tag{1.2}$$

and after the measurement the quantum state becomes

$$\frac{P_n|\psi\rangle}{\sqrt{\langle\psi|P_n|\psi\rangle}} \,. \tag{1.3}$$

1.1.1 Qubit: the simplest quantum system

The indivisible unit of classical information is the bit, an object taking only two possible values: by convention 0 and 1. Similarly, the quantum system with only two orthonormal states is called *quantum bit* or *qubit*, and is the unit of quantum information [1]. This orthonormal states are usually called $|0\rangle$ and $|1\rangle$; they span the smallest nontrivial Hilbert space, i.e. the two-dimensional space of states

$$a|0\rangle + b|1\rangle \,,$$

where a and b are complex numbers satisfying $|a|^2 + |b|^2 = 1$ and the overall phase is physically irrelevant.

Being a bidimensional quantum system, it is natural to interpret the qubit as the spin of a spin-$\frac{1}{2}$ particle. In this picture the states $|0\rangle$ and $|1\rangle$ are nothing but the spin-up state ($|\uparrow\rangle$) and the spin-down state ($|\downarrow\rangle$) along a particular axis, that in this thesis is set by convention to

the z-axis. The two complex numbers a and b define the orientation of the spin in the three dimensional space. Indeed, recalling the quantum theory of angular momentum [4], a finite rotation $R(\vec{n},\alpha)$ of an angle α around the axis specified by $\vec{n}=(\sin\theta\cos\phi,\sin\theta\sin\phi,\cos\theta)$, is given by the following unitary operator

$$U(\vec{n},\alpha)\equiv U(R(\vec{n},\alpha))=e^{-i\frac{\alpha}{2}\vec{n}\cdot\vec{\sigma}}=\mathbb{1}\cos\frac{\alpha}{2}-i\,\vec{n}\cdot\vec{\sigma}\,\sin\frac{\alpha}{2}\,, \tag{1.4}$$

where $\mathbb{1}$ is the identity matrix and

$$\sigma^x=\begin{pmatrix}0&1\\1&0\end{pmatrix},\qquad \sigma^y=\begin{pmatrix}0&-i\\i&0\end{pmatrix},\qquad \sigma^z=\begin{pmatrix}1&0\\0&-1\end{pmatrix}, \tag{1.5}$$

are the Pauli matrices satisfying the algebra

$$\sigma^\mu\sigma^\nu=\delta^{\mu\nu}+i\,\varepsilon^{\mu\nu\gamma}\sigma^\gamma, \tag{1.6}$$

where $\varepsilon^{\mu\nu\gamma}$ is the totally antisymmetric tensor (Levi-Civita symbol) and summation over repeated indices is adopted. As the spin operators transform under SU(2) rotations as a vector

$$U\sigma^\mu U^\dagger=R^{\mu\nu}\sigma^\nu, \tag{1.7}$$

where R is the corresponding SO(3) rotation of the spin operator[5], the rotated state $U|0\rangle$ is an eigenstate of the rotated spin operator $\sum_\mu R^{z\mu}\sigma^\mu$. Therefore, the eigenstate $|\theta,\phi\rangle$ of the spin along the $\vec{n}=(\sin\theta\cos\phi,\sin\theta\sin\phi,\cos\theta)$ axis, shown in Fig. 1.1, is constructed by rotating the spin-up state $|0\rangle$ of an angle θ around the axis $\vec{n}'=\big(\cos(\phi+\pi/2),\sin(\phi+\pi/2),0\big)$, that is $|\theta,\phi\rangle=U(\vec{n}',\theta)|0\rangle$. By direct calculation,

$$|\theta,\phi\rangle=\cos\frac{\theta}{2}|0\rangle+e^{i\phi}\,\sin\frac{\theta}{2}|1\rangle. \tag{1.8}$$

1.1.2 Entanglement

Quantum entanglement is a property of composite quantum systems with no analogues in the classical theory. Indeed, in the classical case the state space (phase space) of a systems composed of n parts is given by the Cartesian product of the n subsystem spaces. Hence, no matter how the systems interact in their physical evolution, the total state is always a product state of n separate systems. In contrast, according to postulate 4 of Quantum Mechanics, the composite state space $\mathscr{H}^{\rm tot}$ is the tensor product of the subsystems' space. A general state in $\mathscr{H}^{\rm tot}$ can be written as a *superposition* of product states

$$|\psi\rangle=\sum_{\alpha_1,\cdots,\alpha_n}c_{\alpha_1,\cdots,\alpha_n}|\alpha_1,\cdots,\alpha_n\rangle\,, \tag{1.9}$$

[5]As it is well known, the spinor representation $U(\vec{n},\alpha)$ of the rotation group is double valued and the two SU(2) matrices U and $-U$ give the same R matrix. But since we are considering a single qubit the sign is irrelevant: only the global phase changes.

where we assumed for simplicity finite dimensional Hilbert spaces with basis $\{|\alpha_j\rangle\}$. In general the state (1.9) can not be written in a *separable* form

$$|\psi\rangle \neq |\psi_1\rangle \cdots |\psi_n\rangle \,, \tag{1.10}$$

with $|\psi_j\rangle \in \mathscr{H}_j$, being $\mathscr{H}_j$ the Hilbert space of subsystem j. The states for which Eq. (1.10) holds are called *entangled* and they span most of the Hilbert space, as the volume fraction of the set of separable states quickly decreases for increasing n [5]. Indeed, the dimension of the total Hilbert space $\dim \mathscr{H}_1 \otimes \cdots \otimes \mathscr{H}_n = \dim \mathscr{H}_1 \times \cdots \times \dim \mathscr{H}_n$ is greater than the sum of the dimensions of the subsystems' Hilbert spaces: the state space grows exponentially with increasing n, unlike the classical (separable) case where the total space grows "only" linearly with n.

Let's consider two systems A and B with Hilbert spaces $\mathscr{H}_A$ and $\mathscr{H}_B$ respectively. The following very important result [6, 7] holds

Schmidt's theorem. *Every state $|\psi\rangle \in \mathscr{H}_A \otimes \mathscr{H}_B$ can be expressed in the form*

$$|\psi\rangle = \sum_{i=1}^{r} \sqrt{\lambda_i} |a_i\rangle \otimes |b_i\rangle \,, \tag{1.11}$$

where $\{|a_i\rangle\}_{i=1}^{d_A}$ is an orthonormal basis for $\mathscr{H}_A$ with $d_A = \dim \mathscr{H}_A$, $\{|b_i\rangle\}_{i=1}^{d_B}$ is an orthonormal basis for $\mathscr{H}_B$ with $d_B = \dim \mathscr{H}_B$; $r \leq \min\{d_A, d_B\}$ is called the **Schmidt rank** *and the λ_i's are called* **Schmidt coefficients**.

The nontrivial result is that there is only one sum in (1.11). In fact, as in Eq. (1.9), every state in $\mathscr{H}_A \otimes \mathscr{H}_B$ can be written as

$$|\psi\rangle = \sum_{i=1}^{d_A} \sum_{j=1}^{d_B} C_{ij} |\tilde{a}_i\rangle \otimes |\tilde{b}_j\rangle \,, \tag{1.12}$$

where C is a complex valued matrix and the bases are arbitrary. The Schmidt theorem is only a changes of basis: performing the singular value decomposition of matrix C

$$C = UDV^\dagger \,,$$

where U is a unitary $d_A \times d_A$ matrix, V is a unitary $d_B \times d_B$ matrix and D is a diagonal $d_A \times d_B$ matrix with non-negative real diagonal entries which, without loss of generality, can be sorted in decreasing order. Setting $|a_i\rangle = \sum_j U_{ji} |\tilde{a}_j\rangle$, $|b_i\rangle = \sum_j V^*_{ji} |\tilde{b}_j\rangle$, and calling $\sqrt{\lambda_i}$ the non-zero diagonal values of D, the Schmidt's theorem follows.

The Schmidt coefficients are uniquely determined by C and obey

$$\sum_i \lambda_i = 1.$$

When the Schmidt rank is equal to one then $\lambda_1 = 1$ and $\lambda_i = 0$, for $i > 1$, and the state is separable. Otherwise when $r = \min\{d_A, d_B\}$ and each $\lambda_i = \frac{1}{r}$ the state is called maximally entangled[6]. The most famous maximally entangled states are the *Bell states*

$$|\Phi^{\pm}\rangle = \frac{|00\rangle \pm |11\rangle}{\sqrt{2}}, \qquad |\Psi^{\pm}\rangle = \frac{|01\rangle \pm |10\rangle}{\sqrt{2}}. \tag{1.13}$$

They are two-qubit ($d_A = d_B = 2$) orthogonal states and are related by local unitary operations

$$(\sigma^z \otimes \mathbb{1})|\Phi^{\pm}\rangle = |\Phi^{\mp}\rangle, \qquad (\sigma^z \otimes \mathbb{1})|\Psi^{\pm}\rangle = |\Psi^{\mp}\rangle, \qquad (\sigma^x \otimes \mathbb{1})|\Phi^{\pm}\rangle = \pm|\Psi^{\pm}\rangle. \tag{1.14}$$

The Bell states are one of the fundamental building blocks of quantum computation [1]: many quantum algorithms, like dense coding or teleportation (explained in the next chapter), start with "*Let two distant parts, Alice and Bob, initially share a Bell state*".

1.2 Quantum subsystems

The Dirac's *ket* formalism is unable to describe in general the state of quantum components when the composite system is in an entangled state, for instance no ket can represent the state of the first qubit in the Bell state (1.13). The reason is the lack of a *certain* knowledge of such a state, for which we need to draw on statistics. Let $|\psi\rangle$ be a ray in the physical Hilbert space, then the **density matrix** associated to that state is

$$\rho_\psi = |\psi\rangle\langle\psi|.$$

Furthermore, the density matrix provides a means for representing quantum systems whose state is not completely known, e.g. when the system could stay in one of the states $|\psi_i\rangle$ with some probability p_i. This happens for instance after the measurement of an observable when the outcome is unknown. In the latter case, the $|\psi_i\rangle$'s are the eigenvectors of the observable and $p_i = |\langle\psi_i|\psi\rangle|^2$, being $|\psi\rangle$ the state before the measurement. The density matrix of the *ensemble* $\{p_i, |\psi_i\rangle\}$ is given by

$$\rho_{\{p_i,|\psi_i\rangle\}} = \sum_i p_i |\psi_i\rangle\langle\psi_i|.$$

[6]The term maximally entangled should depend on the particular measure chosen to quantify entanglement, a subject of still active research [8]. Nevertheless, every entanglement measure should be an *entanglement monotone* (see Section 2.4.2), i.e., it should be non-increasing, on average, under local operations and classical communications (LOCC). However, Nielsen's majorization theorem [9] states that $|\psi\rangle$ can be transformed by LOCC to $|\psi'\rangle$ if and only if the respective Schmidt coefficients λ_i and λ'_i, assumed to be in decreasing order, satisfy

$$\sum_{i=1}^{k} \lambda_i \leq \sum_{i=1}^{k} \lambda'_i \quad \text{for} \quad k = 1, \cdots, n,$$

where n is the dimension of the Hilbert space. The smallest element is obtained for $\lambda_i = 1/n$ and thus no other state can have greater entanglement.

Formally, a density matrix is an operator satisfying the following properties:

- Hermiticity: $\rho = \rho^\dagger$.
- Positivity: $\langle\psi|\rho|\psi\rangle = \sum_i p_i |\langle\psi_i|\psi\rangle|^2 \geq 0$.
- $\mathrm{Tr}\,\rho = \sum_i p_i = 1$.

In the following, the space of density operators on $\mathscr{H}$, i.e., the space of operators satisfying the above conditions, will be denoted with $\mathscr{B}_\mathscr{H}$.

The postulates of quantum mechanics can be rewritten and extended in the density matrix formalism, and in particular:

- The average value of the measurement of an observable A is given by
$$\langle A\rangle = \mathrm{Tr}\,A\rho = \sum_i p_i \langle\psi_i|A|\psi_i\rangle\ .$$
- The density matrix evolves as
$$\rho \xrightarrow{U} U\rho U^\dagger\ .$$
- Measurements are also easily extended to the density operator language. Suppose the measurement is defined by the projection operators P_m. Then, if the initial state was $|\psi_i\rangle$, the probability of getting the result m is $p(m|i) = \langle\psi_i|P_m|\psi_i\rangle$, and after the measurement $|\psi_i\rangle\langle\psi_i| \to \sum_m P_m|\psi_i\rangle\langle\psi_i|P_m$. Accordingly,
$$\rho \xrightarrow{\{P_m\}} \sum_m P_m\rho P_m, \tag{1.15}$$
while the probability of getting the outcome m is
$$p(m) = \sum_i p(m|i)p_i = \mathrm{Tr}\,P_m\rho.$$

When a state can be represented by a ray, such a state is called *pure*. Otherwise it is *mixed*.

Let's consider a bipartite quantum system, composed of subsystems A and B, which is in a generic state (1.12) and suppose that an observer have access only to the system A. A generic observable O_A acting on system A only can be decomposed as $O_A \otimes \mathbb{1}_B = \sum_{a,a',b} \langle a|O_A|a'\rangle|ab\rangle\langle a'b|$ where the rays $|a\rangle$,$|a'\rangle$ span the Hilbert space of system A and the rays $|b\rangle$ span the Hilbert space of system B. The expectation value on the state $|\psi\rangle$ is thus

$$\begin{aligned}\langle O\rangle_A = \langle\psi|O_A\otimes\mathbb{1}_B|\psi\rangle = \sum_{a,a',b} \langle a|O_A|a'\rangle\langle\psi|ab\rangle\langle a'b|\psi\rangle = \\ \sum_{a,a',b} \langle a|O_A|a'\rangle\langle a'b|\psi\rangle\langle\psi|ab\rangle = \mathrm{Tr}\,\rho_A O_A\ ,\end{aligned} \tag{1.16}$$

where

$$\rho_A = \sum_b (\mathbb{1} \otimes \langle b|)|\psi\rangle\langle\psi|(\mathbb{1} \otimes |b\rangle) \equiv \operatorname*{Tr}_B |\psi\rangle\langle\psi| \,, \tag{1.17}$$

is the reduced density matrix of subsystem A obtained with a *partial trace* Tr_B on subsystem B of the global density matrix $|\psi\rangle\langle\psi|$. Because $\langle O\rangle_A$ has the form of Eq. (1.16) for any observable O_A acting on the system A, the density matrix ρ_A fully describes the state of system A on its own. Taking into account Eq. (1.12), it holds $\rho_A = C\,C^\dagger = U\,D^2 U^\dagger$, i.e., in some suitable basis $|a_i\rangle$

$$\rho_A = \sum_i \lambda_i |a_i\rangle\langle a_i|.$$

Therefore, the Schmidt coefficient λ_i represents the probability of system A of being in the state $|a_i\rangle$, and the same can be obviously rephrased for system B. For separable states the Schmidt rank is one and the components are in a pure state. On the other hand, when $r > 1$ A and B are entangled and their state is mixed, represented respectively by the reduced density matrices ρ_A, ρ_B. In particular, when A and B are maximally entangled the reduced density matrix is the maximally mixed state.

With the Schmidt decomposition in hand, also the inverse operation of state reduction follows: given any density matrix ρ on a Hilbert space $\mathscr{H}$ we can use (1.11) to write down a pure state on a larger Hilbert space $\mathscr{H} \otimes \mathscr{H}'$ whose reduction down to $\mathscr{H}$ is ρ. Consider a density matrix $\rho = \sum_{i=1}^r p_i |\psi_i\rangle\langle\psi_i|$ in orhonormal form in the space $\mathscr{H}$. A **purification** of ρ is

$$|\Psi\rangle = \sum_{i=1}^r \sqrt{p_i}|\psi_i\rangle|\phi_i\rangle \,,$$

where $|\phi_i\rangle \in \mathscr{H}'$ are orthogonal rays. The auxiliary Hilbert space must have at least dimension r, but there is a lot of freedom in the choice of purification; for instance $|\Psi\rangle$ and $\mathbb{1} \otimes V|\Psi\rangle$ give the same density matrix ρ, provided V be unitary.

Entanglement between a quantum system and a thermal environment is nowadays an important theoretical tool for studying and rephrasing classical statistical mechanics and thermodynamical concepts [10, 11]. For instance, quantum statistical mechanics is usually teached by considering system-environment interactions: imposing some constraints on physical observables, e.g. energy, the (canonical) density matrices arise provided the extended system to be in a completely mixed state (equal *a priori* probability postulate). However, in [12] it has been shown that the canonical density matrices *typically* result also when the extended system is in pure states. This is clearly a consequence of purification, and the key element is the quantum entanglement between the system and its environment [12] .

1.2.1 Measurement: POVM

In the quantum mechanical description of closed systems measurements are described by a set $\{P_m\}$ of orthogonal projection operators in the Hilbert space. We now briefly generalize the measurement concept by supposing the considered quantum system to be part of an extended quantum system, with bigger Hilbert space $\mathscr{H}^{\text{ext}} = \mathscr{H} \oplus \mathscr{H}^{\perp}$. A generic ray $|\psi\rangle \in H^{\text{ext}}$ is decomposed in two orthogonal parts $|\psi\rangle = |\tilde{\psi}\rangle + |\tilde{\psi}^{\perp}\rangle$ where $|\tilde{\psi}\rangle$ and $|\tilde{\psi}^{\perp}\rangle$ are (unnormalized) vectors in $\mathscr{H}$ and $\mathscr{H}^{\perp}$ respectively. When orthogonal measurements are performed in $\mathscr{H}^{\text{ext}}$ with the projection operators $\{P_m\}$, the observer can know only the component of $|\psi\rangle$ in his Hilbert space. Indeed let's define $P_m = |m\rangle\langle m|$, where $|m\rangle = |\tilde{m}\rangle + |\tilde{m}^{\perp}\rangle$. After the measurement the new state is $|m\rangle$, but the observer knows nothing about $\mathscr{H}^{\perp}$ and for him there is no physical distinction between $|m\rangle$ and $|\tilde{m}\rangle$ (aside from normalization), so the final state of the observer will be $|\tilde{m}\rangle/\sqrt{\langle\tilde{m}|\tilde{m}\rangle}$. The set of operators $\{E_m\}$,

$$E_m = \Pi P_m \Pi = |\tilde{m}\rangle\langle\tilde{m}|\,, \tag{1.18}$$

where Π is the orthogonal projector on $\mathscr{H}$, defines a **POVM, positive operator value measure**, and in abstract terms is composed by a set of non-negative Hermitian operators that sum to unity in $\mathscr{H}$:

$$\sum_m E_m = \Pi \left(\sum_m P_m \right) \Pi = \Pi = \mathbb{1}_{\mathscr{H}}.$$

They are not projectors, unless $\langle\tilde{m}|\tilde{m}\rangle = 1$.

POVMs naturally arise not only with extended measurements on the direct product of two Hilbert spaces. They arise also in the more common setup of composite quantum systems by performing joint projective measurements on the global Hilbert space, i.e., the tensor product of the Hilbert spaces of the components. Indeed, let A and B be two systems with Hilbert spaces $\mathscr{H}_A$ and $\mathscr{H}_B$ initially in the uncorrelated state $\rho = \rho_A \otimes \rho_B$. By performing projective measurements $\{P_m\}$ on the tensor product $\mathscr{H}_A \otimes \mathscr{H}_B$, the final density matrix is $\rho'_{AB} = \sum_m P_m \rho_A \otimes \rho_B P_m$ where the probability of getting the results m is $p(m) = \text{Tr}_{AB}\left[P_m \rho_A \otimes \rho_B\right]$. Therefore, for an observer accessing only system A, the probability of getting the result m can be written as

$$p(m) = \text{Tr}\left[E_m \rho_A\right], \qquad E_m = \operatorname*{Tr}_B\left[P_m(\mathbb{1}_{\mathscr{H}_A} \otimes \rho_B)\right],$$

where the operators $\{E_m\}$ defines a POVM as

$$\sum_m E_m = \sum_m \operatorname*{Tr}_B\left[P_m(\mathbb{1}_{\mathscr{H}_A} \otimes \rho_B)\right] = \operatorname*{Tr}_B \mathbb{1}_{\mathscr{H}_A} \otimes \rho_B = \mathbb{1}_{\mathscr{H}_A}.$$

The opposite point of view is tackled by the following theorem that we state without proof [13]:

Naimark's theorem. *Any POVM* $\{E_m\}$ *in the Hilbert space* $\mathscr{H}$ *can be dilated to an orthogonal resolution of the identity* $\{P_m\}$ *on a larger Hilbert space in such a way that* $E_m = \Pi P_m \Pi$*, where* Π *projects down to* $\mathscr{H}$*.*

1.2.2 Time evolution: Kraus operators

We have seen that the measurement postulate 5 has to be extended when we consider open quantum systems, and in general the measurement is no longer described by a set of projection operators. As it can be expected, postulate 3 has to be generalized as well. Consider an extended system $\mathscr{H} = \mathscr{H}_A \otimes \mathscr{H}_B$, each subspace corresponding to a certain quantum system, and, as in the previous section, assume a closed (unitary) evolution on $\mathscr{H}$. We want to look for the resulting description of the evolution on $\mathscr{H}_A$ or $\mathscr{H}_B$ only. Let's concentrate on A, while B can be either a different known quantum system or an unknown one, such as an *environment* or a *bath*. After a global unitary operation U, e.g. a time evolution $U = U(t)$, the state of subsystem A is clearly

$$\rho'_{_A} = \operatorname*{Tr}_B U \rho\, U^\dagger, \tag{1.19}$$

where ρ is the initial state of the overall system. In general Eq. (1.19) requires the full knowledge of both the state and the evolution of the extended system, but if initially A and B are uncorrelated

$$\rho = \rho_{_A} \otimes \rho_{_B}\,, \tag{1.20}$$

then we can safely trace out B and obtain a complete description of the evolution of A without needing to know the full evolution of the extended system, i.e., the evolution can be described in terms of operators acting on A only. Indeed, let $\rho_{_B} = \sum_b \lambda_b |b\rangle\langle b|$ then

$$\rho'_{_A} = \sum_{b,b'} \lambda_b \langle b'|U|b\rangle \rho_{_A} \langle b|U^\dagger|b'\rangle = \sum_\mu A_\mu \rho_{_A} A_\mu^\dagger\,, \tag{1.21}$$

where μ in this case is a multi-index $\mu = (b', b)$ and the operators $A_\mu \equiv A_{(b',b)} = \sqrt{\lambda_b}\,\langle b'|U|b\rangle$ acting on $\mathscr{H}_A$ are the *Kraus operators* [14]. They satisfy

$$\sum_\mu A_\mu^\dagger A_\mu = \sum_{b,b'} \lambda_b \langle b|U^\dagger|b'\rangle\langle b'|U|b\rangle = \sum_b \lambda_b \langle b|U^\dagger U|b\rangle = \sum_b \lambda_b \mathbb{1}_{\mathscr{H}_A} = \mathbb{1}_{\mathscr{H}_A}\,, \tag{1.22}$$

as U is unitary, and λ_b are the eigenvalues of a density matrix. The form (1.21) is called **operator sum representation**, or *Kraus* or sometimes *Stinespring* decomposition, and is the most general mapping from density operators to density operators [14, 15], as shown in the next section.

The Kraus operators A_μ give an intrinsic description of the dynamics of subsystem A alone. However, the decomposition (1.21) is not unique. Indeed, if we supplement the evolution U with another unitary evolution $\tilde{U}$ on subsystem B alone, clearly $\rho'_{_A}$ does not change,

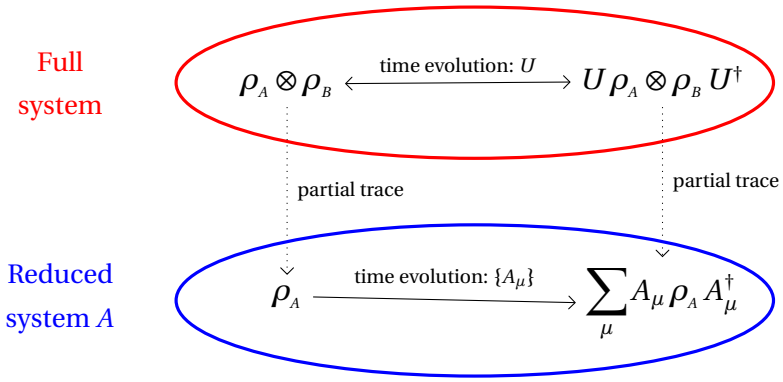

Figure 1.2 – Schematic picture of the time evolution of the full quantum system composed of A and B and the corresponding time evolution of the reduced system A.

but the Kraus operators do

$$A'_{(b',b)} = \sqrt{\lambda_b}\,\langle b'|\left(\mathbb{1}_{\mathscr{H}_A}\otimes\tilde{U}\right)U|b\rangle = \sum_{b''}\langle b'|\tilde{U}|b''\rangle A_{(b'',b)}.$$

In general, two sets of Kraus operators $\{A_\mu\}$ and $\{A'_\mu\}$ give rise to the same evolution provided that $A_\mu = \sum_\nu V_{\mu\nu}A'_\nu$, with V unitary:

$$\sum_\mu A_\mu\,\rho\,A_\mu^\dagger = \sum_{\mu,\nu,\pi} V_{\mu\nu}A'_\nu\,\rho\,(A'_\pi)^\dagger V^*_{\mu\pi} = \sum_{\nu,\pi}\left(V^\dagger V\right)_{\pi\nu} A'_\nu\,\rho\,(A'_\pi)^\dagger = \sum_\nu A'_\nu\,\rho\,(A'_\nu)^\dagger.$$

In this section we have derived the evolution of an open quantum system in a physical way, starting from a unitary evolution in a bigger quantum system. Before going to the axiomatic approach of the next section, let us take the opposite point of view and show that every evolution in the Kraus form (1.21) can be recast as a unitary evolution of a bigger quantum system. Consider the decomposition (1.21) and let $\{|b_\mu\rangle\}$ be a basis on $\mathscr{H}_B$. From the completeness relation (1.22) we can regard the Kraus operators A_μ as the orthogonal columns of a unitary matrix U, by setting $\langle a'|A_\mu|a\rangle = \langle a'b_\mu|U|aB\rangle$ for some $|B\rangle\in\mathscr{H}_B$, i.e. by defining U such that

$$U|\psi_A\rangle|B\rangle = \sum_\mu A_\mu|\psi_A\rangle|b_\mu\rangle.$$

Clearly the freedom in the choice of $|B\rangle$ stems from the freedom in the choice of the Kraus operators, as described before. Then

$$\begin{aligned}\sum_\mu\langle a|A_\mu^\dagger A_\mu|a'\rangle &= \sum_{\mu,a''}\langle aB|U^\dagger|a''b_\mu\rangle\langle a''b_\mu|U|a'B\rangle = \langle a|a'\rangle\\ \sum_\mu\langle a|A_\mu\,\rho_A\,A_\mu^\dagger|a'\rangle &= \sum_{\mu,\tilde{a},\tilde{a}'}\langle ab_\mu|U|\tilde{a}B\rangle\langle\tilde{a}|\rho_A|\tilde{a}'\rangle\langle\tilde{a}'B|U^\dagger|a'b_\mu\rangle\\ &= \langle a|\operatorname*{Tr}_B\left[U\left(\rho_A\otimes|B\rangle\langle B|\right)U^\dagger\right]|a'\rangle\,,\end{aligned}$$

and the equations (1.22) and (1.19) arise with $\rho = \rho_A\otimes|B\rangle\langle B|$, thus providing the so called *environmental representation* of the map (1.21).

1.3 Quantum channels

After obtaining both the measurement and the time evolution of an open quantum system by looking at the corresponding measurement and time evolution of an extended closed quantum system, we now give a formal derivation of the properties that a quantum channel, i.e. a map from density operators to density operators, has to satisfy. We have seen two different quantum channels in (1.15) and (1.21), and we will show here that nothing more is needed.

A quantum channel is a superoperator between (different) spaces of density operators

$$\mathscr{E} : \mathscr{B}_{\mathscr{H}} \longrightarrow \mathscr{B}_{\mathscr{H}'}.$$

Given $\rho \in \mathscr{B}_{\mathscr{H}}$, the quantum channel $\mathscr{E}$

$$\rho' = \mathscr{E}(\rho)\,,$$

must satisfy certain conditions to ensure that the output is a density operator $\rho' \in \mathscr{B}_{\mathscr{H}'}$. The first condition is:

(i) $\mathscr{E}$ **is linear**, as required by the postulates of quantum mechanics. In particular, in order to preserve the probabilistic interpretation of the density matrix, $\mathscr{E}$ has to be a *convex-linear map* on the set of density matrices, i.e.,

$$\mathscr{E}\left(\sum_i p_i \rho_i\right) = \sum_i p_i \mathscr{E}\left(\rho_i\right), \qquad\qquad \sum_i p_i = 1.$$

Indeed, the state $\mathscr{E}(\rho)$, where $\rho = \sum_i p_i \rho_i$ arises by initially preparing the system in the state ρ_i with probability p_i and then letting the system evolve through $\mathscr{E}$. Anyway, the same result has to be obtained when the system, with probability p_i, is initially prepared in ρ_i and then evolved to $\mathscr{E}(\rho_i)$.

In order to describe the other properties of $\mathscr{E}$, let us introduce a convenient matrix representation of the superoperator by defining the so called *Choi matrix* $\hat{\mathscr{E}}$. Let $\{|i\rangle\}$, $i = 1,\ldots,\dim\mathscr{H}$ and $\{|i'\rangle\}$, $i' = 1,\ldots,\dim\mathscr{H}'$ be a basis respectively of $\mathscr{H}$ and $\mathscr{H}'$. The Choi matrix is an operator in the Hilbert space $\mathscr{H}\otimes\mathscr{H}'$ and is defined by

$$\langle k\,i'|\hat{\mathscr{E}}|l\,j'\rangle = \langle i'|\mathscr{E}\big(|k\rangle\langle l|\big)|j'\rangle\,, \tag{1.23}$$

where the range of the indices is straightforward. By exploiting the linearity and using the definition of Choi matrix (1.23) the map $\mathscr{E}$ takes the form

$$\begin{aligned}\mathscr{E}(\rho) &= \sum_{i',j',k,l} \langle k|\rho|l\rangle\,\langle i'|\mathscr{E}\big(|k\rangle\langle l|\big)|j'\rangle\,|i'\rangle\langle j'| = \sum_{i',j',k,l} \langle k|\rho|l\rangle\,\langle k\,i'|\hat{\mathscr{E}}|l\,j'\rangle\,|i'\rangle\langle j'| \\ &= \operatorname*{Tr}_{\mathscr{H}}\left[\left(\rho^T\otimes\mathbb{1}_{\mathscr{H}'}\right)\hat{\mathscr{E}}\right],\end{aligned} \tag{1.24}$$

where $\rho^T = \rho^*$ denotes the transpose of ρ. The matrix $\hat{\mathcal{E}}$ is the only operator satisfying (1.24). In fact, suppose that $\hat{\mathcal{E}}$ and $\hat{\mathcal{E}}'$ give the same map $\mathcal{E}$ by means of Eq. (1.24), then $\mathrm{Tr}_{\mathscr{H}}\left[\rho^T \otimes \mathbb{1}_{\mathscr{H}'}\left(\hat{\mathcal{E}} - \hat{\mathcal{E}}'\right)\right] = 0$ for each $\rho \in \mathscr{B}_{\mathscr{H}}$. By looking at the component expansion in Eq. (1.24) it follows straightforwardly that $\hat{\mathcal{E}} = \hat{\mathcal{E}}'$. In the following the properties of the map $\mathcal{E}$ are introduced and analysed in the more simple language of the Choi matrix:

(ii) $\mathcal{E}$ has to **preserve Hermiticity**:

$$\mathcal{E}(\rho) = \operatorname*{Tr}_{\mathscr{H}}\left[\left(\rho^T \otimes \mathbb{1}_{\mathscr{H}'}\right)\hat{\mathcal{E}}\right] = \mathcal{E}(\rho)^\dagger = \operatorname*{Tr}_{\mathscr{H}}\left[\left(\rho^T \otimes \mathbb{1}_{\mathscr{H}'}\right)\hat{\mathcal{E}}^\dagger\right], \qquad \forall \rho \in \mathscr{B}_{\mathscr{H}}.$$

Accordingly, $\hat{\mathcal{E}}$ is Hermitian.

(iii) $\mathcal{E}$ has to be **trace-preserving**:

$$1 = \mathrm{Tr}\,\mathcal{E}(\rho) = \sum_{i',k,l} \langle k|\rho|l\rangle\, \langle i'|\mathcal{E}\left(|k\rangle\langle l|\right)|i'\rangle = \sum_{i',k,l} \langle k|\rho|l\rangle\, \langle k\,i'|\hat{\mathcal{E}}|l\,i'\rangle, \qquad \forall \rho \in \mathscr{B}_{\mathscr{H}}.$$

Accordingly, $\langle k\,i'|\hat{\mathcal{E}}|l\,i'\rangle = \delta_{kl}$ and thus

$$\operatorname*{Tr}_{\mathscr{H}'} \hat{\mathcal{E}} = \mathbb{1}_{\mathscr{H}}. \tag{1.25}$$

(iv) $\mathcal{E}$ has to be **completely positive**: this means that not only $\mathcal{E}$ has to map positive operators into positive operators, but, furthermore, if we introduce another Hilbert space $\mathscr{K}$ of arbitrary dimensionality, $\mathbb{1} \otimes \mathcal{E}$, where $\mathbb{1}$ is the identity map on $\mathscr{K}$, must map density matrices (positive operators) in $\mathscr{K} \otimes \mathscr{H}$ to density matrices (positive operators) in $\mathscr{K} \otimes \mathscr{H}'$. This physical requirement arises because $\mathcal{E}$ has to be valid when we consider extended systems, i.e., tensor products of Hilbert spaces like $\mathscr{K} \otimes \mathscr{H}$, and $\mathcal{E}$ is only applied locally onto one subsystem of Hilbert space $\mathscr{H}$. Let's prove the following important theorem [16]:

Choi's theorem. *The map $\mathcal{E}$ is completely positive if and only if the corresponding Choi matrix $\hat{\mathcal{E}}$ is positive.*

Proof. Let's consider two states $|\psi\rangle \in \mathscr{K} \otimes \mathscr{H}$ and $|\phi\rangle \in \mathscr{K} \otimes \mathscr{H}'$, expressed in some suitable basis $|\psi\rangle = \sum_{kh} \psi_{kh}|k\,h\rangle$ and $|\phi\rangle = \sum_{kh'} \phi_{kh'}|k\,h'\rangle$. As a mixed state can be *purified* into a pure state in a larger Hilbert space, with the freedom of choosing a large enough $\mathscr{K}$ there is no loss of generality in considering the two states to be pure. As $\hat{\mathcal{E}}$ is Hermitian, it admits the spectral decomposition

$$\hat{\mathcal{E}} = \sum_{\mu} \Lambda_\mu |\chi_\mu\rangle\langle\chi_\mu|. \tag{1.26}$$

Accordingly, setting $\langle hh'|\chi_\mu\rangle = \chi_\mu^{hh'}$, one can test whether $\langle\phi|(\mathbb{1}\otimes\mathscr{E})\big(|\psi\rangle\langle\psi|\big)|\phi\rangle$ is positive:

$$\begin{aligned}\langle\phi|(\mathbb{1}\otimes\mathscr{E})\big(|\psi\rangle\langle\psi|\big)|\phi\rangle &= \sum_{h_1,h_2,h_1',h_2'} \langle\phi|h_1'\rangle\langle h_1|\psi\rangle\,\langle h_1'|\mathscr{E}\big(|h_1\rangle\langle h_2|\big)|h_2'\rangle\,\langle\psi|h_2\rangle\langle h_2'|\phi\rangle \\ &= \sum_{h_1,h_2,h_1',h_2'} \langle\phi|h_1'\rangle\langle h_1|\psi\rangle\langle\psi|h_2\rangle\langle h_2'|\phi\rangle\,\langle h_1h_1'|\hat{\mathscr{E}}|h_2h_2'\rangle \\ &= \sum_\mu \Lambda_\mu \sum_{h_1,h_2,h_1',h_2',k_1,k_2} \phi^*_{k_1h_1'}\psi_{k_1h_1}\,\psi^*_{k_2h_2}\phi_{k_2h_2'}\,\chi_\mu^{h_1h_1'}(\chi_\mu^{h_2h_2'})^* \\ &= \sum_\mu \Lambda_\mu \left|\sum_{h,h',k} \phi_{kh'}\psi_{kh}\chi_\mu^{hh'}\right|^2 \geq 0\,.\end{aligned}$$

This must hold for arbitrary $|\phi\rangle$ and $|\psi\rangle$, and therefore $\Lambda_\mu \geq 0$. The sufficiency of the positivity condition immediately follows as well. □

A completely positive linear map between density matrices is thus uniquely parametrized by the corresponding Choi matrix, which is a Hermitian positive operator satisfying condition (1.25), implying that $\mathrm{Tr}\,\hat{\mathscr{E}} = \sum_\mu \Lambda_\mu = \dim_{\mathscr{H}}$. The matrix $\hat{\mathscr{E}}/\dim_{\mathscr{H}}$ has thus all the properties of a density matrix in $\mathscr{H}\otimes\mathscr{H}'$, a results known as *Choi-Jamiołkowski isomorphism*, and, in fact, the set of completely positive maps is a subset of the set of density matrices. Moreover, from the spectral decomposition (1.26) we can obtain the Kraus decomposition (1.21) of the map:

$$\begin{aligned}\mathscr{E}(\rho) &= \underset{\mathscr{H}}{\mathrm{Tr}}\left[\left(\rho^T\otimes\mathbb{1}_{\mathscr{H}'}\right)\,\hat{\mathscr{E}}\right] = \sum_\mu \Lambda_\mu\,\underset{\mathscr{H}}{\mathrm{Tr}}\left[\left(\rho^T\otimes\mathbb{1}_{\mathscr{H}'}\right)\,|\chi_\mu\rangle\langle\chi_\mu|\right] \\ &= \sum_\mu \Lambda_\mu \sum_{i'j',,k,l} \langle k|\rho|l\rangle\,\langle ki'|\chi_\mu\rangle\langle\chi_\mu|lj'\rangle\,|i'\rangle\langle j'| = \sum_\mu A_\mu\,\rho\,A_\mu^\dagger,\end{aligned}$$

where the Kraus operators can be obtained from the spectral decomposition (1.26)

$$\langle h'|A_\mu|h\rangle = \sqrt{\Lambda_\mu}\,\langle hh'|\chi_\mu\rangle, \tag{1.27}$$

and the condition (1.22) is satisfied thanks to Eq. (1.25). Indeed,

$$\langle i|\sum_\mu A_\mu^\dagger A_\mu|j\rangle = \sum_\mu \Lambda_\mu \sum_{k'}\langle\chi_\mu|ik'\rangle\langle jk'|\chi_\mu\rangle = \sum_{k'}\langle jk'|\hat{\mathscr{E}}|ik'\rangle = \delta_{ij}.$$

A completely positive linear map, i.e., a superoperator mapping quantum states to quantum states, has been described in two ways: in terms of the Kraus decomposition, which is the standard expression in the quantum information community, and by means of the Choi matrix, which has some advantages compared to the Kraus decomposition, as there is a one-to-one correspondence (1.23) between the operator $\hat{\mathscr{E}}$ and the superoperator $\mathscr{E}$, and can be built straightforwardly using the component expansion (1.24) when the relation between the input state ρ and the output state $\mathscr{E}(\rho)$ is known.

1.3.1 One qubit maps

The density matrix of a generic *pure* qubit state can be written in the basis $\{|0\rangle, |1\rangle\}$ thanks to Eq. (1.8)

$$|\theta,\phi\rangle\langle\theta,\phi| = \frac{1}{2}\begin{pmatrix} 1+\cos\theta & e^{i\phi}\sin\theta \\ e^{-i\phi}\sin\theta & 1-\cos\theta \end{pmatrix} . \tag{1.28}$$

As for mixed states, the most general density matrix for the qubit is

$$\rho = \frac{1}{2}\begin{pmatrix} 1+z & x+iy \\ x-iy & 1-z \end{pmatrix} = \frac{1}{2}(\mathbb{1} + \vec{r}\cdot\vec{\sigma}) , \tag{1.29}$$

where the vector $\vec{r} = (x,y,z)$ satisfies $r^2 \leq 1$ because of the requirement that the eigenvalues of ρ are non-negative. The expression (1.28) is recovered for $r^2 = 1$, by setting $\vec{r} = r(\sin\theta\cos\phi, \sin\theta\sin\phi, \cos\theta)$, and in general the space of two qubit density matrices is isomorphic to the **Bloch ball** of Fig. 1.1, whose boundary, the Bloch sphere, corresponds to pure states.

A quantum channel between two qubits is, accordingly, a mapping between Bloch balls $(\mathbb{1} + \vec{r}'\cdot\vec{\sigma})/2 = \mathcal{E}(\mathbb{1} + \vec{r}\cdot\vec{\sigma})/2$ and thus, thanks to the algebra (1.6),

$$\vec{r}' = \mathrm{Tr}\left[\vec{\sigma}\ \mathcal{E}\left(\frac{\mathbb{1} + \vec{r}\cdot\vec{\sigma}}{2}\right)\right] . \tag{1.30}$$

The input and the output Hilbert space ($\mathscr{H}$ and $\mathscr{H}'$) coincide, and since the Pauli matrices (together with the identity matrix) form a basis for the operators acting on the two dimensional space $\mathscr{H}$, the Choi matrix associated to the map (1.30) can be expressed in the form $\hat{\mathcal{E}} \propto \mathbb{1}_4 + \vec{t}\cdot(\mathbb{1}_2 \otimes \vec{\sigma}) + \vec{t}'\cdot(\vec{\sigma}\otimes\mathbb{1}_2) + \sum_{\mu\nu} S_{\mu\nu}\sigma^\mu \otimes \sigma^\nu$, where $\mathbb{1}_n$ is the $n\times n$ identity matrix. Imposing condition (1.25) it follows that the Choi matrix can be parametrized as

$$\hat{\mathcal{E}} = \frac{1}{2}\left(\mathbb{1}_4 + \vec{t}\cdot(\mathbb{1}_2\otimes\vec{\sigma}) + \sum_{\mu\nu} T_{\nu\mu}(\sigma^\mu)^T \otimes \sigma^\nu\right) , \tag{1.31}$$

where we have added a partial transposition for convenience, as it will be clear in the following. Since $(\sigma^\mu)^T = (-1)^{\mu+1}\sigma^\mu$, there are no further assumptions in (1.31) which is obtained simply by setting $S_{\mu\nu} = (-1)^{\mu+1}T_{\nu\mu}$. The coefficients t_μ and $T_{\nu\mu}$ can be obtained from

$$\begin{aligned} 2T_{\nu\mu} &= \mathrm{Tr}\left[(\sigma^\mu)^T \otimes \sigma^\nu\ \hat{\mathcal{E}}\right] = \underset{\mathscr{H}'}{\mathrm{Tr}}\left\{\sigma^\nu \underset{\mathscr{H}}{\mathrm{Tr}}\left[\left(\sigma^{\mu\,T}\otimes\mathbb{1}_{\mathscr{H}'}\right)\ \hat{\mathcal{E}}\right]\right\} = \mathrm{Tr}\left[\sigma^\nu\,\mathcal{E}(\sigma^\mu)\right] , \\ 2t_\nu &= \mathrm{Tr}\left[\mathbb{1}_2\otimes\sigma^\nu\ \hat{\mathcal{E}}\right] = \underset{\mathscr{H}'}{\mathrm{Tr}}\left\{\sigma^\nu \underset{\mathscr{H}}{\mathrm{Tr}}\left[(\mathbb{1}_{\mathscr{H}}\otimes\mathbb{1}_{\mathscr{H}'})\ \hat{\mathcal{E}}\right]\right\} = \mathrm{Tr}\left[\sigma^\nu\,\mathcal{E}(\mathbb{1})\right] . \end{aligned}$$

Thanks to the above equations, the mapping (1.30) can be found explicitly: $r'_\nu = t_\nu + T_{\nu\mu}r_\mu$. Accordingly, a completely positive linear map from qubit to qubit is represented by the following *affine transformation* on the Bloch ball

$$\vec{r}' = T\,\vec{r} + \vec{t} . \tag{1.32}$$

The above transformation has twelve parameters[7]: the 3-dimensional vector t describes a translation of the Bloch ball, while the 3×3 matrix T causes rotations and distortions of the Bloch ball. In particular, the three singular values of T modify the shape of the ball into an ellipsoid while the remaining six parameters define the directions of the deformations and change the orientation of the ellipsoid.

1.3.2 Symmetries

Most common quantum channels can be characterized in terms of symmetries. Let $\mathscr{E}: \mathscr{B}_{\mathscr{H}} \to \mathscr{B}'_{\mathscr{H}}$ be a quantum channel and let $\mathbf{G}$ be a group with unitary representations U and U' on $\mathscr{H}$ and $\mathscr{H}'$ respectively. The quantum channel $\mathscr{E}$ is $\mathbf{G}$-*covariant* if it is not varied by a basis change induced by U and U':

$$\mathscr{E}(U_g\,\rho\,U_g^\dagger) = U'_g\,\mathscr{E}(\rho)\,{U'_g}^\dagger, \qquad \forall g\in\mathbf{G} \text{ and } \forall\rho\in\mathscr{B}_{\mathscr{H}}, \tag{1.33}$$

or, equivalently, $\mathscr{E}(\rho) = {U'_g}^\dagger\,\mathscr{E}(U_g\,\rho\,U_g^\dagger)\,U_g$. In order to verify the $\mathbf{G}$-covariance one has not to check all the elements of the group: the generators are sufficient. In fact, suppose that $g = g_1 g_2$, then $U_g = U_{g_1}U_{g_2}$ and $U'_g = U'_{g_1}U'_{g_2}$. By direct calculation it straightforward to check that if (1.33) holds for g_1 and g_2, than it holds also for g. Accordingly, it is sufficient to require that Eq. (1.33) holds for all the generators of the group. The condition (1.33) can be written also by means of the Choi matrix

$$\begin{aligned}\mathscr{E}(\rho) = \operatorname*{Tr}_{\mathscr{H}}\left[\left(\rho^T\otimes\mathbb{1}_{\mathscr{H}'}\right)\hat{\mathscr{E}}\right] &= \operatorname*{Tr}_{\mathscr{H}}\left[\left(U_g^*\rho^T U_g^T\otimes\mathbb{1}_{\mathscr{H}'}\right)\left(\mathbb{1}_{\mathscr{H}}\otimes {U'_g}^\dagger\right)\hat{\mathscr{E}}\left(\mathbb{1}_{\mathscr{H}}\otimes U'_g\right)\right]\\ &= \operatorname*{Tr}_{\mathscr{H}}\left[\left(\rho^T\otimes\mathbb{1}_{\mathscr{H}'}\right)\left(U_g^T\otimes {U'_g}^\dagger\right)\hat{\mathscr{E}}\left(U_g^*\otimes U'_g\right)\right].\end{aligned}$$

Hence, the $\mathbf{G}$-covariance is equivalent to this simple condition on the Choi matrix

$$[\hat{\mathscr{E}},\, U_g^*\otimes U'_g] = 0, \qquad \forall g\in\mathbf{G}, \tag{1.34}$$

where $\mathbf{G}$ is the set of generators of the group $\mathbf{G}$. If $\mathbf{G}$ is a Lie group, it can be studied by linearizing the group in the neighbourhood of its identity, and studying the associated Lie algebra: $U_g \simeq \mathbb{1} - i\epsilon A_g$ where A_g is Hermitian, being U_g unitary. In this case $U_g^*\otimes U'_g \simeq \mathbb{1}\otimes\mathbb{1} - i\epsilon\left(A_g^*\otimes\mathbb{1} - \mathbb{1}\otimes A'_g\right)$ and $\mathbf{G}$-covariance condition takes the form

$$[\hat{\mathscr{E}},\, A_g^*\otimes\mathbb{1}] = [\hat{\mathscr{E}},\, \mathbb{1}\otimes A'_g], \qquad \forall g\in\mathbf{G}. \tag{1.35}$$

Let us show some examples of two-qubit quantum channels where the input and output Hilbert space are the same ($U_g = U'_g$):

[7] These parameters have to satisfy some inequalities [17, 18], for making (1.32) a mapping between Bloch balls.

1. **Invariance under rotation around the α axis**: $[\hat{\mathcal{E}},\ (\sigma^\alpha)^*\otimes\mathbb{1}] = [\hat{\mathcal{E}},\ \mathbb{1}\otimes\sigma^\alpha]$ can be expressed thanks to the expression (1.31) and (1.6)

$$\begin{aligned} -T_{\nu\mu}\varepsilon_{\mu\alpha\gamma}(\sigma^\gamma)^T\otimes\sigma^\nu &= T_{\nu\mu}\varepsilon_{\nu\alpha\gamma}(\sigma^\mu)^T\otimes\sigma^\gamma + t_\mu\varepsilon_{\mu\alpha\gamma}\mathbb{1}\otimes\sigma^\gamma \\ &= T_{\mu\gamma}\varepsilon_{\mu\alpha\nu}(\sigma^\gamma)^T\otimes\sigma^\nu + t_\mu\varepsilon_{\mu\alpha\gamma}\mathbb{1}\otimes\sigma^\gamma, \end{aligned}$$

where the sum over repeated indices is understood. The conditions appear thus

$$T_{\nu\mu}\varepsilon_{\mu\alpha\gamma} + T_{\mu\gamma}\varepsilon_{\mu\alpha\nu} = 0, \quad \forall\nu,\gamma, \qquad \text{and} \quad t_{\mu\neq\alpha} = 0. \tag{1.36}$$

The explicit form of the matrices T for $\alpha = 1,2,3$ is

$$T^{\alpha=1} = \begin{pmatrix} s_1 & 0 & 0 \\ 0 & s_3 & s_2 \\ 0 & -s_2 & s_3 \end{pmatrix}, \quad T^{\alpha=2} = \begin{pmatrix} s_1 & 0 & s_3 \\ 0 & s_2 & 0 \\ -s_3 & 0 & s_1 \end{pmatrix}, \quad T^{\alpha=3} = \begin{pmatrix} s_1 & s_2 & 0 \\ -s_2 & s_1 & 0 \\ 0 & 0 & s_3 \end{pmatrix}, \tag{1.37}$$

for some s_i. For example, when the system is invariant under rotation around the z axis, the Choi matrix is

$$\hat{\mathcal{E}} = \begin{pmatrix} \frac{1+s_3+t}{2} & 0 & 0 & s_1 - is_2 \\ 0 & \frac{1-s_3-t}{2} & 0 & 0 \\ 0 & 0 & \frac{1-s_3+t}{2} & 0 \\ s_1+is_2 & 0 & 0 & \frac{1+s_3-t}{2} \end{pmatrix},$$

which describes the so-called *squeezed generalized amplitude damping channel* [19] which represents a dissipative interaction of a qubit with a squeezed thermal bath. The more common **amplitude damping** channel is obtained in the particular case $s_1 = \sqrt{1-\gamma}$, $s_2 = 0$, $s_3 = 1-\gamma$, $t = \gamma$, and describes the decay of the state $|1\rangle$ to $|0\rangle$ with probability γ. The amplitude damping channel is an effective description of many important relaxation processes, as the spontaneous emission from an atom, or the relaxation process due to the coupling of the qubit with its surrounding environment [1].

2. $SU(2)$ **invariance**: the conditions (1.36) and (1.37) must hold all together and hence $t_\mu = 0$ and $T_{\nu\mu} = s\delta_{\mu\nu}$. The affine transformation of the Bloch ball is simply $\vec{r}' = s\vec{r}$ and hence

$$\rho' = s\rho + \frac{1-s}{2}\,\mathbb{1}_2. \tag{1.38}$$

The quantum channel described by Eq. (1.38) is the so-called **depolarising channel**. It describes a qubit which with probability s is left untouched and with probability $1-s$ is transformed to the completely mixed state.

3. **Invariance under exchange** $|0\rangle \longleftrightarrow |1\rangle$. There are essentially two SU(2) transformations which cause this reflection, being $\sigma^\alpha \sigma^z \sigma^\alpha = -\sigma^z$ for $\alpha = x, y$. This is not a Lie group and we have to use (1.34) with $U_g = U'_g = \sigma^\alpha$. As $\sigma^\alpha \sigma^\beta \sigma^\alpha = (2\delta_{\alpha\beta} - 1)\sigma^\beta$

$$t_\mu \mathbb{1} \otimes \sigma^\mu (2\delta_{\alpha\mu} - 2) + T_{\nu\mu} (\sigma^\mu)^T \otimes \sigma^\nu [(2\delta_{\alpha\mu} - 1)(2\delta_{\alpha\nu} - 1) - 1] = 0 \,.$$

The conditions are only those that have to be simultaneously verified for both $\alpha = x$ and $\alpha = y$, and accordingly

$$t_3 = 0, \qquad T_{3\alpha} = T_{\alpha 3} = 0, \qquad \text{for } \alpha = 1, 2. \tag{1.39}$$

2

Quantum information transmission

A classical bit (such as a memory element or a wire carrying a digital signal) is usually a macroscopic system, and is generally described by one continuous parameter such as voltage. Within this parameter space two well separated regions are chosen by the designer to represent the boolean values 0 and 1. A quantum bit or *qubit* in contrast, is typically a microscopic system, such as an atom or a nuclear spin or a photon. The boolean states $|0\rangle$ and $|1\rangle$ are represented by a fixed pair of reliably distinguishable states of the qubit (for example, horizontal and vertical photon polarizations or the states $\left|S^z = \pm\frac{1}{2}\right\rangle$ of a spin $S = \frac{1}{2}$ particle). According to the principles of quantum mechanics, a qubit can also exist in a superposition of the basis states $|0\rangle$ and $|1\rangle$, and a pair of qubits is capable of existing in four boolean states, $|00\rangle$, $|01\rangle$, $|10\rangle$ and $|11\rangle$, as well as all possible superpositions of them. These include states such as $\frac{1}{2}(|0\rangle + |1\rangle) \otimes (|0\rangle + |1\rangle)$ which are describable as a tensor product of states of the individual qubits, as well as entangled states such as $\frac{1}{\sqrt{2}}(|00\rangle + |11\rangle)$ which do not admit such a description. More generally, a quantum state of n qubits is represented by a complex vector in a Hilbert space of 2^n dimensions. The exponentially large dimensionality of this space distinguishes quantum computers from classical analog computers, whose states, being separable, are represented by a number of parameters that grows only linearly with the system size. The ability to preserve and manipulate entangled states is the distinguishing feature of quantum computers, responsible both for their power and for the difficulty of building them.

Just as any classical algorithm can be expressed as a sequence of one- and two-bit operations, any quantum algorithm (see Fig. 2.1 for an example of a quantum circuit) can be expressed as a sequence of one- and two-qubit quantum gates, that is, unitary operations acting on one or two qubits at a time. By using quantum gates and wires, with entangled states flowing through them in the intermediate stages of a computation, certain computations mapping classical inputs to classical outputs can be done in far fewer steps than any known sequence of classical gate operations. Most famously [20], a quantum computer can factorise large integers in a time that is polynomial in the logarithm of the best classical time, thereby threatening the security of cryptosystems based on the presumed difficulty

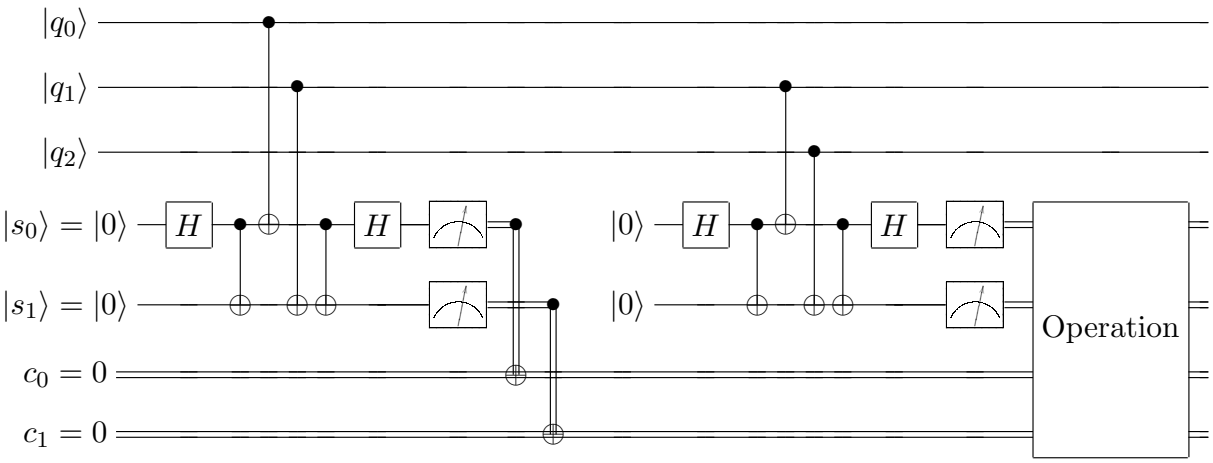

Figure 2.1 – Example of quantum circuit operating on the qubits $|q_i\rangle$ and $|s_i\rangle$ and on the classical bits c_i.

of factorising[1]. Another class of problems for which quantum computers seem to provide exponential speed-up is the simulation of many-particle quantum systems [21, 22].

Quantum information theory generalizes the classical notions of source and channel and introduces a new resource, entanglement, for achieving communication schemes that have no classical analogue. For example, two forms of quantum information transmission that have no classical counterpart are quantum teleportation and quantum superdense coding [1]. These involve an initial stage in which a pair of particles in a maximally-entangled state is shared between two parties, followed by a second stage in which this shared entanglement is used to achieve, respectively, transmission of a qubit via two classical bits, or transmission of two classical bits via one qubit.

2.1 Teleportation

Quantum teleportation is one of the most fascinating discoveries of quantum information theory. It is a process of transmission of a generic unknown quantum state from one part ("Alice") to another ("Bob") which is implemented not by directly sending particles through a quantum channel, but via local operations, classical communication, and initially shared entanglement.

Suppose indeed that Alice and Bob share the Bell state $|\Phi^+_{AB}\rangle$, written in Eq. (1.13). Alice also has another unknown qubit $|\psi_Q\rangle = \alpha|0\rangle + \beta|1\rangle$ (see Fig. 2.2) and she wants to teleport it to Bob. The state must be unknown to Alice, because otherwise she can just phone Bob and

[1]This exponential speed-up depends on the quantum computer's ability to vastly parallelize the performance of a fast Fourier transform, using destructive interference among a number of parallel computation paths that increases exponentially with the number of physical qubits involved in the computation.

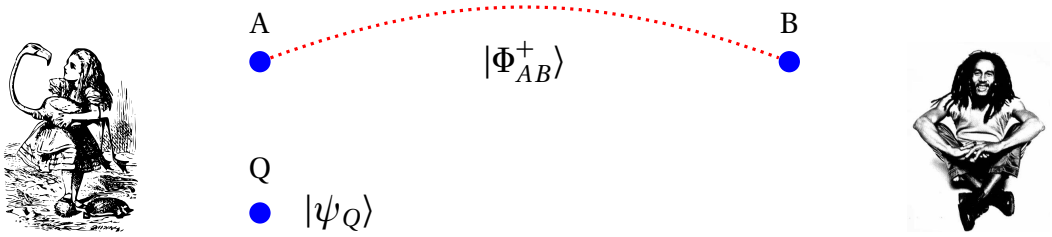

Figure 2.2 – Schematic picture of teleportation: Alice and Bob initially share a maximally entangled state.

Alice's measurement	Bob's state	Bob's operation
$\|\Phi^+\rangle$	$\alpha\|0\rangle+\beta\|1\rangle$	$\mathbb{1}_2$
$\|\Phi^-\rangle$	$\alpha\|0\rangle-\beta\|1\rangle$	σ^z
$\|\Psi^+\rangle$	$\alpha\|1\rangle+\beta\|0\rangle$	σ^x
$\|\Psi^-\rangle$	$\alpha\|1\rangle-\beta\|0\rangle$	$\sigma^z\sigma^x$

Table 2.1 – Unitary operation to be performed by Bob depending on the state obtained by Alice after the measurement.

tell him all the details of the state, so that he can recreate it. Moreover, Alice is not able to obtain all the information about the unknown state $|\psi_Q\rangle$ by performing measurements: she would obtain only the two diagonal states, e.g. $|0\rangle$ and $|1\rangle$, with some probability. However, even if the state $|\psi_Q\rangle$ is unknown to her, Alice can teleport it to Bob via local operations and classical communications. The initial state of the three qubits is

$$|\psi_Q\rangle|\Phi^+_{AB}\rangle=\left(\alpha|0_Q\rangle+\beta|1_Q\rangle\right)\frac{1}{\sqrt{2}}\left(|0_A0_B\rangle+|1_A1_B\rangle\right).$$

This can be expanded and rewritten as

$$\begin{aligned}|\psi_Q\rangle|\Phi^+_{AB}\rangle&=\frac{1}{\sqrt{2}}\left(\alpha|0_Q0_A0_B\rangle+\alpha|0_Q1_A1_B\rangle+\beta|1_Q0_A0_B\rangle+\beta|1_Q1_A1_B\rangle\right)\\&=\frac{1}{2}\Big[|\Phi^+_{QA}\rangle\left(\alpha|0_B\rangle+\beta|1_B\rangle\right)+|\Phi^-_{QA}\rangle\left(\alpha|0_B\rangle-\beta|1_B\rangle\right)\\&+\quad|\Psi^+_{QA}\rangle\left(\alpha|1_B\rangle+\beta|0_B\rangle\right)+|\Psi^-_{QA}\rangle\left(\alpha|1_B\rangle-\beta|0_B\rangle\right)\Big].\end{aligned}$$

Alice's two qubits (QA) are now written in terms of the four Bell states (1.13), while the state of B is written in terms of the original state to be teleported. Alice now measures in the Bell basis her two qubits and then phones Bob to tell him the results of her measurement. Bob then knows which of the four states $\alpha|0\rangle\pm\beta|1\rangle$, $\alpha|1\rangle\pm\beta|0\rangle$ he has and can apply a unitary operation to his qubit, according to table 2.1, in order to obtain the original $|\psi_Q\rangle$.

In the standard teleportation scheme Alice and Bob initially share a maximally entangled state for performing teleportation. What happens instead if Alice and Bob initially share

a generic state τ_{AB}? This could happen for instance if the maximally entangled state has undergone some noise. What requirements τ_{AB} has to fulfil for making Alice able to perform teleportation? In order to describe this situation in general let us consider a mixed state ρ_Q to be teleported. As in the standard teleportation scheme, Alice performs a measurement over the Bell basis, described by the set of projection operators $|\chi^\mu_{QA}\rangle\langle\chi^\mu_{QA}|$ where $\{|\chi^\mu_{QA}\rangle\} = \{|\Phi^\pm_{AB}\rangle, |\Psi^\pm_{AB}\rangle\}$, while Bob applies a μ dependent unitary operation U^μ_B on his qubit B. The quantum channel which describes this process is

$$\rho_Q \otimes \tau_{AB} \quad \longrightarrow \quad \sum_\mu |\chi^\mu_{QA}\rangle\langle\chi^\mu_{QA}| \otimes U^\mu_B \left(\rho_Q \otimes \tau_{AB}\right) |\chi^\mu_{QA}\rangle\langle\chi^\mu_{QA}| \otimes (U^\mu_B)^\dagger \,.$$

The resulting state ρ'_B of Bob is obtained by taking the partial trace over A and Q, thus

$$\rho'_B = \sum_\mu U^\mu_B \,\langle\chi^\mu_{QA}|\rho_Q \otimes \tau_{AB}|\chi^\mu_{QA}\rangle\,(U^\mu_B)^\dagger.$$

Now we use the following trick [23]: let S_{QB} be the unitary idempotent operator exchanging Q and B, i.e. $\rho_Q \otimes \tau_{AB} = S_{QB}\,\tau_{QA} \otimes \rho_B\, S_{QB}$ where ρ_B is exactly the same state ρ_Q, but on qubit B and the same holds for τ_{QA}. Moreover, by ordering the state $|\chi^\mu_{QA}\rangle$ such that $|\chi^\mu_{QA}\rangle = \sigma^\mu_Q \otimes \mathbb{1}_A|\Phi^+_{QA}\rangle$, as in Eq. (1.14), it follows

$$\begin{aligned}
\rho'_B &= \sum_\mu U^\mu_B \,\langle\Phi^+_{QA}|\,\sigma^\mu_Q S_{QB}\left(\tau_{QA} \otimes \rho_B\right) S_{QB}\sigma^\mu_Q|\Phi^+_{QA}\rangle\,(U^\mu_B)^\dagger \\
&= \sum_\mu U^\mu_B \,\langle\Phi^+_{QA}|\,S^2_{QB}\,\sigma^\mu_Q S_{QB}\left(\tau_{QA} \otimes \rho_B\right) S_{QB}\sigma^\mu_Q\, S^2_{QB}|\Phi^+_{QA}\rangle\,(U^\mu_B)^\dagger \\
&= \sum_\mu U^\mu_B \,\langle\Phi^+_{QA}|S_{QB}\left(\tau_{QA} \otimes \sigma^\mu_B \rho_B\, \sigma^\mu_B\right) S_{QB}\,|\Phi^+_{QA}\rangle\,(U^\mu_B)^\dagger.
\end{aligned}$$

The operator S_{QB} has a simple expression in terms of the Pauli matrices that can be checked by direct calculation: $S_{QB} = \frac{1}{2}\sum_\nu \sigma^\nu_Q \otimes \mathbb{1}_A \otimes \sigma^\nu_B$. Then

$$\rho'_B = \frac{1}{4}\sum_{\mu,\nu,\lambda} \langle\Phi^+_{QA}|\sigma^\nu_Q \otimes \mathbb{1}_A\,\tau_{QA}\sigma^\lambda_Q \otimes \mathbb{1}_A|\Phi^+_{QA}\rangle\; U^\mu_B\sigma^\nu_B\sigma^\mu_B\rho_B\,\sigma^\mu_B\sigma^\lambda_B(U^\mu_B)^\dagger.$$

By comparing Table (2.1) with Eq. (1.14) is straightforward to check that the standard teleportation scheme arises when we consider $U^\mu_B = \sigma^\mu_B$. Then, dropping the unimportant indices,

$$\begin{aligned}
\rho'_B &= \frac{1}{4}\sum_{\mu,\nu,\lambda} \langle\chi^\nu|\tau|\chi^\lambda\rangle\;\sigma^\mu_B\sigma^\nu_B\sigma^\mu_B\rho_B\,\sigma^\mu_B\sigma^\lambda_B\sigma^\mu_B \\
&= \sum_\mu \langle\chi^\mu|\tau|\chi^\mu\rangle\;\sigma^\mu_B\rho_B\,\sigma^\mu_B,
\end{aligned} \tag{2.1}$$

where the last equality follows from direct calculations. Eq. (2.1) associates a quantum channel to the teleportation procedure that, being in the Kraus form (1.21), is completely positive. Therefore, the teleportation procedure can be also easily extended to the case in which

the qubit to be teleported is part of a *quantum register*, i.e. an array of (possibly entangled) qubits.

Moreover, the result of Eq. (2.1) can be generalized to higher dimensional systems [24, 25] by using the generators of the unitary group of $d \times d$ matrices

$$\Upsilon^{nm} = \sum_k e^{\frac{2\pi i k n}{d}} |k\rangle\langle k \oplus m|, \tag{2.2}$$

where $\oplus$ denotes the addition modulo d and $n, m = 0, \ldots, d-1$. They are clearly unitary, satisfy the algebra

$$\Upsilon^{nm}\Upsilon^{n'm'} = e^{\frac{2\pi i}{d}(n'm - nm')}\,\Upsilon^{n'm'}\Upsilon^{nm}\,, \qquad \mathrm{Tr}\,\Upsilon^{nm} = d\,\delta_{n0}\delta_{m0}\,, \tag{2.3a}$$

$$\mathrm{Tr}[\Upsilon^{nm}(\Upsilon^{n'm'})^\dagger] = d\,\delta_{nn'}\delta_{mm'}, \tag{2.3b}$$

and accordingly form a basis of the space of $d \times d$ unitary operators [26]. Moreover, the set of maximally entangled bipartite states, i.e., those whose reduced density matrices in diagonal form are proportional to the identity, can be constructed from the state

$$|\Phi^+\rangle = \frac{1}{\sqrt{d}} \sum_i |i\rangle|i\rangle. \tag{2.4}$$

Indeed, the others maximally entangled states can be constructed by applying local unitary operations on $|\Phi^+\rangle$ for not changing the eigenvalues of the reduced density matrices. However, since $U \otimes V|\Phi^+\rangle = UV^T \otimes \mathbb{1}|\Phi^+\rangle$, the set of maximally entangled states is

$$|\chi^\mu\rangle \equiv |\chi^{nm}\rangle = \Upsilon^{mm} \otimes \mathbb{1}\,|\Phi^+\rangle = \frac{1}{\sqrt{d}} \sum_k e^{\frac{2\pi i k n}{d}} |k\rangle|k \oplus m\rangle, \tag{2.5}$$

where we have defined the multi-index $\mu = (n, m)$. Let us generalize the qubit teleportation to the case of d-dimensional systems, by considering also more general local quantum operations on B described by a set of μ-dependent Kraus operators $B^\nu(\mu)$. As in the simplest case of qubit teleportation, the teleportation quantum channel can be written as

$$\begin{aligned}\rho'_B &= \sum_{\mu,\nu} B^\nu(\mu)\langle\Phi^+_{QA}|(\Upsilon^\mu_Q)^\dagger S_{QB}\left(\tau_{QA} \otimes \rho_B\right) S_{QB}\Upsilon^\mu_Q|\Phi^+_{QA}\rangle\, B^\nu(\mu)^\dagger \\ &= \sum_{\mu,\nu} B^\nu(\mu)\langle\Phi^+_{QA}|S_{QB}\left(\tau_{QA} \otimes (\Upsilon^\mu)^\dagger\rho_B\Upsilon^\mu\right) S_{QB}|\Phi^+_{QA}\rangle\, B^\nu(\mu)^\dagger,\end{aligned}$$

where the swap operator can be found by generalizing the previous qubits' case using the definition (2.2): it is straightforward to prove that the Hermitian idempotent swap operator is

$$S_{QB} = \frac{1}{d}\sum_{mn} \Upsilon^{mn}_Q \otimes \mathbb{1}_A \otimes \left(\Upsilon^{mn}_B\right)^\dagger = \frac{1}{d}\sum_{mn} \left(\Upsilon^{mn}_Q\right)^\dagger \otimes \mathbb{1}_A \otimes \Upsilon^{mn}_B.$$

Specialising to the case in which Bob performs only unitary operations $B^{\nu}(\mu) = \Upsilon^{\mu}$

$$\begin{aligned}\rho' &= \frac{1}{d^2}\sum_{\mu,\mu',\mu''} \langle\Phi^+|\left((\Upsilon^{\mu'})^\dagger \otimes \mathbb{1}\right)\tau\left(\mathbb{1}\otimes\Upsilon^{\mu''}\right)|\Phi^+\rangle\,\Upsilon^{\mu}\Upsilon^{\mu'}(\Upsilon^{\mu})^\dagger\,\rho\,\Upsilon^{\mu}(\Upsilon^{\mu''})^\dagger(\Upsilon^{\mu})^\dagger \\ &= \sum_{\mu}\langle\chi^{\mu}|\tau|\chi^{\mu}\rangle\,\Upsilon^{\mu}\rho\,(\Upsilon^{\mu})^\dagger\,. \end{aligned} \tag{2.6}$$

where the commutation relations (2.3) have been used. In particular, thanks to $\Upsilon^{nm}\Upsilon^{m'n'}(\Upsilon^{nm})^\dagger = e^{\frac{2\pi i}{d}(n'm-nm')}\,\Upsilon^{m'n'}$, by summing over m, n and by recalling $(m',n') = \mu$ equation (2.6) follows.

Quantum teleportation with a shared arbitrary Bell state guarantees a perfect teleportation of the state, whereas in general, when the shared state τ is not a Bell state the teleportation channel (2.1),(2.6) gives imperfect teleportation. In the next section a generic transmission of a quantum state using a generic quantum channel $\mathscr{E}$ is considered and rigorous measures of the transmission quality are defined.

2.2 State transmission

In the previous section the quantum teleportation protocol has been analyzed and described as a quantum channel between the qubit Q, held by Alice, and the qubit B held by Bob. Now we generalize the concept of state transmission[2], by considering Alice and Bob connected by a generic quantum channel $\mathscr{E}$ (see Fig. 2.3). This quantum channel can arise by assuming, as in the teleportation scheme, that the distant parts share an entangled state and perform local operations and classical communications, or that Alice and Bob are connected by a physical medium, i.e. a *quantum wire*. In the latter case, it is the dynamics of the composite system formed by the two qubits and the wire to trigger the transmission, for instance when the qubit is encoded in a photon and the photon is let to fly over an optical fiber or when the qubits and the wire are made of localized particles and the many-body dynamics of these particles effectively induces the transmission. Each of these schemes can be described by a quantum channel between Alice and Bob, provided that Alice and the rest of the system are initially disentangled (1.20).

Suppose that Alice wants to transfer the state $|\psi\rangle$ to Bob via the quantum channel $\mathscr{E}$. This quantum channel could be noisy, e.g., due to the interaction with an external environment or due to the internal interactions between the constituents of the channel which might entrap the state inside without transferring it to the distant part. In order to check the quality of transmission we can look at the overlap between the transmitted state $\mathscr{E}(|\psi\rangle\langle\psi|)$ and the initial state $|\psi\rangle$, i.e. we can calculate the fidelity of transmission

$$\langle\psi|\mathscr{E}(|\psi\rangle\langle\psi|)|\psi\rangle. \tag{2.7}$$

[2]Notice that a quantum state can be transmitted, but not cloned, because of the *no-cloning theorem* [27].

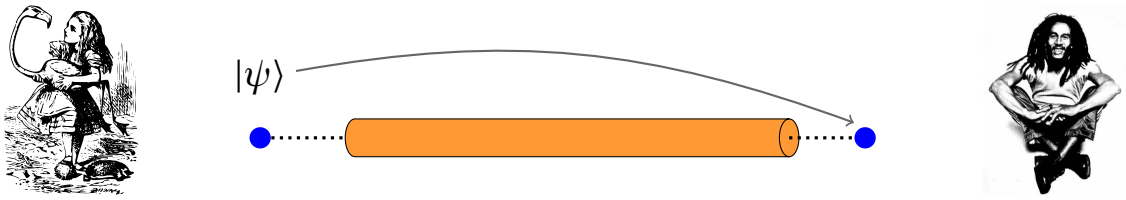

Figure 2.3 – Schematic picture of state transmission: Alice wants to transfer the state $|\psi\rangle$ of one of her qubits to a qubit held by Bob.

The above quantity depends on the state $|\psi\rangle$ to be transmitted. Thus, in order to have a quantity which does not depend on the initial state we can consider the worst scenario by minimizing (2.7) over the possible $|\psi\rangle$'s. However, the resulting quantity is highly non-linear and an explicit formula can be found only in very simple cases (see the next section). Another simpler possibility stems by considering the average, instead of the minimum, over all possible initial states, i.e.,

$$\mathfrak{F} = \int d\psi \, \langle\psi|\mathcal{E}(|\psi\rangle\langle\psi|)|\psi\rangle \, ,$$

where $d\psi$ is the unitary invariant measure over the pure-state space. This quantity, called the **average transmission fidelity**, can be found explicitly using the twirling operator (A.1). Indeed, thanks to (A.3),

$$\int d\psi \, |\psi\rangle^{\otimes 2}\langle\psi|^{\otimes 2} = \int dU \, U^{\otimes 2}|00\rangle\langle 00|(U^\dagger)^{\otimes 2} = \frac{1}{d(d+1)}(\mathbb{1}\otimes\mathbb{1} + S), \tag{2.8}$$

where d is the dimension of the Hilbert space and S is the swap operator. Projecting the above equation onto a suitable basis

$$\int d\psi \, \langle k|\psi\rangle\langle j|\psi\rangle\langle\psi|i\rangle\langle\psi|l\rangle = \frac{1}{d(d+1)}\left(\delta_{ik}\delta_{jl} + \delta_{kl}\delta_{ji}\right) \, ,$$

and thus

$$\begin{aligned}\bar{\mathfrak{F}} &= \int d\psi \, \langle\psi|\mathcal{E}(|\psi\rangle\langle\psi|)|\psi\rangle = \sum_{ijkl}\langle i|\mathcal{E}(|k\rangle\langle l|)|j\rangle \int d\psi \, \langle j|\psi\rangle\langle\psi|i\rangle\langle k|\psi\rangle\langle\psi|l\rangle \\ &= \sum_{ij}\frac{\langle i|\mathcal{E}(|i\rangle\langle j|)|j\rangle + \langle i|\mathcal{E}(|j\rangle\langle j|)|i\rangle}{d(d+1)} = \frac{1}{d+1} + \frac{1}{d(d+1)}\sum_{ij}\langle ii|\hat{\mathcal{E}}|jj\rangle \\ &= \frac{1+\langle\Phi^+|\hat{\mathcal{E}}|\Phi^+\rangle}{d+1} \, ,\end{aligned} \tag{2.9}$$

where we used the trace preserving condition and $|\Phi^+\rangle$ is defined in (2.4). As described in the previous chapter the Choi matrix divided by d is isomorphic to a quantum state. So what is the physical meaning of $\langle\Phi^+|\hat{\mathcal{E}}|\Phi^+\rangle$?

Figure 2.4 – Schematic picture of entanglement transmission: Alice has two systems A and A' in the maximally entangled state $|\Phi^+\rangle$ and transmit the state of A to the system B held by Bob via a quantum channel.

Immagine that Alice holds a maximally entangled pair (A', A) and transfers the state of A through a channel $\mathscr{E}$, as in Fig. 2.4, while A' is assumed to be isolated. If the pair (A, A') was initially in the state $|\Phi^+\rangle$ then the state of the pair (A', B) after the transmission is

$$\rho_{A'B} = (\mathbb{1}\otimes\mathscr{E})(|\Phi^+\rangle\langle\Phi^+|) = \frac{1}{d}\sum_{\substack{a\tilde{a}\\ b\tilde{b}}}\left(\mathbb{1}\otimes|b\rangle\langle b|\mathscr{E}|\tilde{b}\rangle\langle\tilde{b}|\right)(|aa\rangle\langle\tilde{a}\tilde{a}|)$$
$$= \frac{1}{d}\sum_{\substack{a\tilde{a}\\ b\tilde{b}}}\langle b|\mathscr{E}(|a\rangle\langle\tilde{a}|)|\tilde{b}\rangle\,|ab\rangle\langle\tilde{a}\tilde{b}| = \frac{1}{d}\sum_{\substack{a\tilde{a}\\ b\tilde{b}}}\langle ab|\hat{\mathscr{E}}|\tilde{a}\tilde{b}\rangle\,|ab\rangle\langle\tilde{a}\tilde{b}| = \frac{1}{d}\hat{\mathscr{E}}. \tag{2.10}$$

The Choi matrix $\hat{\mathscr{E}}$ associated to the quantum channel $\mathscr{E}$ is thus the state resulting from the application of the channel $\mathbb{1}\otimes\mathscr{E}$ to the maximally entangled pair $|\Phi^+\rangle$. Therefore, the quantity

$$\bar{\mathfrak{f}} = \frac{1}{d}\langle\Phi^+|\hat{\mathscr{E}}|\Phi^+\rangle \tag{2.11}$$

is the **entanglement transmission fidelity** for the state $|\Phi^+\rangle$, i.e. it represents the fidelity that the maximally entangled state in the local pair (A', A) turns into a maximally entangled state in the pair (A', B) made by two distant systems. Moreover, every maximally entangled state can be generated from $|\Phi^+\rangle$ via a local unitary operation on A'; but since A' is an isolated system these local operations do not affect the entanglement transmission: the entanglement transmission fidelity $\bar{\mathfrak{f}}$ does not depend on the particular maximally entangled state to be teleported, that is why it is called **entanglement transmission fidelity**. In Eq. (2.11) we have thus proved the following theorem [28]

Horodecki's theorem. *The average transmission fidelity $\bar{\mathfrak{F}}$ is related to the entanglement transmission fidelity $\bar{\mathfrak{f}}$ by*

$$\bar{\mathfrak{F}} = \frac{d\,\bar{\mathfrak{f}}+1}{d+1}, \tag{2.12}$$

where d is the dimension of the Hilbert space of the state to be trasported.

There are essentially two mechanisms that cause the average fidelity to deteriorate during a transmission process: collective phenomenon due to the channel being an interacting

system (possibly dissipative), and local rotations. As a matter of fact, the average fidelity does not distinguish between bad transmission, i.e. due to decoherence or dispersion of the state all over the channel, and good transmission with an extra rotation during the dynamics; on the other hand, the latter can be safely handled by letting Bob to perform an extra unitary rotation R. The maximal average fidelity achievable after removing such a local rotation is

$$\mathfrak{F} = \max_{R\in \mathrm{SU}(d)} \int d\psi \, \langle\psi|R^\dagger \mathscr{E}(|\psi\rangle\langle\psi|) R|\psi\rangle \tag{2.13a}$$

$$= \max_{R\in \mathrm{SU}(d)} \frac{d}{d+1} \langle\Phi^+| \left(\mathbb{1}\otimes R^\dagger \mathscr{E} R\right)(|\Phi^+\rangle\langle\Phi^+|)|\Phi^+\rangle + \frac{1}{d+1} \tag{2.13b}$$

$$= \frac{d\,\mathfrak{f}+1}{d+1} \,. \tag{2.13c}$$

We call $\mathfrak{f}$ the maximal entanglement fidelity

$$\mathfrak{f} = \max_{R\in \mathrm{SU}(d)} \frac{1}{d} \langle\Phi^+|(\mathbb{1}\otimes R^\dagger)\hat{\mathscr{E}}(\mathbb{1}\otimes R)|\Phi^+\rangle = \max_{\chi \text{ m.e.}} \frac{1}{d} \langle\chi|\hat{\mathscr{E}}|\chi\rangle \,, \tag{2.14}$$

where the maximum is taken over the maximally entangled states $|\chi\rangle$. Indeed, the states $(\mathbb{1}\otimes R)|\Phi^+\rangle$, with varying R, give all the possible maximally entangled states.

2.2.1 Fidelity of teleportation

Thanks to the tools developed in the previous sections for general quantum channels we can now calculate the fidelity of teleportation, i.e. the transmission fidelity with the teleportation channel (2.6). In particular we will prove the following theorem:

Theorem 1. *The maximal entanglement teleportation fidelity of the teleportation channel* $\mathscr{E}^{telep.}$ *is*

$$\mathfrak{f}^{telep.} = \max_{\chi \ m.e.} \langle\chi|\tau|\chi\rangle \,, \tag{2.15}$$

where the expression in the RHS of Eq. (2.15) *is the* **fully entangled fraction** *of the shared state* τ.

Before going to the proof of the theorem, let's discuss the main consequence of this result. In fact, according to (2.15), there are two possible ways for transferring a state over a noisy quantum channel:

1. Directly transfer the state over the channel, as in Fig. 2.4.

2. First share an entangled state by sending entanglement over the channel, as in Fig. 2.4, and then perform teleportation, as in Fig. 2.2, using the shared resource.

Eq. (2.15) states that these two transmission methods give the same fidelity.

Proof. The Choi matrix for a channel expressed in the Kraus form (1.21) is in general

$$\hat{\mathcal{E}} = \sum_{\substack{a\tilde{a}\\ b\tilde{b}}} \langle b|\mathcal{E}(|a\rangle\langle\tilde{a}|)|\tilde{b}\rangle\, |ab\rangle\langle\tilde{a}\tilde{b}| = \sum_{\mu}\sum_{\substack{a\tilde{a}\\ b\tilde{b}}} \langle b|A^{\mu}|a\rangle\langle\tilde{b}|A^{\mu}|\tilde{a}\rangle^{\dagger}|ab\rangle\langle\tilde{a}\tilde{b}|\,,$$

and accordingly the entangled fraction is

$$\langle\Phi^+|\hat{\mathcal{E}}|\Phi^+\rangle = \frac{1}{d}\sum_{\mu} |\operatorname{Tr} A^{\mu}|^2\,. \tag{2.16}$$

The fully entangled fraction $\hat{\mathcal{E}}^{\text{telep.}}$ for the teleportation channel (2.6) is the maximum over the operators R of $\frac{1}{d}\langle\Phi^+|(\mathbb{1}\otimes R^{\dagger})\hat{\mathcal{E}}(\mathbb{1}\otimes R)|\Phi^+\rangle$. The latter is given by Eq. (2.16) with $A^{\mu} = \sqrt{\langle\chi^{\mu}|\tau|\chi^{\mu}\rangle}\, R^{\dagger}\Upsilon^{\mu}$ and then

$$\begin{aligned}
\max_{\chi\ \text{m.e.}} \frac{1}{d}\langle\chi|\hat{\mathcal{E}}^{\text{telep.}}|\chi\rangle &= \max_{R\in\mathrm{SU}(d)} \frac{1}{d^2}\sum_{\mu}\langle\chi^{\mu}|\tau|\chi^{\mu}\rangle \sum_{a\tilde{a}}\langle a|R^{\dagger}\Upsilon^{\mu}|a\rangle\langle\tilde{a}|R^{\dagger}\Upsilon^{\mu}|\tilde{a}\rangle^{\dagger}\\
&= \max_{R\in\mathrm{SU}(d)} \sum_{\mu}\langle\chi^{\mu}|\tau|\chi^{\mu}\rangle\, \langle\Phi^+|\mathbb{1}\otimes(R^{\dagger}\Upsilon^{\mu})|\Phi^+\rangle\langle\Phi^+|\mathbb{1}\otimes(R^{\dagger}\Upsilon^{\mu})^{\dagger}|\Phi^+\rangle\\
&= \max_{R\in\mathrm{SU}(d)} \sum_{\mu}\langle\Phi^+|(\mathbb{1}\otimes R^{\dagger})|\chi^{\mu}\rangle\langle\chi^{\mu}|\,\tau\,|\chi^{\mu}\rangle\langle\chi^{\mu}|(\mathbb{1}\otimes R)|\Phi^+\rangle\\
&= \max_{R\in\mathrm{SU}(d)} \langle\Phi^+|(\mathbb{1}\otimes R^{\dagger})\,\tau\,(\mathbb{1}\otimes R)|\Phi^+\rangle = \max_{\chi\ \text{m.e.}}\langle\chi|\tau|\chi\rangle\,,
\end{aligned}$$

where in the penultimate equality we used the orthogonality of the maximally entangled states. □

2.3 Entanglement as a resource

As we have seen, the problem of state transfer is directly connected to quantum teleportation with a shared resource τ. When τ is a maximally entangled state the standard teleportation protocol guarantees a perfect transmission. On the other hand, for a generic state τ the fidelity of teleportation is uniquely determined by the fully entangled fraction (2.15). When the fully entangled fraction is lower than a certain threshold, which will be derived in this section, the teleportation does not provide a better transmission fidelity than that of an ordinary classical communication channel [29]. To do better than a classical channel, *the shared quantum state must be entangled.*

It is clear indeed that Alice can measure the state $|\phi\rangle$ of her qubit, by applying a set of projection operators $|\psi^{\mu}\rangle\langle\psi^{\mu}|$, and send the measurement outcome to Bob, who will prepare his state in the state obtained by Alice. After the measurement the state of Alice is described by the density operator $\rho = \sum_{\mu=1}^{d} |\langle\phi|\psi^{\mu}\rangle|^2\, |\psi^{\mu}\rangle\langle\psi^{\mu}|$, i.e., the measurement defines a quantum channel with Kraus operators $A^{\mu} = |\psi^{\mu}\rangle\langle\psi^{\mu}|$. The entanglement fraction of

this quantum channel, as given by (2.16), is $\bar{\mathfrak{f}} = 1/d$ and, accordingly, the fidelity between $|\phi\rangle$ and the state after the measurement is, on average,

$$\bar{\mathfrak{F}}^{\text{cl.}} = \frac{2}{d+1}. \tag{2.17}$$

In the remaining part of this section we will prove [30] that the teleportation cannot do better than a classical channel when the shared resource τ is not entangled, that is $\mathfrak{f} \leq \frac{1}{d}$ for any separable state. A general mixed separable state [31] can be written as a classical mixture of product mixed states

$$\rho = \sum_i p_i \rho_{_A}^i \otimes \rho_{_B}^i \,. \tag{2.18}$$

These states satisfy the so-called *reduction criterion for separability*. It is given by the following conditions that are satisfied by all separable states [31]

$$\rho_{_A} \otimes \mathbb{1} - \rho \geq 0, \qquad\qquad \mathbb{1} \otimes \rho_{_B} - \rho \geq 0. \tag{2.19}$$

where $\rho_{_A}$ and $\rho_{_B}$ are obtained by taking the partial trace of ρ over B and A respectively. We will now prove that $\mathfrak{f} \leq \frac{1}{d}$ for any state satisfying the reduction criterion (2.19). However, the reduction criterion is not equivalent to separability (with the exception of the two-qubit case), as there are also some entangled states satisfying the reduction criterion [30, 28].

Let $\mathfrak{f}_R = \langle\Phi^+|(\mathbb{1}\otimes R^\dagger)\tau(\mathbb{1}\otimes R)|\Phi^+\rangle$ be the entanglement fraction with respect to the maximally entangled state $(\mathbb{1}\otimes R)|\Phi^+\rangle$. Clearly, $\mathfrak{f} = \max_R \mathfrak{f}_R$. By observing that $\mathbb{1}\otimes U|\Phi^+\rangle = U^T \otimes \mathbb{1}|\Phi^+\rangle$, and accordingly $|\Phi^+\rangle$ is invariant under the application of $U\otimes U^*$ rotations, it follows that the entanglement fidelities obtained from both states $(\mathbb{1}\otimes R^\dagger)\tau(\mathbb{1}\otimes R)$ and

$$\tilde{\tau}_R = \int dU\, (U^\dagger \otimes U^T R^\dagger)\tau(U\otimes RU^*) = \left[\int dU\, U^\dagger\otimes U^\dagger \left(\mathbb{1}\otimes R^\dagger\right)\tau(\mathbb{1}\otimes R)\Big)^{T_2} U\otimes U\right]^{T_2},$$

where T_2 is the transposition operation over the second Hilbert space only, are the same. Using the expression (A.3) and noting that $\mathrm{Tr}\, O^{T_2} = \mathrm{Tr}\, O$ and $\mathrm{Tr}\, O^{T_2} S = \mathrm{Tr}\, O S^{T_2}$, where $S^{T_2} = d|\Phi^+\rangle\langle\Phi^+|$, we obtain

$$\begin{aligned}\tilde{\tau}_R &= \frac{1-\langle\Phi^+|(\mathbb{1}\otimes R^\dagger)\tau(\mathbb{1}\otimes R)|\Phi^+\rangle}{d^2-1}\,\mathbb{1}\otimes\mathbb{1} + \frac{d^2\,\langle\Phi^+|(\mathbb{1}\otimes R^\dagger)\tau(\mathbb{1}\otimes R)|\Phi^+\rangle - 1}{d^2-1}\,|\Phi^+\rangle\langle\Phi^+|, \\ &= \frac{1-\mathfrak{f}_R}{d^2-1}\,\mathbb{1}\otimes\mathbb{1} + \frac{d^2\mathfrak{f}_R - 1}{d^2-1}\,|\Phi^+\rangle\langle\Phi^+|.\end{aligned}$$

The reduced density matrix of the above state is $\left(d\,\frac{1-\mathfrak{f}_R}{d^2-1} + \frac{d^2\mathfrak{f}_R-1}{d(d^2-1)}\right)\mathbb{1} = \frac{1}{d}\,\mathbb{1}$. Since the identity operator can be expressed in the basis given by $|\Phi^+\rangle\langle\Phi^+|$ and the other maximally entangled states, the state $\tilde{\tau}_R$ satisfies the reduction criterion (2.19) if $\frac{1}{d} \geq \frac{1-\mathfrak{f}_R}{d^2-1} + \frac{d^2\mathfrak{f}_R-1}{d^2-1}$, i.e. if $\mathfrak{f}_R \leq \frac{1}{d}$ for each R. Hence, the fully entangled fraction for separable states is bounded from above by $\frac{1}{d}$. We have thus proved that in oder to teleport a state with an average fidelity larger than the classical value (2.17) the shared state between Alice and Bob must be entangled.

2.4 Explicit formulas for two-qubits channels

In the case of a quantum channel between qubit states, thanks to the parametrization (1.31) for the Choi matrix, the entanglement fraction is

$$\begin{aligned}\bar{\mathfrak{f}}^{\text{qubit}} &= \frac{1}{4}\langle\Phi^+|\left(\mathbb{1}_4+\vec{t}\cdot(\mathbb{1}_2\otimes\vec{\sigma})+\sum_{\mu\nu}T_{\nu\mu}(\sigma^\mu)^T\otimes\sigma^\nu\right)|\Phi^+\rangle \\ &= \frac{1}{4}\left(1+\sum_{\mu\nu}T_{\nu\mu}\langle\Phi^+|\mathbb{1}\otimes\sigma^\mu\sigma^\nu|\Phi^+\rangle\right)=\frac{1+\operatorname{Tr}T}{4},\end{aligned} \tag{2.20}$$

and accordingly

$$\bar{\mathfrak{F}}^{\text{qubit}}=\frac{1}{2}+\frac{1}{6}\operatorname{Tr}T. \tag{2.21}$$

Moreover, thanks to (1.7),

$$\mathfrak{f}=\max_{R\in\mathrm{SO}(3)}\frac{1+\operatorname{Tr}[RT]}{4}.$$

Let thus $T=UDV^T$ be the singular value decomposition of T, where D is diagonal and $U,V\in\mathrm{O}(3)$. Thanks to the Cauchy-Schwartz inequality for the Hilbert-Schmidt inner product $(X,Y)=\operatorname{Tr}X^TY$ [1] it holds that $\operatorname{Tr}[RT]\leq\operatorname{Tr}D$, where the equality arise by setting $R=UV^T$. However, when $\det T<0$, the matrix UV^T does not belong to SO(3). In such a case we have to set $R=UV^T\operatorname{diag}(1,1,-1)$. In general [32], if τ_i are the singular values of T ordered in decreasing order

$$\mathfrak{f}=\frac{1+\tau_1+\tau_2+\operatorname{sign}(\det T)\tau_3}{4}, \tag{2.22}$$

$$\mathfrak{F}=\frac{1}{2}+\frac{1}{6}\left(\tau_1+\tau_2+\operatorname{sign}(\det T)\tau_3\right). \tag{2.23}$$

2.4.1 Minimum fidelity

The state dependent fidelity for the two qubit case is

$$\begin{aligned}\langle\psi|\mathcal{E}(|\psi\rangle\langle\psi|)|\psi\rangle &= \operatorname{Tr}\left[\frac{\mathbb{1}+\vec{r}\cdot\vec{\sigma}}{2}\mathcal{E}\left(\frac{\mathbb{1}+\vec{r}\cdot\vec{\sigma}}{2}\right)\right]=\frac{1}{2}\left(1+\vec{r}\cdot\operatorname{Tr}\left[\vec{\sigma}\,\mathcal{E}\left(\frac{\mathbb{1}+\vec{r}\cdot\vec{\sigma}}{2}\right)\right]\right) \\ &= \frac{1+\vec{r}\cdot T\vec{r}+\vec{r}\cdot\vec{t}}{2}.\end{aligned} \tag{2.24}$$

where we used (1.30) and (1.32). The minimization of the above equation in the general case is a difficult problem which can not be solved analytically [33]. However, when the channel is covariant under rotation around some axis, this minimization can be performed analytically. Indeed, let us consider the case in which the system is covariant with respect to rotations around the z axis (1.37) and set as usual $\vec{r}=(\sin\theta\cos\phi,\sin\theta\sin\phi,\cos\theta)$. Then, Eq. (2.24) takes the form

$$\langle\psi|\mathcal{E}(|\psi\rangle\langle\psi|)|\psi\rangle=\frac{(s_3-s_1)\cos^2\theta+t_3\cos\theta+s_1+1}{2},$$

which has a stationary point in $\cos\theta_{\text{s.p.}} = \frac{t_3}{2(s_1-s_3)}$. Then,

$$\mathfrak{F}^{\min} = \begin{cases} \frac{1+s_1}{2} - \frac{t_3^2}{8(s_3-s_1)} & \text{if } s_3 > s_1 + \frac{|t_3|}{2} \\ \frac{1+s_3-|t_3|}{2} & \text{otherwise,} \end{cases} \tag{2.25}$$

$$\mathfrak{F}^{\max} = \begin{cases} \frac{1+s_1}{2} + \frac{t_3^2}{8(s_1-s_3)} & \text{if } s_1 > s_3 + \frac{|t_3|}{2} \\ \frac{1+s_3+|t_3|}{2} & \text{otherwise.} \end{cases} \tag{2.26}$$

Hence, if $t_3 = 0$ the system possesses also invariance under the exchange $|0\rangle \longleftrightarrow |1\rangle$, as shown in (1.39), and the two computational states $|0\rangle$ and $|1\rangle$ are the best (worst) transmitted if $s_3 > s_1$ ($s_1 > s_3$).

2.4.2 Concurrence

The fully entangled fraction $\mathfrak{f} = \max_{\chi \text{ m.e.}} \langle\chi|\rho|\chi\rangle$, i.e. the maximum overlap of a state ρ with the maximally entangled states, is one of the most important quantities for checking the quality of state- and entanglement transmission, but is not a true measure of entanglement. Indeed, an entanglement measure $\mathfrak{E}$ has to satisfy the following requirements [34]

(i) $\mathfrak{E}(\rho) = 0$ if and only if the state is separable and $\mathfrak{E}(\rho) = 1$ for maximally entangled states (2.5).

(ii) $\mathfrak{E}$ must be an **entanglement monotone**: $\mathfrak{E}$ must be invariant under local unitary operations, i.e. $\mathfrak{E}(U\otimes U\rho U^\dagger\otimes U^\dagger) = \mathfrak{E}(\rho)$, and decrease, on average, under *LOCC*. This acronym stays for *local operations and classical communications* and includes all quantum operations, e.g. measurements, performed locally in each subsystem. The entanglement monotone is the key paradigm of any entanglement measure: *entanglement cannot be created or increased by local operations*, global operations are needed.

(iii) $\mathfrak{E}$ is convex, i.e. entanglement cannot be increased by mixing: $\mathfrak{E}\left(\sum_i p_i\rho_i\right) \leq \sum_i p_i \mathfrak{E}(\rho_i)$.

The fully entangled fraction does not satisfy the first condition, and is not an entanglement monotone [32]. Provided that a good entanglement measure $\mathfrak{E}$ is given, the quality of entanglement transmission, in the scheme depicted in Fig. 2.4, is measured by the *entanglement transmission ratio*

$$\mathfrak{R}_{\mathscr{E}} = \frac{\mathfrak{E}^{\text{out}}}{\mathfrak{E}^{\text{in}}} = \frac{\mathfrak{E}[\mathbb{1}\otimes\mathscr{E}(\rho_{A'A})]}{\mathfrak{E}(\rho_{A'A})} = \frac{\mathfrak{E}(\rho_{A'B})}{\mathfrak{E}(\rho_{A'A})}, \tag{2.27}$$

i.e. the ratio between the transmitted entanglement $\mathfrak{E}(\rho_{A'B})$ and the initial entanglement $\mathfrak{E}(\rho_{A'A})$ held by Alice. Clearly, $\mathfrak{R} \leq 1$ as $\mathfrak{E}$ is an entanglement monotone.

Finding a proper and general measure of entanglement is a subject of active research [8] and currently there is only one general measure of entanglement, the so-called **concurrence**, which holds only for the two qubits case. The physical meaning of this quantity is unclear, though it is related with the so-called entanglement of formation [35], which quantifies how many Bell states (1.13) are needed per copy of to prepare many copies of ρ using local operations and classical communication. The mathematical proof that the concurrence is an entanglement measure and that it provides a computable formula for the entanglement of formation is quite long [36, 37, 38]. Therefore, here we only state the definition without a proof.

The concurrence of a two-qubits state is

$$\mathfrak{C}(\rho) = \max\{0, \sqrt{\lambda_1} - \sqrt{\lambda_2} - \sqrt{\lambda_3} - \sqrt{\lambda_3}\}, \tag{2.28}$$

where λ_i are the decreasingly ordered eigenvalues of

$$R = \rho\,(\sigma^y \otimes \sigma^y)\,\rho^T\,(\sigma^y \otimes \sigma^y)\,, \tag{2.29}$$

and the transpose is performed in the standard basis $\{|00\rangle, |01\rangle, |10\rangle, |11\rangle\}$. This quantity has a simple analytical expression when ρ is block-diagonal [39], and thus the eigenvalues are simply those of the two block. Indeed, let

$$\rho = \begin{pmatrix} A & 0 & 0 & f \\ 0 & B & e & 0 \\ 0 & e^* & C & 0 \\ f^* & 0 & 0 & D \end{pmatrix}, \quad \Longrightarrow \quad R = \begin{pmatrix} AD+|f|^2 & 0 & 0 & 2Af \\ 0 & BC+|e|^2 & 2Be & 0 \\ 0 & 2Ce^* & BC+|e|^2 & 0 \\ 2Df^* & 0 & 0 & AD+|f|^2 \end{pmatrix}.$$

The eigenvalues of the R matrix are $(\sqrt{BC} \pm |e|)^2$ and $(\sqrt{AD} \pm |f|)^2$. As ρ is positive, $|f|^2 \leq AD$ and $|e|^2 \leq BC$ and hence the concurrence is given by

$$\mathfrak{C}(\rho) = 2\,\max\{0,\, |f| - \sqrt{BC},\, |e| - \sqrt{AD}\}. \tag{2.30}$$

Let us consider now the entanglement transmission, as in Fig. 2.4, and let $|\lambda\rangle_{A'A}$ be a two-qubit state initially held by Alice. As we are interested in the entanglement properties of this state we assume $|\lambda\rangle_{A'A}$ to be in the Schmidt form (1.11),

$$|\lambda\rangle_{A'A} = \sqrt{\lambda}\,|00\rangle_{A'A} + \sqrt{1-\lambda}\,|11\rangle_{A'A} = \Lambda \otimes \mathbb{1}|\Phi^+\rangle_{A'A}, \qquad \text{where } \Lambda = \sqrt{2}\begin{pmatrix} \sqrt{\lambda} & 0 \\ 0 & \sqrt{1-\lambda} \end{pmatrix}$$

as a generic state can be put in the Schmidt form by local unitary operations without thus changing the entanglement content of the state. This initial state has a concurrence that can be obtained straightforwardly: $\mathfrak{C}^{\text{in}} = 2\sqrt{\lambda(1-\lambda)}$. When the state of A is sent to Bob via a quantum channel $\mathscr{E}$ the resulting state is $\mathbb{1} \otimes \mathscr{E}(\Lambda \otimes \mathbb{1}|\Phi^+\rangle\langle\Phi^+|\Lambda \otimes \mathbb{1}) = \left(\Lambda \otimes \mathbb{1}\,\hat{\mathscr{E}}\,\Lambda \otimes \mathbb{1}\right)/2$,

where we have removed the indices of the Hilbert space for compactness. The concurrence of the transmitted state is obtaind thus by diagonalizing the matrix

$$R^{\text{out}} = \left(\Lambda\otimes\mathbb{1}\,\frac{\hat{\mathscr{E}}}{2}\,\Lambda\otimes\mathbb{1}\right)\sigma^y\otimes\sigma^y\left(\Lambda\otimes\mathbb{1}\,\frac{\hat{\mathscr{E}}^T}{2}\,\Lambda\otimes\mathbb{1}\right)\sigma^y\otimes\sigma^y.$$

As $\Lambda\sigma^y\Lambda\otimes\sigma^y = \mathfrak{C}^{\text{in}}\sigma^y\otimes\sigma^y$ it follows that

$$R^{\text{out}} = \left(\mathfrak{C}^{\text{in}}\right)^2\,\Lambda\otimes\mathbb{1}\left(\frac{\hat{\mathscr{E}}}{2}\,\sigma^y\otimes\sigma^y\,\frac{\hat{\mathscr{E}}^T}{2}\;\sigma^y\otimes\sigma^y\right)\Lambda^{-1}\otimes\mathbb{1}\,,$$

and since the eigenvalues of the matrices A and UAU^{-1} are the same, we have shown the important result [40]

$$\mathfrak{C}^{\text{out}} = \mathfrak{C}^{\text{in}}\,\mathfrak{C}\left(\frac{\hat{\mathscr{E}}}{2}\right) \equiv \mathfrak{C}^{\text{in}}\,\mathfrak{C}\left[(\mathbb{1}\otimes\mathscr{E})(|\Phi^+\rangle\langle\Phi^+|)\right]. \tag{2.31}$$

This means that, provided that Alice initially holds an entangled pair ($\mathfrak{C}^{\text{in}}\neq 0$), the entanglement transmission ratio (2.27) for the concurrence does not depend on the initial entangled state but depends only on the capability of the channel to send a maximally entangled pair. In other words, the entanglement transmission ratio is given by the concurrence of one half of the Choi matrix $\hat{\mathscr{E}}$ associated to a channel $\mathscr{E}$

$$\mathfrak{R}_{\mathscr{E}} = \frac{1}{2}\mathfrak{C}\left(\hat{\mathscr{E}}\right). \tag{2.32}$$

3

Quantum communication through spin chains dynamics

Quantum Computers, when realized, hold the promise of speeding up the solution of certain problems perceived as difficult on a classical computer [41, 20, 42, 1]. They also hold the promise of enabling controlled simulations of the behaviour of complex quantum systems [21, 1]. The typical quantum computer is regarded as a collection of quantum two state systems (or "qubits") on which arbitrary unitary operations can be performed. Different quantum registers, i.e. arrays of qubits, are connected to each other by quantum communication channels (which could effectively be physical shuttling of qubits [43, 44]). Most operations would take place between qubits of the same register through, say, a common bus mode, or direct interactions together with very fast qubit transfers within the register. Occasionally, quantum channels would be used to transfer qubits from one register to another, and thereby enable quantum gates between qubits of different registers.

Even if we are able to scale up quantum computers by some technology which does not require internal communication channels, such channels will still be necessary to hook up distinct quantum computers. For reasons of compactness, mobility and cost, we might just prefer to have small sized quantum computers. However one may need to tackle very complex problems for which the power of a single quantum computer will not suffice. It will then become very important to combine the processing powers of distinct quantum computers to obtain a computer with a greater processing power. Moreover, as the channel connects quantum computers, some encoding and decoding of quantum states should easily be possible inside the quantum computers. The transmitted state (after decoding, if applicable) should be transferable to a qubit or a group of qubits of the quantum computer that receives it.

The usual approach envisaged for connecting quantum computers and registers, as depicted in Fig. 3.1, is to first map the state to be transmitted from the qubits of one processor to a *flying* or *mobile* qubit. This flying qubit then traverses through a channel and reaches a second processor, where its state is mapped on to the qubits of that processor. However,

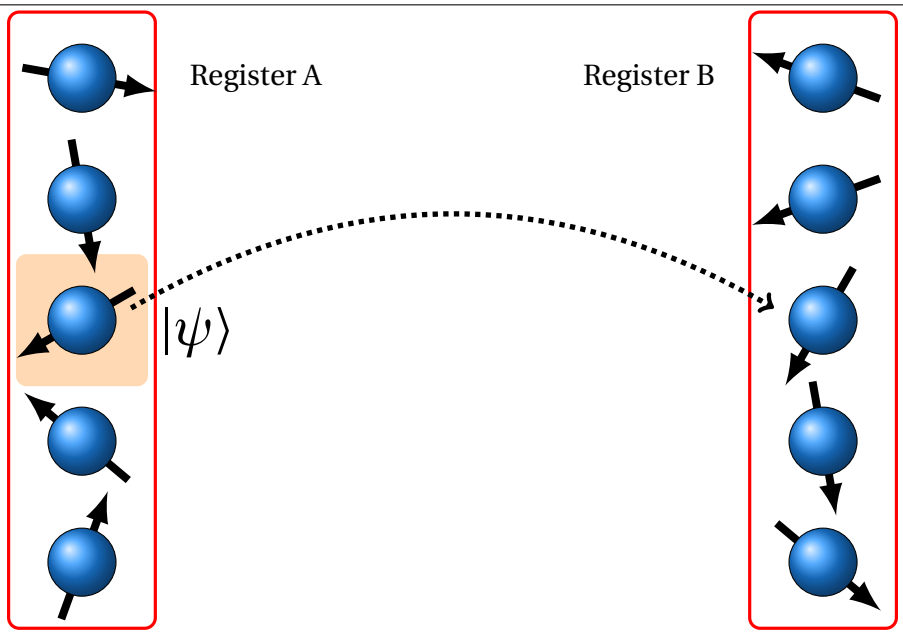

Figure 3.1 – Quantum state transmission between two distant quantum registers. The state of one qubit in the register A has to be transmitted to the a qubit of a distant register B.

depending on the physical nature of the qubits of the processors, this approach could involve either (a) interfacing between different physical systems such as stationary spins and photons [45] or stationary and mobile spins [46] or (b) physically moving a quantum system and subsequently bringing it to a halt elsewhere such as shuttling ions [43] or electrons [44]. All the above can be complicated in many respects. So one can ask the question: is it possible to transfer quantum information from place to place *using only stationary qubits*? The first idea that comes to mind is to have a chain of qubits as shown in Fig.3.2, and swap a quantum state perfectly in succession from one qubit to the next. A quantum state encoded on a qubit at one end of the line can be transported perfectly through a series of swaps to the qubit at the opposite end of the line. For example, in Fig.3.3, the strategy is to swap the state in the following order: $A \rightarrow 1, 1 \rightarrow 2, \ldots$ and so forth until the state reaches the qubit on the register B. This kind of data-bus, called a *swapping channel*, has been discussed, for example, in Ref.[47]. However, such a data-bus requires the ability to modulate the strength or nature of interactions between pairs of adjacent qubits (such as 1 and 2 or 3 and 4) in time. Typically, this would require control fields on the wire varying over the scale of the spacing between the qubits. If so much control is available on a chain of qubits, then why not use the chain as a quantum computer? It will then be a gross under-utilization to use it merely as a data-bus. Moreover, the requirement of so much control for the transfer of a quantum state naturally implies that such a protocol is also very susceptible to errors in these controls. For example, there are many pair-wise interactions to be switched on and off in succession for transmission of the state of qubit A to that of qubit B in Fig.3.3, and errors

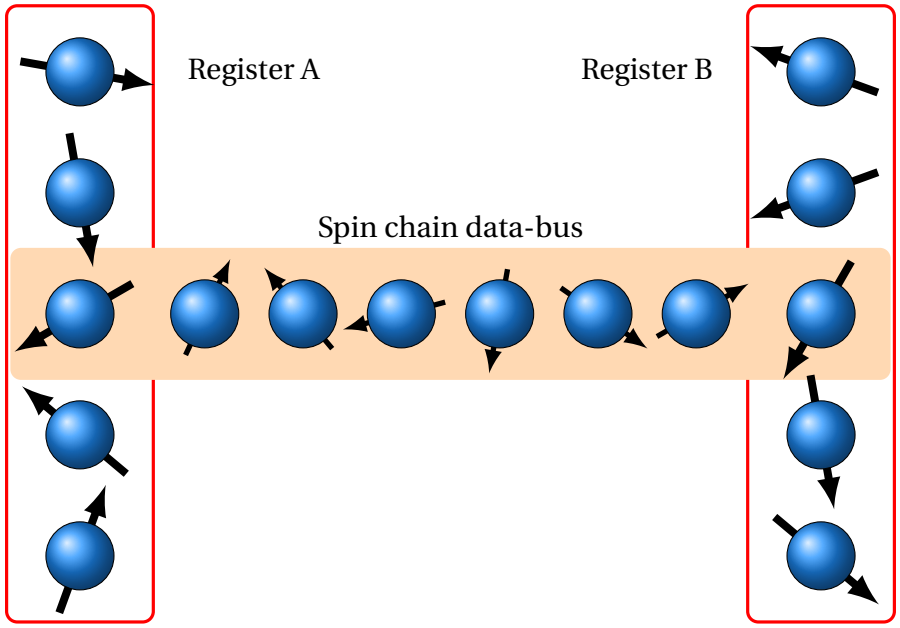

Figure 3.2 – This figure depicts the possibility of transporting quantum information from one quantum processor to another through a line of stationary qubits.

would accumulate in each of these steps. Thus the question arises as to whether we can utilize systems with much lower control for connecting quantum registers. For example, if the interactions between qubits in a chain are permanent and uncontrollable (always on and constant in strength), and we are not allowed to apply any control fields to the single qubits, could the chain still act as a quantum data-bus? The validity of the above possibility will enable us to use such a qubit chain as a data-bus in the true sense of the word. This is because in the normal everyday use of the word "data-bus", such as to denote a cable connecting two computers, we do not envisage controlling every individual part of the cable and we mostly let the information flow through it in its own natural way. A qubit chain in which inter-qubit interactions are permanent, is an example of a *spin-*$\frac{1}{2}$ *chain.*

In quantum mechanics, spins are systems endowed with tiny quantized magnetic moments. Bulk materials often have a large collection of spins permanently coupled to each other. The mutual interaction of these spins makes them prefer alignment or anti-alignment with respect to each other, resulting in diverse phenomena such as ferromagnetism and anti-ferromagnetism. A spin chain models a large class of such materials in which the spins are arranged in one dimension (as in Fig. 3.3) and permanently coupled to each other, usually with an interaction strength decreasing with distance. A common form of the Hamiltonian for the interaction between the nth and the mth spin is written as

$$H_{nm} = \sum_{\alpha} J^{\alpha}_{nm}\, S^{\alpha}_{n} S^{\alpha}_{m}, \tag{3.1}$$

where S^{x}_{n}, S^{y}_{n}, S^{z}_{n} are the operators for the components of the nth spin along the x, y and z

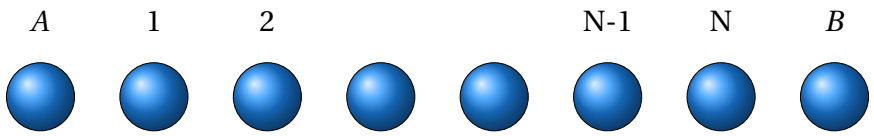

Figure 3.3 – The figure shows a spin chain: a system of spins perpetually coupled to each other with an interaction strength which generally decreases with distance.

directions, respectively. An interaction of the above form is termed as Heisenberg interaction, after his inventor, or *exchange interaction*, as it usually arises from the pure exchange of the electrons' states between neighbouring ions in a metal. Not only do examples of such systems exist in nature [48], but they can also be fabricated in systems of any kind of qubits [49, 50, 51], as qubits are isomorphic to spin-1/2 systems. If one indeed fabricates artificial systems, why would one fabricate a spin chain *i.e.,* a system with permanent couplings rather than a system where such couplings are also switchable? The obvious answer is that such a system should have a much lower complexity of fabrication because they do not require an attached mechanism (such as electrodes) varying over the scale of the separation of the qubits to modulate their interactions.

3.1 Quantum communication with unmodulated chain

Depending on the specific physical realization of the overall system, it might be easier to act on the structure of the Hamiltonian (3.1) ruling the channel dynamics or to prepare the channel in a specific initial state. For instance, spin chains in solid state physics represent a vast reservoir of possible quantum channels, characterized by the most diverse Hamiltonians, though with fixed parameters [52, 53]. On the other hand, initializing a spin chain embedded in a solid-state matrix might be a hard task. Quite complementary, recent progresses in optical lattices are making a real chance out of several theoretical proposals for realizing spin chains with cold atoms [54, 55, 56, 57, 58, 59], though with some restrictions on the structure of the effective spin Hamiltonians actually attainable [60]. Moreover, different initial states can be realized in an optical lattice [61, 62, 63], and new cooling techniques [64] also provide the possibility of reaching temperatures in which the magnetic phases are not disturbed by thermal fluctuations and so the real magnetic ground state of the system becomes reachable.

There are two essential features that characterize quantum channels made of interacting localized objects: their dynamics is dispersive, due to the non trivial structure of the many-body Hamiltonian that describes the channel, and it depends on the initial state of the channel itself. Dispersion is always detrimental to quantum information transmission, and designing a non dispersive channel requires a detailed engineering of the local cou-

plings [65, 66], which is hard to achieve practically. It is therefore relevant to understand up to what extent according to the type, the parameters and the length, a homogeneous non locally engineered spin chain is usable for quantum communication. In particular, and at variance with some recent works in which high quality transmission is achieved independently of the system initialization [66, 67, 68] we would like to see whether or not one can improve the quality of transmission by means of a specific initialization. Another issue which is less studied in the literature (unless very few cases for the case of engineered chains [69, 66]) is the effect of Hamiltonians which do not conserve the number of excitations. In fact, our investigation includes a wide class of Hamiltonians which change the number of excitations during the time evolution.

We consider quantum channels realized by finite spin-1/2 chains with homogeneous nearest-neighbor exchange interaction of the Heisenberg type, possibly in the presence of a uniform external magnetic field. As for the initial state of the channel we consider the ferromagnetic state, with all the spins parallel to each other, the Nèel state, where neighbouring spins are anti-parallel, the state built as a series of singlets, and the ground state. In order to study the interplay between the properties of the channel Hamiltonian and the structure of the initial state in determining the quality of the transmission processes, we specifically deal with different Hamiltonians and different initial states. We present a comprehensive study for the transmission quality over the whole phase diagram of the XY and XXZ Hamiltonians with the above initial states.

The quantum channel consists of $N+1$ spin-1/2 particles sitting at sites 1 to $N+1$ of a one dimensional lattice and interacting through the Hamiltonian

$$H_{\rm ch} = \sum_{n=1}^{N} \left(j_x S_n^x S_{n+1}^x + j_y S_n^y S_{n+1}^y + j_z S_n^z S_{n+1}^z \right) + h \sum_{n=1}^{N+1} S_n^z, \tag{3.2}$$

where j_α ($\alpha = x, y, z$) are the exchange integrals, h is an external uniform magnetic field applied in the z direction, and $S_n^\alpha = \sigma_n^\alpha/2$ are the operators of the spin sitting at site n. We prepare the channel in some initial pure state $|\psi_{\rm ch}\rangle$, which can be either entangled or separable with respect to single-spin states. An extra qubit which carries the information is labelled by A, sits on the site with index 0, and is initially set in some arbitrary state $\rho_A(0)$. The schematic picture of the system is shown in Fig. 3.3.

At $t = 0$ the interaction between the qubit and the channel is suddenly switched on, via

$$H_I = j_x S_0^x S_1^x + j_y S_0^y S_1^y + j_z S_0^z S_1^z + h S_0^z. \tag{3.3}$$

We use sudden switching for computational simplicity as the dynamics is not altered by a more realistic finite switching time, provided that it is small compared to the characteristic times set by the couplings of the Hamiltonian H_I, as shown in Fig. 7.3(b) that will be discussed in Chapter 7.

The total Hamiltonian $H = H_{\rm ch} + H_I$ rules the dynamics of the overall system, whose state at time t reads $\rho(t) = e^{-iHt}\,\rho(0)\,e^{iHt}$ where $\rho(0) = \rho_{_A}(0) \otimes |\psi_{\rm ch}\rangle\langle\psi_{\rm ch}|$ and $\hbar = 1$. The density matrix of the qubit B, standing on site $N+1$, namely $\rho_{_B}(t)$, is obtained by tracing out the qubits $A \equiv 0, 1, ..., N$ from $\rho(t)$. On the other hand, one can define the superoperator $\mathscr{E}_t$ which maps the initial density matrix of the qubit A, i.e. $\rho_{_A}(0)$, to the density matrix of qubit B at time t, i.e. $\rho_{_B}(t)$, according to

$$\rho_{_B}(t) = \mathscr{E}_t[\rho_{_A}(0)]. \tag{3.4}$$

This mapping defines a quantum channel (see Section 1.3). When the transmission of a generic pure quantum state $|\psi_{_A}\rangle$ is in order, according to the scheme depicted in Fig. 2.3, we set $\rho_{_A}(0) \equiv |\psi_{_A}\rangle\langle\psi_{_A}|$ and quantify the quality of transmission by the average transmission fidelity (2.9) between the initial state $|\psi_{_A}\rangle$ and the final state $\rho_{_B}(t)$. There are essentially two mechanisms that cause the average fidelity to deteriorate during a transmission process of the type we are describing: dispersion, which is a collective phenomenon due to the channel being an interacting many-body system, and local rotations. As a matter of fact, the average fidelity does not distinguish between bad transmission, i.e. dispersion of the state all over the chain, and good transmission with an extra rotation during the dynamics; on the other hand, the latter can be safely handled with an extra unitary operation on the qubit B, thus leaving dispersion as the *only* destructive effect in transmitting quantum states.

Assume a unitary operator R, independent of the state $|\psi_{_A}\rangle$, is found such that the average fidelity for the rotated final state $R^\dagger \rho_{_B}(t) R$ equals the maximum attainable value through the specific channel, then one could get a quantitative estimate of the dispersiveness of transmission, which might be a very useful tool for characterizing the channel's suitability for state-transfer processes. Aiming at such goal, we use the Optimal Average Fidelity (OAF) given by Eq. (2.13). The Optimal Average Fidelity, once computed via Eq. (2.23), gives a quantitative indication about how well a channel behaves, as far as pure-state transmission is concerned.

When entanglement transmission comes into play, mixed state transmission must be considered, and other strategies are necessary. Let us prepare the qubit A in a maximally entangled state with an isolated qubit A', see Fig. 2.4. The dynamical evolution causes the mixed state of qubit A to be transmitted to qubit B, thus generating entanglement between qubit A' and B. We can quantify the quality of such transmission by the entanglement transmission ratio (2.32), which is nothing but the concurrence $\mathfrak{C}(t)$ of the state of the qubits A' and B at time t, when initially A and A' are in the maximally entangled state $|\Phi^+\rangle = (|00\rangle + |11\rangle)/\sqrt{2}$.

Consistently with the transfer process, our scheme implies the existence of an arrival time when both the optimal average fidelity $\mathfrak{F}(t)$ and the concurrence $\mathfrak{C}(t)$ get their maximum value. In fact, due to the finite size of the chain, the information travels from A to B and viceversa multiple times, and the above quantities display multiple peaks during the

dynamics. Here we concentrate on the first peak, whose position defines the arrival time $t = t^*$, as in a practical situation waiting for longer times is unwise due to the effect of decoherence.

3.2 Quasi-free Hamiltonians

In this section we consider the XY model defined by Eq. (3.2) with

$$j_x = j(1+\gamma), \quad j_y = j(1-\gamma), \quad j_z = 0, \tag{3.5}$$

where, j is the exchange coupling and γ is the anisotropy parameter. This model is exactly solvable, as it turns into a free fermionic system, which makes valuable analytical results available. Despite being mapped into a non-interacting system, the model in the infinite N limit has a rich phase diagram featuring a quantum phase transition [70] at $h = 1$ and, as far as the entanglement properties are concerned, the divergence of the entanglement range when approaching the curve $h^2 + \gamma^2 = 1$, where pairwise entanglement vanishes [71, 72, 73]. Moreover, its peculiar non equilibrium dynamics has been studied in the framework of dynamical entanglement sharing [74], with periodic boundary conditions assumed.

Defining the operators $\sigma^{\pm} = \frac{\sigma^x \pm i\sigma^y}{2} \equiv S^x \pm iS^y$ which satisfy the algebra

$$[\sigma^z, \sigma^{\pm}] = \pm 2\sigma^{\pm}, \qquad [\sigma^+, \sigma^-] = \sigma^z, \tag{3.6}$$

$$\sigma^+ = (\sigma^-)^\dagger \qquad (\sigma^+)^2 = 0, \tag{3.7}$$

the total XY Hamiltonian reads

$$H^{\mathrm{XY}} = \frac{j}{2}\sum_{n=0}^{N}\left(\sigma_n^+\sigma_{n+1}^- + \gamma\sigma_n^+\sigma_{n+1}^+ + \mathrm{h.c.}\right) + \frac{h}{2}\sum_{n=0}^{N+1}\sigma_n^z. \tag{3.8}$$

This Hamiltonian can be mapped to a quadratic fermionic Hamiltonian through the Jordan-Wigner transformation

$$c_n = \prod_{m=0}^{n-1}\left(-\sigma_m^z\right)\sigma_n^-, \tag{3.9}$$

where the operators c_n are fermionic annihilation operators which satisfy the algebra (B.2), as it can be easily proven. By substituting the spin operators with their fermionic counterparts Eq. (3.8) takes the form

$$H = \sum_{n,m=0}^{N+1}\left[c_n^\dagger A_{nm} c_m + \frac{1}{2}(c_n^\dagger B_{nm} c_m^\dagger - c_n B_{nm} c_m)\right], \tag{3.10}$$

where, A is a symmetric matrix with elements $A_{nm} = \frac{j}{2}(\delta_{n,m+1} + \delta_{n,m-1}) + h\delta_{n,m}$ and B is an antisymmetric matrix with elements $B_{nm} = \frac{j\gamma}{2}(\delta_{n,m-1} - \delta_{n,m+1})$. This fermionic Hamiltonian can then be diagonalized with the procedure described in the appendix B. In the here

considered case of finite N and open boundary conditions the analytical expressions of the energies and of the diagonalizing matrices for finite γ and h are complicated [75], but they can be determined numerically as explained in section B.2.

The spin data-bus can be conveniently characterized in terms of its dynamical behaviour, which is investigated in the Heisenberg representation. The fermionic operators $c_n(t) = e^{+iHt} c_n e^{-iHt}$ read

$$c_n(t) = \sum_{m=0}^{N+1} U_{nm}(t) c_m + V_{nm}(t) c_m^\dagger, \tag{3.11}$$

where the dynamical matrices $U(t)$ and $V(t)$ are written in (B.18). The dynamics of the z-component of the spins follows as

$$\sigma_n^z(t) = 2\, c_n^\dagger(t) c_n(t) - 1\,, \tag{3.12}$$

while that of the other components is complicated by the Jordan-Wigner string of operators (3.9). However, the dynamics of the boundary spins, i.e. those in position 0 and $N+1$ is straightforward since

$$\sigma_0^- = c_0\,, \qquad \sigma_{N+1}^- = \Pi\, c_{N+1} = -c_{N+1}\,\Pi\,, \tag{3.13a}$$

$$\sigma_0^+ = c_0^\dagger\,, \qquad \sigma_{N+1}^+ = -\Pi\, c_{N+1}^\dagger = c_{N+1}^\dagger\,\Pi, \tag{3.13b}$$

being the parity operator $\Pi = \exp\left(i\pi \sum_{n=0}^{N+1} c_n^\dagger c_n\right) \equiv \prod_{n=0}^{N+1}\left(-\sigma_n^z\right)$ a constant of motion, as $[H,\Pi]=0$. Accordingly, the dynamics of the last spin is given by

$$\sigma_{N+1}^-(t) = \Pi \left[\sum_{n=0}^{N+1} U_{N+1n}(t)\, c_n + V_{N+1n}(t)\, c_n^\dagger\right]\,. \tag{3.14}$$

When the channel is initialized in some state with a given parity $(-1)^p$, that is $\prod_{k=1}^{N+1}\left(-\sigma_k^z\right)|\psi_{\rm ch}\rangle = (-1)^p|\psi_{\rm ch}\rangle$, the time evolution of the expectation values $\langle\sigma^\alpha(t)\rangle$ in the Heisenberg picture reads

$$\langle\sigma_{N+1}^-(t)\rangle = e^{i\phi_u}\, u(t)\langle\sigma_0^-\rangle + e^{-i\phi_v}\, v(t)\langle\sigma_0^+\rangle\,, \tag{3.15a}$$

$$\langle\sigma_{N+1}^+(t)\rangle = e^{-i\phi_u}\, u(t)\langle\sigma_0^+\rangle + e^{i\phi_v}\, v(t)\langle\sigma_0^-\rangle\,, \tag{3.15b}$$

$$\langle\sigma_{N+1}^z(t)\rangle = -1 + u^2(t)\left[1+\langle\sigma_0^z\rangle\right] + v^2(t)\left[1-\langle\sigma_0^z\rangle\right] + 2A(t)\,, \tag{3.15c}$$

where

$$u(t) = |U_{N+1,0}(t)|, \qquad \phi_u(t) = \arg[U_{N+1,0}(t)] + p\pi, \tag{3.16a}$$

$$v(t) = |V_{N+1,0}(t)|, \qquad \phi_v(t) = -\arg[V_{N+1,0}(t)] + (p+1)\pi, \tag{3.16b}$$

and $A(t)$ is the real function

$$A(t) = \sum_{j,l=1}^{N+1} U_{N+1j}^*(t) U_{N+1l}(t)\langle\psi_{\rm ch}|c_j^\dagger c_l|\psi_{\rm ch}\rangle + V_{N+1j}^*(t) V_{N+1l}(t)\langle\psi_{\rm ch}|c_j c_l^\dagger|\psi_{\rm ch}\rangle + \tag{3.17}$$

$$U_{N+1j}^*(t) V_{N+1l}(t)\langle\psi_{\rm ch}|c_j^\dagger c_l^\dagger|\psi_{\rm ch}\rangle + V_{N+1j}^*(t) U_{N+1l}(t)\langle\psi_{\rm ch}|c_j c_l|\psi_{\rm ch}\rangle.$$

We prepare the qubit 0 in the density matrix which is parametrized by the vector $\vec{a} = \langle \vec{\sigma}_0 \rangle$ of the Bloch sphere via $\rho_A(0) = (I + \vec{a}\cdot\vec{\sigma})/2$. Correspondingly, the time evolution of the state of the qubit $N+1$, $\rho_B(t) = (I + \vec{b}(t)\cdot\vec{\sigma})/2$, is parametrized by the vector $\vec{b}(t) = \langle \vec{\sigma}_{N+1}(t) \rangle$, which is determined from (3.15). The mapping (3.15) defines a quantum channel from A to B, i.e. from qubit 0 to qubit $N+1$, which is represented as in (1.32) by the affine transformation $\vec{b} = T\,\vec{a} + \vec{t}$ generated by the matrix T

$$\begin{aligned} T &= \begin{pmatrix} u\cos\phi_u + v\cos\phi_v & u\sin\phi_u + v\sin\phi_v & 0 \\ -u\sin\phi_u + v\sin\phi_v & u\cos\phi_u - v\cos\phi_v & 0 \\ 0 & 0 & u^2 - v^2 \end{pmatrix} \\ &= S_{\phi_v - \phi_u} \begin{pmatrix} u - v & 0 & 0 \\ 0 & u + v & 0 \\ 0 & 0 & u^2 - v^2 \end{pmatrix} S^T_{\phi_v + \phi_u}\,, \end{aligned} \tag{3.18a}$$

and the vector $\vec{t}$

$$\vec{t} = \begin{pmatrix} 0 \\ 0 \\ u^2 + v^2 - 1 + 2A \end{pmatrix}, \tag{3.18b}$$

where the rotation matrix is

$$S_{2\phi} = \begin{pmatrix} \sin\phi & \cos\phi & 0 \\ -\cos\phi & \sin\phi & 0 \\ 0 & 0 & 1 \end{pmatrix}.$$

Eqs. (3.18) show that the evolution in the xy-plane involves the two rotations $S_{\phi_v - \phi_u}$, $S^T_{\phi_v + \phi_u}$ as well as the shrinking towards the center of the Bloch sphere embodied in $u(t) - v(t)$ and $u(t) + v(t)$. Notice that none of the quantities involved depends on the initial state $|\psi_{\rm ch}\rangle$, thus relating the dynamics in the xy-plane only with the phase-diagram γ-h of the model. In fact, the only dependence on the initial state is in the quantity $A(t)$ which uniquely affects the shift in the z direction, and represents the interference of $|\psi_A\rangle$ with $|\psi_{\rm ch}\rangle$ during the evolution. Notice that in the XX case, where $V_{ij}(t) = 0$ (see appendix B.3.1), the dynamics (3.18) realizes a generalized amplitude damping channel [1].

The OAF, which measures the quality of state transmission, can be computed from the affine map (3.18) using the formula (2.23): the singular values of T are $|u(t) + v(t)|$, $|u(t) - v(t)|$, and $|u^2(t) - v^2(t)|$, from which

$$\mathfrak{F}^{\rm XY}(t) = \frac{1}{2} + \frac{1}{6}\left|u^2(t) - v^2(t)\right| + \frac{1}{3}\max\{u(t), v(t)\}. \tag{3.19}$$

This is a remarkable result as it is fully *independent* of the initial state of the channel (i.e. the parameter $A(t)$) and depends only on the Hamiltonian parameters. Moreover, the rotation

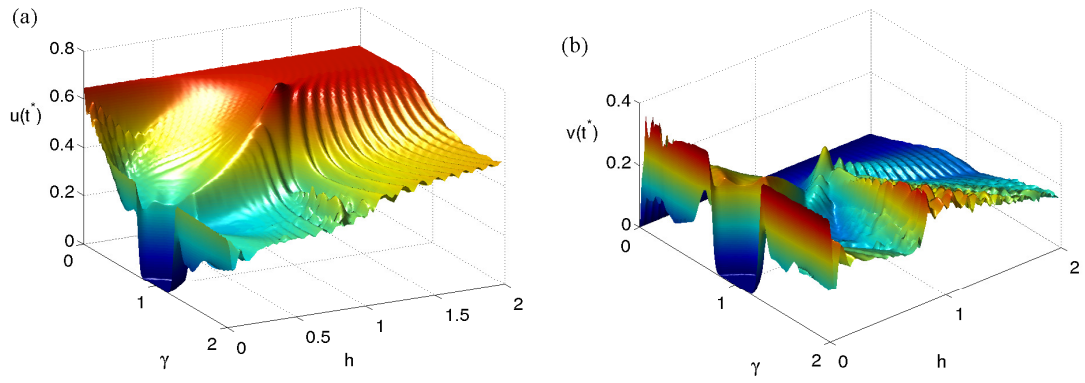

Figure 3.4 – (a) $u(t^*)$ vs. γ and h; the peak is located at $\gamma = 0.7$ and $h = 1$. (b) $v(t^*)$ vs. γ and h. Both figures are for $N = 50$.

that maximizes the average fidelity is found to be

$$R = \begin{cases} e^{-i\frac{\phi_u}{2}\sigma^z} & \text{for } u > v\ , \\ e^{i\frac{\pi}{2}\sigma^x} e^{i\frac{\phi_v}{2}\sigma^z} & \text{for } u < v\ . \end{cases} \tag{3.20}$$

In the XX case the effect of the magnetic field on the dynamics is only in the phase ϕ_u, as shown in appendix C.2, and therefore one can always choose the magnetic field such that at the arrival time t^*, i.e. when fidelity peaks, $\phi_u(t^*) = 0$. On the other hand, in the XY case the dynamical quantities depend on h in a complicated way, making the explicit rotation R, given in Eq. (3.20), necessary.

From Eq. (3.19) we see that the larger the difference between $u(t^*)$ and $v(t^*)$ the larger the OAF. In particular, as seen in Fig. 3.4, we find that, whenever the fidelity is large, we see that $u(t^*) \gg v(t^*)$, so the qualitative behavior of the OAF is the same of $u(t^*)$. Moreover, in the region $0 \leq \gamma \leq 1$ and $1 \leq h \leq 2$, $u(t^*)$ is large, taking its maximum value for $\gamma = 0$ (XX case) and for $\gamma = 0.7$ and $h = 1$. This means that in the γ-h phase-diagram the line $\gamma = 0$ and the point $(0.7, 1)$ set the best possible Hamiltonian parameters, corresponding to the least dispersive channel. This can be explained following the techniques of Chapters 5 and 6. Indeed, the distribution of excited states is centered around an energy $\approx h$. When $\gamma = 0$, or when $\gamma = \frac{1}{\sqrt{2}} \simeq 0.7$ and $h = 1$, this distribution is centered around the inflection point of the dispersion relation (6.4): the dynamics involves mostly the excitations with almost-linear dispersion relation and, accordingly, the transmission is more coherent.

The scaling of $\mathfrak{F}^{\mathrm{XY}}(t^*)$ for increasing length N is shown in Fig. 3.5 where it is clear that for the best parameters ($\gamma = 0$, $h = 0$ and $\gamma = 0.7$, $h = 1$) the OAF decreases very slowly, and it is larger than the classical value (2.17), i.e. $2/3$, even for chains up to $N = 240$. This can be proved in the XX case thanks to the analytical results of appendix C.2. In fact, using

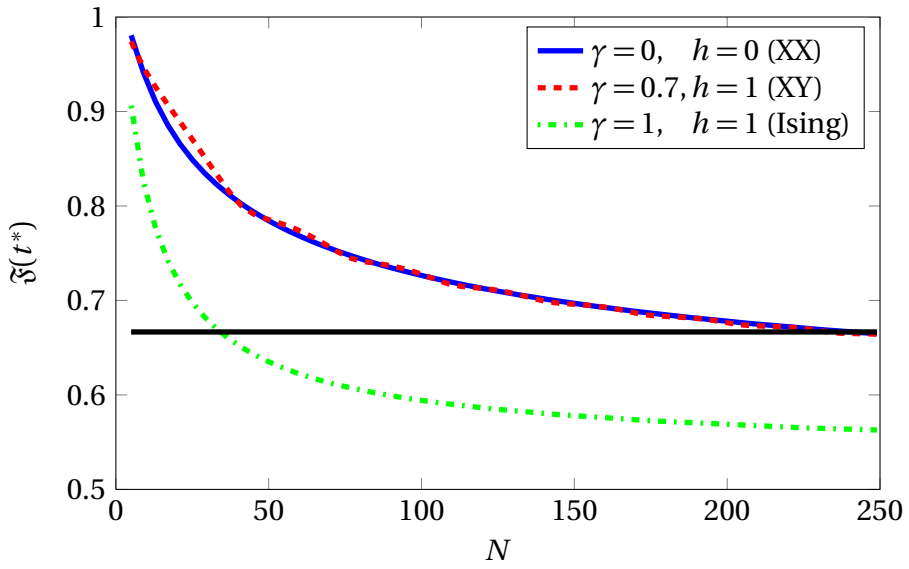

Figure 3.5 – Scaling of the OAF at the arrival time t^* versus length N, for different parameters of the Hamiltonian.

Eq. (C.32), we can show that the solution of equation $\mathfrak{F}^{\mathrm{XY}}(t^*) = 2/3$ is $N = 240$, in excellent agreement with Fig. 3.5. The weak dependence of $\mathfrak{F}^{\mathrm{XY}}(t^*)$ on N for the best parameters strengthens the statement that these indeed define the least dispersive channel, no matter the length. Conversely, for non optimal parameters (for example $\gamma = 1$, $h = 1$) the OAF decreases quickly and becomes lower than the classical threshold value 2/3 for chains longer than $N = 32$.

Let us now consider the entanglement transmission. The Choi matrix associated with the channel is derived from the affine map (3.18) using (1.31). By explicit calculation the Choi matrix is

$$\begin{pmatrix} u^2(t)+A(t) & 0 & 0 & u(t)e^{i\phi_u(t)} \\ 0 & 1-u^2(t)-A(t) & v(t)e^{i\phi_v(t)} & 0 \\ 0 & v(t)e^{-i\phi_v(t)} & v^2(t)+A(t) & 0 \\ u(t)e^{-i\phi_u(t)} & 0 & 0 & 1-v^2(t)-A(t) \end{pmatrix}. \tag{3.21}$$

The quality of entanglement transmission, as measured by the entanglement ratio according to (2.32), is thus given by one half of the concurrence of (3.21), which being in bloch diagonal form, is given by (2.30), i.e.

$$\mathfrak{C}(t) = \max\{0,\ \hat{C}(u(t), v(t)),\ \hat{C}(v(t), u(t))\} \tag{3.22}$$

where,

$$\hat{C}(x,y) = x - \sqrt{(y^2+A(t))(1-x^2-A(t))}.$$

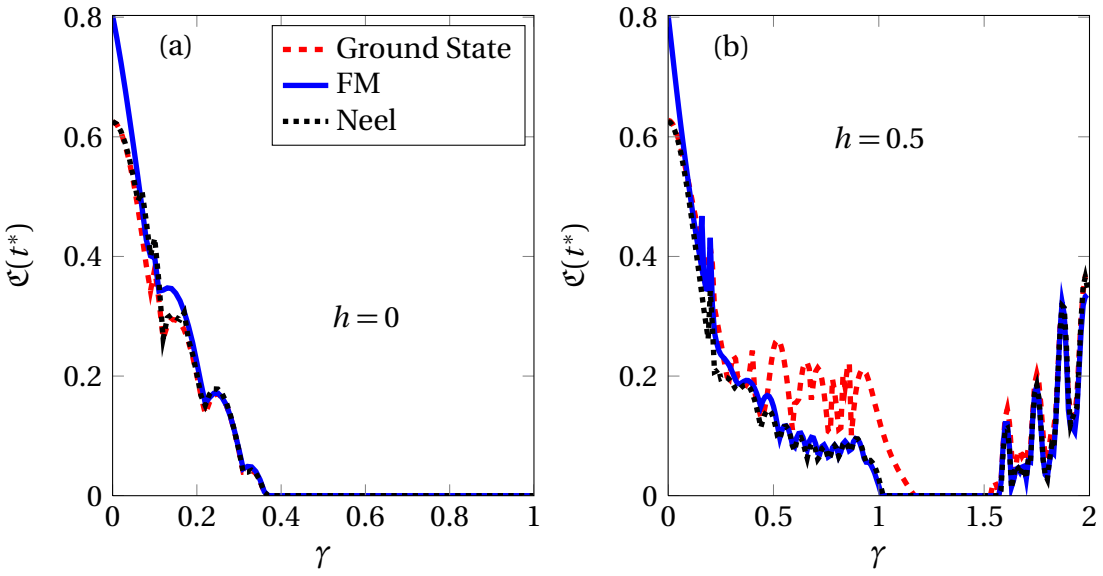

Figure 3.6 – Entanglement versus γ in a chain of length $N=20$ for different initial states while the magnetic field takes the values: (a) $h=0$ and (b) $h=0.5j$.

One can see that, at variance with the OAF, the entanglement transmission depends on the initial state as it is a function of $A(t)$; this is due to the fact that during the dynamics the initial state of qubits A and A' interferes with the initial state of the chain and deteriorates the quality of the transmission.

In the following, we investigate different initial states of the channel in order to find out to which state a better quality transmission might correspond. In particular, we will refer to two fully separable states, namely the ferromagnetic state, with all the spins aligned along the z direction, e.g. $|0,0,...,0\rangle$, and the Nèel state, with neighbouring spins antiparallel to each other, e.g. $|0,1,0,1,...,0,1\rangle$. Moreover, we will also study two different entangled initial states, namely that defined by a series of singlet states, and the ground state of the channel Hamiltonian.

Let us first consider the XX ($\gamma=0$) model, so as to exploit the analytical expressions available (see appendix C). We can prove that the concurrence achieves its maximum value, i.e. $u(t)$, when $|\psi_{\rm ch}\rangle$ is initialized in a ferromagnetic state. In fact in this case, since $V_{ij}(t)\equiv 0$, it is

$$A(t)=\sum_{j,l=1}^{N+1} U^*_{N+1j}(t)U_{N+1l}(t)\langle\psi_{\rm ch}|c_j^\dagger c_l|\psi_{\rm ch}\rangle. \tag{3.23}$$

which is equal to 0 (1) when $|\psi_{\rm ch}\rangle$ consists in a tensor product of down (up) spins. For other initial states, in which $0<A(t)<1$, the concurrence is lower than $u(t)$. In particular, when $h=0$ and the channel is initialized in its ground state, the system is invariant for exchange of up and down spins, and thanks to (1.39), $2A(t)=1-u^2(t)-v^2(t)$. Accordingly, $\mathfrak{C}(t)=1/2\max\{0,2u(t)-1+u^2(t)\}$, which is evidently lower than $u(t)$, i.e. of the concurrence

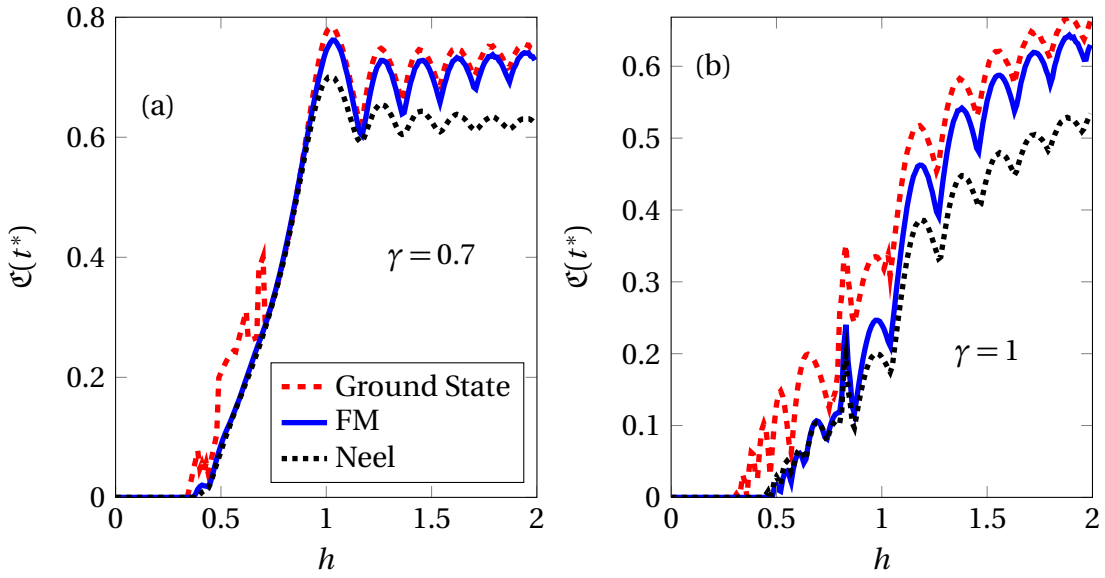

Figure 3.7 – Entanglement versus h in a chain of length $N = 20$ for different initial states while the anisotropy parameter takes: (a) $\gamma = 0.7$ and (b) $\gamma = 1$.

when the channel is initialized in a tensor product of up or down states.

In Fig. 3.6(a) we plot the concurrence as a function of the anisotropy γ when $h = 0$ for different initial states. As the figure clearly shows, increasing the anisotropy decreases the quality of transmission.

In the limit of $\gamma \to 1$ the Hamiltonian H_{ch} becomes Ising-like which has a poor transmitting quality. As one can see, in Fig. 3.6(a), in the absence of magnetic field the ferromagnetic initial state always gives the highest entanglement; in particular, when the anisotropy γ is small the difference between this initialization and the others is evident.

One may improve the poor ability of entanglement transmission in highly anisotropic chains (large γ) by switching on the magnetic field. This is clearly seen in Fig. 3.6(b) where we set $h = 0.5$. Furthermore, we notice that the field does not essentially affect the transmission for small γ and, quite surprisingly, makes the ground state the best possible initial state for strongly anisotropic chains.

In order to better understand the role of the magnetic field we consider the transmitted entanglement for different initial states as a function of h. In Fig. 3.7 we plot the concurrence for $\gamma = 0.7$ and $\gamma = 1$ and see that there exists a value of the field, slightly depending on the initial state of the chain, above which the transmission becomes possible, even for large anisotropies.

The existence of an exact solution for the XY Hamiltonian allows us to study the quality of transmission for very long chains. In Fig. 3.8 we plot $\mathfrak{C}(t^*)$ as a function of N for different initial states, which evidently differentiate the entanglement transmission through long

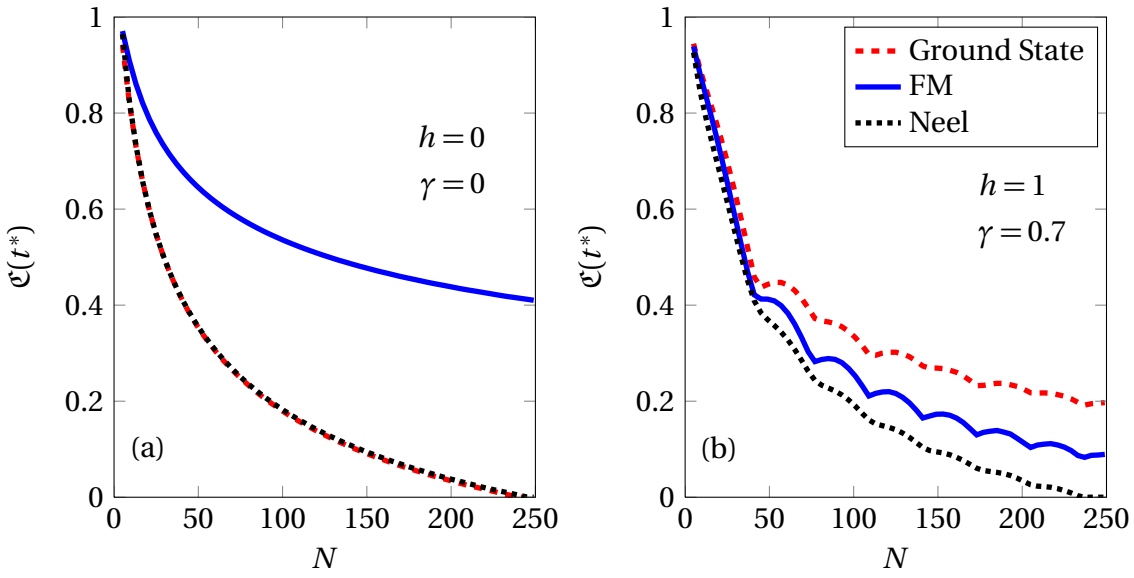

Figure 3.8 – Scaling of the obtained entanglement at the arrival time versus length N for different initial states: (a) isotropic XX Hamiltonian ($\gamma = 0$ and $h = 0$); (b) anisotropic XY Hamiltonian ($\gamma = 0.7$ and $h = 1$).

chains. In particular, in Fig. 3.8(a), we see that in the XX chain the ferromagnetic initial state not only gives the highest concurrence amongst the different initializations but it also provides the best scaling with N. In Fig. 3.8(b) we plot $\mathfrak{C}(t^*)$ as a function of N for $\gamma = 0.7$ and $h = 1$, i.e. for the parameters that define the less dispersive XY-like channel (see Fig. 3.4). At variance with the state transmission case, where for such parameters the transmission quality is as high as in the XX case (see Fig. 3.5), during entanglement transmission through an XY chain we cannot avoid the interference $A(t)$ by properly choosing the initial state of the chain, and a strong dependence on the length N appears; Fig. 3.8(b) in fact shows that this gives rise to a significant lowering of the transferred concurrence.

Results for the Nèel state and the series of singlets are found to be very close to each other (therefore only those for the former state are plotted): This shows that the inherent entanglement in the initial state has a very little effect when a state is attached at one end of a spin chain.

3.3 Interacting Systems

After studying the effect of the initial state on the transmission quality in free fermionic systems, interacting models must also be considered, not only because they represent the large majority of many-body systems, but also because they are usually characterized by an extremely rich, though often difficult to be physically deciphered, phenomenology.

For simulating interacting systems we cannot use the theory described in Section 3.2; we have to consider the full $2^{N+2} \times 2^{N+2}$ sparse Hamiltonian matrix given by (3.2) and (3.3). However, though the ground state can be efficiently computed using well-established techniques [76], the full diagonalization of large (sparse) matrices, required for the dynamics, can be effectively obtained only for very small N. Nevertheless, the dynamics can be efficiently calculated using the Chebyshev expansion technique [77, 78, 79].

Let $\tilde{H} = (H - b\mathbb{1})/a$ be the rescaled Hamiltonian, where $a = (E^{\max} - E^{\min})/(2-\epsilon)$ and $b = (E^{\max} + E^{\min})/2$, being $E^{\max}$ ($E^{\min}$) the largest (smallest) eigenvalue of H. Here we introduced the small parameter ϵ for making the eigenvalues of $\tilde{H}$ well inside the range $[-1, 1]$; in practice we have used $\epsilon = 0.01$. The evolution operator can be expanded as [78]

$$U(t) = e^{-itH} = e^{-it(a\tilde{H}+b)} = e^{-ibt}\left[\mathscr{J}_0(at) + 2\sum_{k=1}^{\infty}(-i)^k \mathscr{J}_k(at)\mathbb{T}_k(\tilde{H})\right], \tag{3.24}$$

where the $\mathscr{J}_k$'s are the Bessel functions and the $\mathbb{T}_k$'s are the Chebyshev polynomials of the first kind [80]. The importance of the Chebyshev expansion stems from the fact that the Bessel function $\mathscr{J}_k(x)$ starts to differ from zero only after $x \approx k$. In particular, as $\mathscr{J}_{x+\xi(x/2)^{\frac{1}{3}}}(x) \simeq (2/x)^{\frac{1}{3}}\mathrm{Ai}(\xi)$, for large x [80], being Ai the Airy function, one can prove that $\mathscr{J}_{x+8x^{\frac{1}{3}}}(x) \approx 10^{-10}/x^{\frac{1}{3}}$. When we are interested on time scales $t < t^{\max}$ we can safely cut (3.24) up to some order $\chi = [at^{\max} + 8(at^{\max})^{\frac{1}{3}}]$, with negligible errors. Here we used $\chi = [1.5at^{\max}]$ for safety.

For calculating the evolution of the initial state $|\psi_0\rangle$ one has to accumulate the (sparse) vectors $|v_k\rangle = (-i)^k\mathbb{T}_k(\tilde{H})|\psi_0\rangle$ for k up to χ. Thanks to the recurrence relations of the Chebyshev polynomials, the vectors $|v_k\rangle$ can be obtained [78] via

$$|v_{k+1}\rangle = -2i\tilde{H}|v_k\rangle + |v_{k-1}\rangle\,,$$

where $|v_0\rangle = |\psi_0\rangle$ and $|v_1\rangle = -i\tilde{H}|v_0\rangle$. The evolved state is thus

$$|\psi(t)\rangle = e^{-ibt}\left[\mathscr{J}_0(at)|v_0\rangle + 2\sum_{k=1}^{\chi}\mathscr{J}_k(at)|v_k\rangle\right]. \tag{3.25}$$

The Choi matrix of the quantum channel is calculated thanks to the explicit definition $\hat{\mathscr{E}}(t) = \mathrm{Tr}_{0\cdots N}\left[\mathbb{1}\otimes U(t)|\Phi^+\rangle\langle\Phi^+|\otimes|\psi_{\mathrm{ch}}\rangle\langle\psi_{\mathrm{ch}}|\mathbb{1}\otimes U^\dagger(t)\right]$ and all the figures of merit are evaluated.

3.3.1 XXZ Hamiltonian

Amongst the interacting Hamiltonians the XXZ spin model here discussed, and defined by Eq. (3.2) with

$$j_x = j_y = j\,, \qquad\qquad j_z = j\Delta\,, \tag{3.26}$$

is known to describe many real systems and compounds, thus playing an essential role, especially in one dimensional physics [53, 60].

This model has a very rich phase diagram: $\Delta < -1$ is the ferromagnetic phase with a simple separable ground state with all spins aligned in the same direction. For $-1 < \Delta \leq 1$ the Hamiltonian is gapless and the region is called XY phase. $\Delta > 1$ defines the *Nèel phase*, where the spectrum is gapped and a finite staggered magnetization arises. In the Ising limit $\Delta \gg 1$ the ground state is the Nèel state.

Dynamical transmission in interacting fermionic models is very different from the free fermionic case, as it results from a complex combination of many different effects amongst which the scattering between interacting excitations and the existence of localized states. As a matter of fact, there is no transmission process which is generally independent of the initial state of the channel. In particular we find that, depending on the value of Δ, the best transmission processes correspond to different initializations of the chain.

Let us first discuss the state transfer process. In Fig. 3.9(a) we see that even the OAF strongly depends on $|\psi_{\rm ch}\rangle$: for $\Delta > 0$ the ground state clearly gives the best possible initialization, while for $\Delta < 0$ the phenomenology is much more complicated. When considering the entanglement transmission in Fig. 3.9(b) the situation is somehow reversed, with a specific state, namely the ferromagnetic one, granting the best possible initialization for $\Delta < 0$, and a more complex scenario for $\Delta > 0$.

The general phase diagram in Fig. 3.9 embodies the complex balance between the effect of interference, which can be varied by acting on the initial state of the chain, and the dispersiveness of the channel which depends on Δ. As we already noted, in the XXZ case also the OAF is affected by interference, and the overlap of $\mathfrak{F}(t^*)$ observed in Fig. 3.9(a) in the $\Delta = 0$ point is due to its corresponding to a non-interacting model, for which, as proved in section 3.2, the OAF does not depend on the initial state. On the other hand, there is no Δ value where the entanglement transmission is independent of the destructive effects of interference. Therefore, the only mechanism for removing such effect is that of choosing a ferromagnetic initial state, whose dynamics can be resolved in the single particle sector [81] where interference does not occur. The absence of interference is the reason why for $\Delta = 0$ the $\mathfrak{C}(t^*)$ obtained with the ferromagnetic initial state is by far larger than the others. Finally, in Figs. 3.9(a) and (b) we see that, given the initial state, $\mathfrak{F}(t^*) - 2/3$ and $\mathfrak{C}(t^*)$ have a similar behaviour as a function of Δ, with a shift in $\mathfrak{C}(t^*)$ for the FM initial state, consistent with the exact analysis given above for the XX case.

Indications about the effects of dispersiveness of the channel on the transmission processes can also be extracted: the ground state is seen to minimize such effects for whatever Δ, though this implies a better entanglement transmission only for $\Delta > 0.5$ where interference probably plays a minor role leaving dispersion as the main destructive effect.

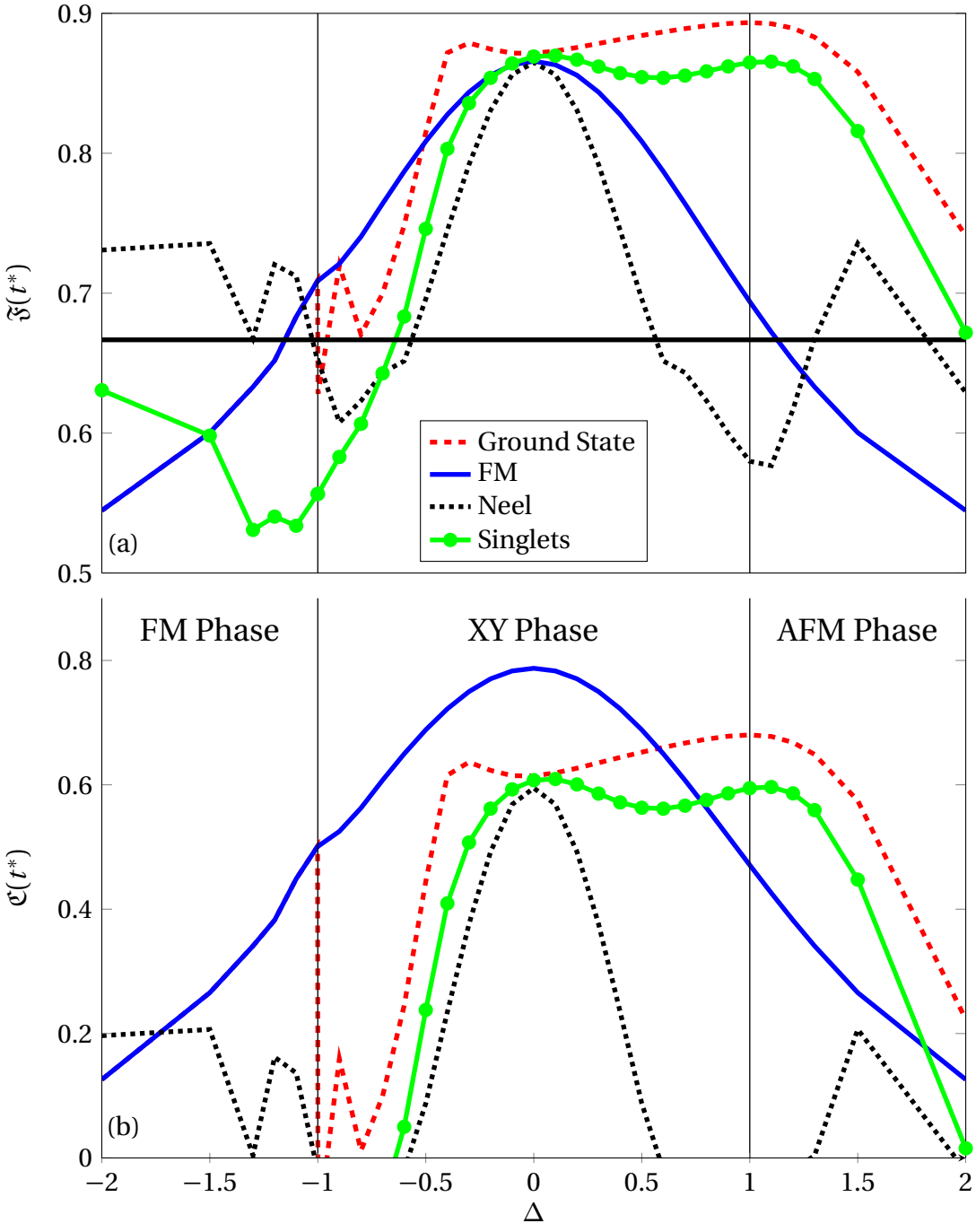

Figure 3.9 – Transferring properties of a XXZ chain with the length of $N = 20$ in its whole phase diagram for different initial states: (a) optimized average fidelity at the arrival time t^* (the black line indicates the classically obtained fidelity 2/3); (b) obtainable entanglement at the arrival time t^*.

3.4 Concluding remarks

In [82] we have studied the quality of state and entanglement transmission through quantum channels described by spin chains varying both the Hamiltonian parameters and the initial state of the channel. We have considered a vast class of Hamiltonians, including interacting and non-interacting fermionic systems, which contains some of the most relevant experimental realizations of one dimensional many-body systems, both in the framework of solid state physics and in the realm of cold atoms in optical lattices.

We find that if a free-fermionic model is available and an XY-like spin Hamiltonian can be effectively realized, then the best possible tuning of the parameters is that corresponding to the XX model with a ferromagnetic initial state, both for state and entanglement transfer, whose quality stays surprisingly high even for chains as long as $N \simeq 240$. In the anisotropic case, a state transfer of the same quality as that attained at $\gamma = 0$, is obtained for $\gamma = 0.7$ and $h = 1$: referring to the framework developed in Ref. [68] and analyzed in chapter 5, we infer that the relevant excitations lie in the linear zone of the dispersion relation and the resulting dynamics is essentially dispersionless. Moreover, good results for both state and entanglement transmission are found in a wide range of the parameters γ and h, providing the channel is initialized in its ground state. When an interacting XXZ model with a specific Δ is at hand, one has to choose whether to optimize the state or the entanglement transmission, since these goals are obtained with different initial states. In fact, we find that the optimal average fidelity is more sensitive to the dispersiveness of the channel, while the entanglement transmission is more sensitive to the interference with the initial state of the chain. As a matter of fact the former gets its maximum in the antiferromagnetic isotropic ($\Delta = 1$) channel initialized in its ground state, while the latter is maximized by an XX ($\Delta = 0$) channel initialized in a ferromagnetic state.

Our analysis shows that the fidelity and the entanglement do not necessarily quantify the quality of quantum communication in the same way. Namely, highest entanglement transfer can occur along a spin chain which is different from that giving the highest average fidelity. In fact, to the best of our knowledge, these results are the first example in which state and entanglement transmission show different features due to the different role played in such processes by dispersion, essentially set by the parameters of the Hamiltonian, and interference, which explicitly depends on the initial state of the channel. However, when we have higher entanglement one can always purify/distill entanglement using local operations [83] and subsequently use it for teleportation and eventually end up with a higher fidelity.

4

Routes to perfection and near perfection

The protocol for state transfer described in the previous section has the advantage of being the simplest experimental setup, as no dynamical control, no encoding, and no fine-design of interactions is required. It might be the best procedure, thanks to its simplicity, for early testing the transport properties of solid-state implementations of spin data-bus, for checking the quality of a qubit array and for studying the quantum response to a "quantum impulse", which are all important aims. However, once the transport properties of spin-chains are investigated, in order to really use them for connecting two distant registers in a quantum computer, which is by far the main motivation, only perfect or near to perfect state transfer is relevant. For example, the realization of a quantum gate between qubits in two separate registers, as in Fig. (2.1), requires to perfectly transfer the state of a qubit from the first register to the second one, do a gate between that qubit and a qubit of the second register, and then perfectly transfer its state back to the first register. How to obtain such a perfect communication bus is the problem to which many authors have proposed different solutions, some based on the idea of engineering the bus itself by the specific design of its internal interactions, others on that of intervening on the initialization process, by preparing the bus in a configuration found to serve the purpose, and still others using local or global dynamical control on the chain. In each case, a severe external action on the physical system is required. Another approach considers a uniform spin chain data-bus weakly coupled to the external qubits, where both the fidelity of state and entanglement transmission can be made arbitrarily high, provided that the interaction between the bus and the qubits is arbitrarily small. This approach has both the advantage of being experimentally feasible and of having a theoretical near to perfect state transfer. However, due to the weak couplings involved, the transmission times are very long, and the overall system could suffer from decoherence in such a long time.

In this section we first review some of these proposals which have most inspired our research, and finally we introduce our idea for inducing a coherent ballistic transmission, that will be further analysed an applied in detail in the next chapters. The main guideline is the fact that excitations characterized by a linear dispersion relation are substantially transmit-

ted coherently along a chain. We develop a general procedure for stirring up the coherent excitations in quadratic (quasi-free) models, permitting the design of a fast transmission bus without requiring engineering, nor pulse-shaping.

4.1 Perfect mirroring

The idea of perfect mirroring is to consider statically interacting qubits, with engineered interactions between the neighbouring sites. With *ad-hoc* constructions, engineered chains are suitable not only for transmitting states between the ends of the chain, but also for transferring whatever state (both pure and mixed) in position x to the position $N-x+1$, being N the length of the chain. This method has been introduced in [84] for a single excitation and then extended in [85] to multiple excitations. We give an overview of the main ideas using an engineered spin-1/2 model. For a more rigorous treatment, being a mathematical subject, there is a detailed review [86].

Let's consider an XX model with arbitrary (different) interactions between nearest neighbours

$$H=\frac{1}{2}\sum_{n=1}^{N-1} j_n\left(\sigma_n^x\sigma_{n+1}^x+\sigma_n^y\sigma_{n+1}^y\right)+\frac{1}{2}\sum_{n=1}^{N} h_n\,\sigma_n^z\,. \tag{4.1}$$

This Hamiltonian is solved again by mapping (4.1) into a quasi-free fermionic model, $H=\sum_{nm}A_{nm}\,c_n^\dagger c_m$ as in section 3.2 where

$$A=\begin{pmatrix} h_1 & j_1 & & & & & \\ j_1 & h_2 & j_2 & & & & \\ & j_2 & h_3 & j_3 & & & \\ & & & \ddots & & & \\ & & & j_{N-2} & h_{N-1} & j_{N-1} \\ & & & & j_{N-1} & h_N \end{pmatrix}. \tag{4.2}$$

Being isotropic in the x-y plane the matrix B (see Section 3.2) is null, and accordingly the time evolution is given by (B.22). The Hilbert space has a natural Fock space structure, thanks to the Jordan-Wigner mapping (3.9), and an arbitrary initial state of the chain can be written as

$$|\psi\rangle=\sum_{\{n\}}\psi(n_1,n_2,\ldots,n_N)(c_1^\dagger)^{n_1}(c_2^\dagger)^{n_2}\cdots(c_N^\dagger)^{n_N}|0\rangle\,, \tag{4.3}$$

where $|0\rangle$ is the vacuum of the Fermi operators. The perfect mirroring occurs if there exist a transmission time t^* such that the state in position n is transported to the position $N-n+1$,

i.e.

$$\begin{aligned}|\psi(t^*)\rangle &= \sum_{\{n\}}\sum_{\{i_n\}}\psi(n_1,n_2,\dots,n_N)\,(U_{1,i_1}(t^*)c_{i_1}^\dagger)^{n_1}(U_{2,i_2}(t^*)c_{i_2}^\dagger)^{n_2}\cdots(U_{N,i_N}(t^*)c_{i_N}^\dagger)^{n_N}|0\rangle \\ &= \sum_{\{n\}}\psi(n_1,n_2,\dots,n_N)\,(c_N^\dagger)^{n_1}(c_{N-1}^\dagger)^{n_2}\cdots(c_1^\dagger)^{n_N}|0\rangle\,, \\ &= \sum_{\{n\}}(-1)^{\frac{\tilde{n}(\tilde{n}-1)}{2}}\psi(n_N,n_{N-1},\dots,n_1)\,(c_1^\dagger)^{n_1}(c_2^\dagger)^{n_2}\cdots(c_N^\dagger)^{n_N}|0\rangle\,, \end{aligned} \tag{4.4}$$

where $\tilde{n}=\sum_i n_i$ and $(-1)^{\frac{\tilde{n}(\tilde{n}-1)}{2}}$ is an overall phase in each sector with constant number of fermions. This happens when at the transmission time t^*

$$U(t^*)\propto X\,, \qquad\qquad X_{nm}\equiv\delta_{n,N-m+1}\,, \tag{4.5}$$

being X the reflection operator. As $U(t)=O^T e^{-iEt}O$, where $A=O^T E O$ is the spectral decomposition of A, Eq. (4.5) means that $OXO^T\propto e^{-iEt^*}$ for some t^*. Accordingly X has to be diagonal in the same basis of the matrix A and thus

$$[A,X]=0\,. \tag{4.6}$$

The above condition means that A has to be mirror-symmetric, i.e. symmetric with respect to the "anti-diagonal", a property called *persymmetry* in the mathematical literature [87]: $j_n=j_{N-n}$ and $h_n=h_{N-n+1}$. Furthermore, Eq. (4.5) forces the existence of a time t^* such that $e^{-iE_kt^*}$ is proportional to the eigenvalues of X. Accordingly, by properly choosing the order of the eigenvalues $\{E_k\}$

$$e^{-iE_kt^*}=e^{i\alpha}(\text{-}1)^k\,, \tag{4.7}$$

with some unessential α. When the matrix A is persymmetric and the condition (4.7) holds then perfect transmission is obtained between whatever sites which are at the same distance from the opposite boundaries. Eq. (4.7) can be solved numerically using the inverse eigenvalue techniques, i.e. algorithms giving an Hamiltonian with the required spectrum [88]. An analytic solution has been found in [85]: indeed by setting $h_n=0$ and $j_n=\sqrt{n(N-n)}$, the condition (4.7) is satisfied and the eigenvectors are written in terms of known special polynomials.

This approach, despite giving perfect state transmission, is complicated in an experimental perspective, as an experimentalist should be able to perform a fine tuning of the interactions according to the law $j_n=\sqrt{n(N-n)}$, *a fortiori*, as the quality deteriorates in the presence of static noise [89]. Moreover, the dependence on N of the coupling strengths avoids scalability: when the transmission distances are varied, all the nearest-neighbour interactions has to be changed as well. Nonetheless, the condition (4.7) is one of the main building blocks of our scheme. Indeed, the condition (4.7) is automatically satisfied in a quasi-uniform system at the ballistc time $t^*\approx(N+1)/v$ if the relevant excitations for the dynamics have mostly a linear dispersion relation, i.e. $E_k=vk$, as in a finite uniform open ended chain $k=k_n=\frac{\pi n}{N+1}$.

4.1.1 Generalization to XY models

Here we introduce our generalization of the above arguments to XY models

$$H=\sum_{n=1}^{N-1}\left(j_n\frac{1+\gamma_n}{2}\,\sigma_n^x\sigma_{n+1}^x+j_n\frac{1-\gamma_n}{2}\sigma_n^y\sigma_{n+1}^y\right)+\frac{1}{2}\sum_{n=1}^{N}h_n\,\sigma_n^z\,, \tag{4.8}$$

i.e. quadratic fermionic models not conserving the number of "particles", where the matrix A (see Section 3.2) is given by (4.2) and the pairing anti-symmetric matrix B is non-null

$$B=\begin{pmatrix} 0 & -j_1\gamma_1 & & & & & \\ j_1\gamma_1 & 0 & -j_2\gamma_2 & & & & \\ & j_2\gamma_2 & 0 & -j_3\gamma_3 & & & \\ & & & \ddots & & & \\ & & & j_{N-2}\gamma_{N-2} & 0 & -j_{N-1}\gamma_{N-1} & \\ & & & & j_{N-1}\gamma_{N-1} & 0 & \end{pmatrix}. \tag{4.9}$$

In this case the perfect mirroring condition reads $U(t^*)=e^{i\alpha}X$ and $V(t^*)=0$, i.e. in matrix language (see Section B.2.2)

$$\begin{pmatrix} P^\dagger & Q^T \\ Q^\dagger & P^T \end{pmatrix}\begin{pmatrix} e^{-iEt^*} & 0 \\ 0 & e^{iEt^*} \end{pmatrix}\begin{pmatrix} P & Q \\ Q^* & P^* \end{pmatrix}=\begin{pmatrix} e^{i\alpha}X & 0 \\ 0 & e^{-i\alpha}X \end{pmatrix}.$$

As in the XX case, this means that the matrix on the r.h.s. of the above equation can be diagonalized using the same matrices of P and Q and that the energy-eigenvalues have to satisfy the condition (4.7). Accordingly, these necessary conditions must hold

$$\left[\begin{pmatrix} A & B \\ -B^* & -A^* \end{pmatrix},\begin{pmatrix} e^{i\alpha}X & 0 \\ 0 & e^{-i\alpha}X \end{pmatrix}\right]=0 \quad\Longrightarrow\quad XAX=A,\quad XBX=e^{2i\alpha}B\,. \tag{4.10}$$

The matrix A has to be persymmetric while there is still some freedom in the symmetry properties of B. However, if B is real (as in the XY model), the parameter α, which in the $B=0$ case is a free parameter, has to be a multiple of $\frac{\pi}{2}$: the matrix B thus has to be persymmetric, when for instance $\alpha=\frac{\pi}{2}$ or anti-persymmetric, i.e. $\gamma_{N-n}=-\gamma_n$, when for instance $\alpha=\pi$. The physical origin of these constraints is still unclear, but there is a nice argument supporting the persymmetric case $\alpha=\frac{\pi}{2}$. Indeed, the XY model does not conserve the number of particles and the phase $(-1)^{\frac{\tilde{n}(\tilde{n}-1)}{2}}$ in (4.4) is not a constant of motion. However, the parity is conserved and $(-1)^{\frac{\tilde{n}(\tilde{n}-1)}{2}}e^{i\pi\tilde{n}/2}=e^{i\pi\tilde{n}^2/2}$ has a fixed value in each sector with constant parity. In the persymmetric case insofar, the dynamics effectively mirrors the state $\psi(n_1,\ldots,n_N)\to\psi(n_N,\ldots,n_1)$ without relative phases when the initial state has constant parity.

4.1.2 Perfect transmission without mirroring

A many-body quantum system described by an XY spin model or by a quasi-free fermionic model acts as a quantum mirror provided that the Hamiltonian is persymmetric and the energy eigenvalues satisfy the condition (4.7). However, for designing a quantum bus connecting two distant registers, only the perfect transmission between the boundary spins of the chain is required. We generalize thus the Lemma 2 of Ref. [86] for showing that, even in the less-stringent case of perfect transmission only between the boundary qubits, the Hamiltonian has to satisfy some symmetry, and as a particular case it can be persymmetric.

Indeed, let us assume that

$$\begin{pmatrix} P^\dagger & Q^T \\ Q^\dagger & P^T \end{pmatrix} \begin{pmatrix} e^{-iEt^*} & 0 \\ 0 & e^{iEt^*} \end{pmatrix} \begin{pmatrix} P & Q \\ Q^* & P^* \end{pmatrix} e_1 = e^{i\alpha} e_N \,,$$

being e_i the vector with components $(e_i)_j = \delta_{ij}$. Then it must be true that

$$e^{-iE_k t^*} P_{k1} = e^{i\alpha} P_{kN}, \qquad e^{iE_k t^*} Q_{k1} = e^{-i\alpha} Q_{kN}, \qquad \forall k \,.$$

In particular, this reveals that $|P_{k1}|^2 = |P_{kN}|^2$ and $|Q_{k1}|^2 = |Q_{kN}|^2$, and by rising the Hamiltonian matrix S of (B.11) to an integer power, m, we can relate

$$e_1^T S^m \, e_1 = \sum_k E_k^m (|P_{k1}|^2 - |Q_{k1}|^2) = e_N^T S^m \, e_N .$$

For $m = 1$, this gives that $h_1 = h_N$. For $m = 2$, we find that $h_1^2 + j_1^2(1+\gamma_1^2) = h_N^2 + j_{N-1}^2(1+\gamma_{N-1}^2)$ which can be solved for instance by setting $j_1 = \pm j_{N-1}$ and $\gamma_1 = \pm\gamma_{N-1}$. Each time that m is increased by 1, new variables are introduced on each side of the equation. Since this sides must be equals the required symmetry properties occur.

4.2 Wave packet encoding

Near to perfect state transmission can be obtained also by conveniently encoding the initial state to be transfered into a "wave packet" over multiple sites of the chain. In this case, classical results about wave packet transmission can be exploited for designing the optimal shape of the packet for better transmission [90, 91], depending on the Hamiltonian.

In fact, when a spin chain conserves the number of spin up (down)[1], and the bus is initialized in the fully polarized state $|\mathbf{0}\rangle \equiv |00\cdots0\rangle$, the dynamics becomes very alike that of a classical wave packet: by initially setting the qubit A in the state $\alpha|0\rangle + \beta|1\rangle$ the whole chain evolves according to

$$|\psi(t)\rangle = \alpha|\mathbf{0}\rangle + \beta \sum_B f_{BA}(t)|\mathbf{B}\rangle \,, \tag{4.11}$$

[1] This means that $[H, S^z_{\text{tot}}]$, where $S^z = \sum_n \sigma_n^z/2$ is the total magnetization operator along the direction z.

where $|\mathbf{B}\rangle$ is the state $|00\cdots010\cdots0\rangle$, with $|1\rangle$ in position B, and $f_{BA}(t)=\langle\mathbf{B}|e^{-itH}|\mathbf{A}\rangle$. If the Hamiltonian is translationally invariant, then it can be diagonalized with a Fourier transformation[2] and accordingly

$$f_{AB}(t)=\frac{1}{N}\sum_k e^{2\pi i\frac{(B-A)k}{N}}e^{-it\omega_k}\ ,$$

where N is the length of the chain, and ω_k is the energy as a function of the momentum index k, i.e. the dispersion relation up to an unimportant constant. Equation (4.11) is nothing but the evolution of a *delta-like* wave-packet centered at position A. In typical cases, such as a particle in a box or a harmonic oscillator, such a wave-function is known to disperse (spread) rapidly in space. The standard solution is to place the particle in a Gaussian wave-packet, which usually has a low dispersion and travels with a definite group velocity. The same trick can be applied to spin chains by initially encoding the state $\alpha|0\rangle+\beta|1\rangle$ onto a (Gaussian) wave-packet over multiple sites: $|\psi(0)\rangle=\alpha|\mathbf{0}\rangle+\beta\sum_a\phi_a|\mathbf{a}\rangle$, where $\phi_a\propto e^{-\left(\frac{a-A}{\sigma}\right)^2}$. The time evolved state $|\psi(t)\rangle=\alpha|\mathbf{0}\rangle+\beta\sum_b\phi_b(t)|\mathbf{b}\rangle$ is then described by the evolution of the wave packet

$$\phi_b(t)=\sum_a f_{ba}(t)\,\phi_a=\sum_k e^{-it\omega_k}\frac{1}{N}\sum_a e^{2\pi i\frac{(b-a)k}{N}}\phi_a=\frac{1}{\sqrt{N}}\sum_k e^{-i\left(t\omega_k-\frac{2\pi k}{N}b\right)}\tilde{\phi}_k\ , \qquad (4.12)$$

where $\tilde{\phi}_k$ is the discrete Fourier transform of ϕ_a. It is clear that if $\omega_k=ck$ for some velocity c the wave-packet travels coherently during the evolution without dispersion. On the other hand, most systems have a non trivial dispersion relation and the wave-packet is expected to spread during the evolution. Nevertheless, most dispersion relations have an inflection point, i.e. there exists a certain k_0 such that $\omega''(k_0)=0$, around which the dispersion relation can be approximated as a linear one. If the initial wave-packet $\tilde{\phi}_k$ is centered around k_0 in the momentum space then it is expected that the wave-function remains coherent during the evolution. Consider indeed an initial Gaussian wave-packet centered around A in coordinate space, and centered around k_0 in the momentum space: $\phi_a\propto e^{-\left(\frac{a-A}{\sigma}\right)^2+2\pi i\frac{a}{N}k_0}$. When $\sigma\gg1$ such a wave packet is very narrow in momentum space, centered around k_0, and we can expand ω_k around k_0 up to the third order, which is the first dispersive term, being $\omega''(k_0)=0$. In this case a Gaussian pulse does not remain Gaussian but modifies its shape becoming an Airy function [92, 93]. The wave-packet's spread increases during the transmission according to the formula [94]

$$\sigma(t)^2=\sigma^2+\frac{1}{2}\left(\frac{\omega'''(k_0)t}{2^5\sigma^2}\right)^2\ .$$

In order to minimize the dispersion during the transmission over distances of the order of N, the above equation has to be minimized for $t=N/\omega'(k_0)$. The result is

$$\sigma\propto N^{\frac{1}{3}}\ , \qquad (4.13)$$

[2] For translationally invariant Hamiltonians we have $H=\sum_k\omega_k|k\rangle\langle k|$ where $\langle\mathbf{B}|k\rangle=\frac{1}{\sqrt{N}}e^{2\pi i\frac{Bk}{N}}$.

which is then the *optimal encoding width* of the state onto a Gaussian wave packet. When (4.13) holds the encoded wave-packet reaches the destination B without a significant change of its shape. The transmitted Gaussian wave-packet can then be decoded. At the end, the procedure effectively induces a state transmission between A and B where the corresponding fidelity of transmission is observed to be very high [90], as expected.

Thanks to the Heisenberg principle, when (4.13) holds, the width Δ of the wave-packet in the momentum space is

$$\Delta \propto N^{-\frac{1}{3}} . \tag{4.14}$$

This means that in order to minimize the dispersion, the number of involved modes in the dynamics should scale with N as $N^{\frac{2}{3}}$.

4.3 Qubits weakly coupled to the bus

Another approach for sending quantum information with near to perfect fidelity is by weakly coupling distant qubits to a many-body system. Say for instance that the quantum many body system is an arbitrary graph of spins interacting with each other via a coupling strength $J \simeq 1$, while the sending and receiving qubits are coupled to the system through a coupling ϵ where $\epsilon \ll 1$. Then one can derive an effective Hamiltonian, acting on the distant qubits only, provided that the local energies of the qubits are not in resonance with the energies of the spin bus [95, 96, 97, 67]. One can also consider the resonant regime [95, 98, 99] where practically one ends up to a three body Hamiltonian, i.e. the distant qubits and the resonant mode. In the off-resonant case the effective Hamiltonian can be derived using the Fröhlich method [95]. Let $H_{\text{tot}} = H + \epsilon V$ be the total Hamiltonian, $H = H_b + H_q$, where H_q is the Hamiltonian of the qubits, H_b is the Hamiltonian of the spin bus, and ϵV is the coupling between the qubits and the bus. Let F be an Hermitian operator and set $H'_{\text{tot}} = e^{i\epsilon F} H_{\text{tot}}\, e^{-i\epsilon F}$. Expanding H'_{tot} in series of ϵ we get

$$H^{(2)}_{\text{tot}} = H + \epsilon\big(V + i\,[F,H]\big) + \epsilon^2\left(i\,[F,V] + \frac{i^2}{2}[F,[F,H]]\right) + \mathcal{O}(\epsilon^3) .$$

The best quadratic expansion is the obtained by choosing F such that

$$V + i\,[F,H] = 0 . \tag{4.15}$$

For such a condition the second-order Hamiltonian $H^{(2)}_{\text{tot}}$ becomes

$$H^{(2)}_{\text{tot}} = H + \frac{i\,\epsilon^2}{2}\,[F,V] + \mathcal{O}(\epsilon^3) .$$

Let $\{|n\rangle\} \equiv \{|q,b\rangle\}$ be the set of eigenvectors of H with eigenvalues $E_n \equiv \omega_q + \Omega_b$, assumed to be non-degenerate for simplicity: $|q\rangle$ and ω_q (respectively $|b\rangle$ and Ω_b) are the eigenvectors

and eigenvalues of H_q (respectively H_b). A solution of Eq. (4.15), which is a particular case of Sylvester equation [100], is

$$F = -i\sum_{n,m}\frac{\langle n|V|m\rangle}{E_n - E_m}|n\rangle\langle m| = -\frac{1}{2}\int_{-\infty}^{\infty} e^{itH}\,V\,e^{-itH}\,\mathrm{sign}(t)\,dt\,.$$

Then the effective Hamiltonian acting only on the external qubits can be obtained by tracing out the bus, i.e.

$$\begin{aligned} H^{\mathrm{eff}} &\simeq H_q + \frac{\epsilon^2}{2}\operatorname*{Tr}_b \Im\left[\rho\int_{-\infty}^{\infty} e^{itH}\,V\,e^{-itH}\,V\,\mathrm{sign}(t)\,dt\right] \qquad (4.16)\\ &= H_q + \frac{\epsilon^2}{2}\sum_{\substack{qq'\tilde{q}\\ b\tilde{b}}}\rho_b\langle qb|V|\tilde{q}\tilde{b}\rangle\langle\tilde{q}\tilde{b}|V|q'b\rangle\left(\frac{1}{\omega_q+\Omega_b-\omega_{\tilde{q}}-\Omega_{\tilde{b}}}+\frac{1}{\omega_{q'}+\Omega_b-\omega_{\tilde{q}}-\Omega_{\tilde{b}}}\right)|q\rangle\langle q'|\,, \end{aligned}$$

where $\Im x = (x - x^\dagger)/(2i)$ and ρ is the initial state of the bus, assumed to be diagonal: $\rho = \sum_b \rho_b|b\rangle\langle b|$. The integral in (4.16) can be expressed in terms of "standard" time dependent correlation functions of the bus [101], and can be calculated analytically in some cases [95, 96]. For example when $H_q = h_0(\sigma_A^z + \sigma_B^z)$ and $V = \sum_{q=A,B}\sigma_q^+\sigma_{b_q}^- + \mathrm{h.c.}$, where b_A, b_B are two arbitrary qubits of the bus, then

$$H^{\mathrm{eff}} = h_A^{\mathrm{eff}}\sigma_A^z + h_B^{\mathrm{eff}}\sigma_B^z + j^{\mathrm{eff}}(\sigma_A^+\sigma_B^- + h.c)\,.$$

where the effective couplings depend both on the Hamiltonian of the bus H_b and on the initial state ρ, as well as the positions b_A and b_B. Forgetting the local rotations caused by h_A^{eff} and h_B^{eff} which do not affect entanglement and can be safely handled with local counter-rotations, the dynamics induced by the above Hamiltonian acts as a perfect permutation operator between sites A and B on times $t \propto 1/j^{\mathrm{eff}} \propto 1/\epsilon^2$.

This method is powerful, as different kind of interactions, different initial states, and different attachment positions can be safely handled with a proper effective coupling. It ensures an almost perfect transmission, where the imperfections arise as the effective Hamiltonian is not exact, and does make sense in an experimental point of view. However, the drawback is that the time scales involved are very long, being of the order of $1/\epsilon^2$ where $\epsilon \ll 1$, and in such a long time the system could suffer from decoherence, as an interaction with the (thermal) environment can never be entirely removed.

4.4 Coherent ballistic dynamics

Now we introduce the idea of our method, that will be further analysed in the next chapters, for inducing a coherent ballistic dynamics in systems modeled with quasi-free Hamiltonians. In some sense, our method gathers the three approaches described before in an unique, simple idea.

Indeed we consider a scheme similar to the latter one, where the interactions between the qubits of the bus are uniform, whereas the couplings j_0 between the boundaries of the bus and the external qubits A and B are different. This setting is the most natural one for connecting distant registers, as it is clear from Fig. 3.2. We assume that the distant registers are initially detached from the bus, and that the couplings j_0, can be switched on and set to a particularly tuned value. In the limit of very weak j_0, according to (4.16) only the modes which are in resonance with the local energies h_0 of the qubits are involved in the dynamics, but the resulting transmission times are very long, as we have seen. On the other hand, when j_0 increases, more and more normal modes in the neighbourhood of the resonant region are involved. Considering quasi-free models, these modes do not interact and the resulting dynamics emulates a wave packet dynamics. Indeed, being the system almost translationally invariant in the limit of big N, the energy eigenvalues E_k can be interpreted as a dispersion relation, with k a quasi-momentum index. In this momentum space, the wave-packet is peaked around the local energy h_0 and has a width $\Delta(j_0)$ which increases for increasing j_0, as more modes come into play. A coherent ballistic evolution of the wave-packet is obtained, as described in section 4.2, by setting the value of h_0 to the inflection-point energy (the center of the linear zone) and by setting j_0 such that (4.14) holds. The difference with the approach of section 4.2 is that the wave-packet lies in the quasi-momentum space, and its width can be controlled only by properly choosing j_0, without requiring the control of multiple qubits in the neighbourhood of A and B. Moreover, as in finite systems $k = k_n \approx \pi n/N$, thanks to the system's mirror symmetry, when $t^* \approx N/v$, being v the group velocity in the linear zone, the perfect transmission condition (4.7) is almost satisfied and a perfect reconstruction of initial state on the qubit B is expected as well.

The advantages are evident. Only the couplings j_0 and the local interaction h_0 need to be controlled, and in some particular cases, notably the XX model, only the tuning of j_0 is sufficient. There is no need for engineering, nor for controlling many ($N^{\frac{1}{3}}$) qubits and, thanks to the non-weak couplings, the transmission times are fast. Recently it has been shown [89] that our results are also stable against static perturbation. Indeed, in most situations the transmission performance of our approach renders the full engineering of the couplings of a spin chain unnecessary in order to obtain quantum state transmission with high fidelity under static perturbations.

In the next chapters our approach will be derived more rigorously for both XX and XY models.

5

Optimal dynamics with the XX model

After the general introduction of the previous chapters, we consider here a specific model, the XX spin chain, and we analyze in detail how to obtain the ballistic regime. As outlined in Section 4.4, in the ballistic regime the transmission can be depicted [68, 90, 102] in terms of a travelling wavepacket carrying the information about the state of the endpoint qubit A, eventually yielding the state reconstruction at the opposite endpoint qubit B thanks to the overall system's mirror symmetry [84, 103, 66, 104]. The ballistic regime differs from that arising in the limit of very weak endpoint couplings [97, 105, 106, 107, 67] where (almost) perfect state transfer occurs at very long times as a result of a Rabi-like population transfer involving only two or three single-particle modes. Understanding the basic mechanism of ballistic transfer, where the number of involved single-particle modes will be shown to be of the order of $N^{2/3}$, as in Section 4.2, allows us to devise an optimal value of the endpoint interactions for any N, and vice versa. Remarkably, the corresponding transmission quality, as witnessed by the state- and the entanglement fidelity, does not decrease to zero when the data-bus becomes very long, but remains surprisingly high.

We consider the setup illustrated in figure 5.1: the data-bus connecting the qubits A and B is a one-dimensional array of N localized $S = 1/2$ spins with exchange interactions of XX Heisenberg type and a possible external magnetic field applied along the z direction. This gives the total Hamiltonian the following structure

$$H = \sum_{i=1}^{N-1} \left(S_i^x S_{i+1}^x + S_i^y S_{i+1}^y\right) + h \sum_{i=1}^{N} S_i^z + \\ + j_0 \sum_{i=0,N} \left(S_i^x S_{i+1}^x + S_i^y S_{i+1}^y\right) + h_0 \left(S_0^z + S_{N+1}^z\right) , \tag{5.1}$$

where $S_i^\alpha = \frac{1}{2}\sigma_i^\alpha$ and the qubits A and B sit at the endpoint sites 0 and $N+1$ of a one-dimensional discrete lattice on whose sites $1, 2, ..., N$ the spin chain is set. The exchange interaction (chosen as energy unit) and the magnetic field h are homogeneous along the chain, and an overall mirror symmetry is assumed, implying the endpoint coupling j_0 and field h_0 to be the same for both ends. The N spins constituting the XX data-bus are collectively indicated by Γ. We will focus our attention on how the state of the qubit B evolves

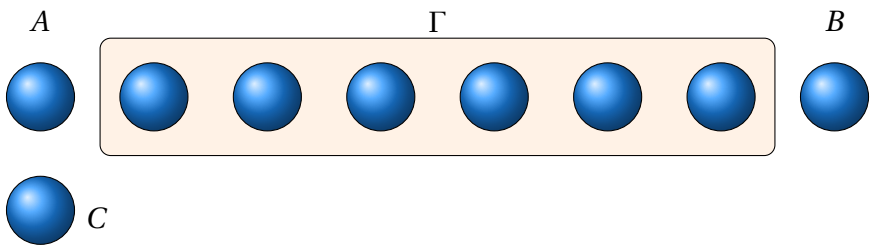

Figure 5.1 – The endpoints of a quantum data-bus Γ are coupled to the qubits A and B, via the interaction j_0; A can be entangled with an external qubit C.

under the influence of the chain Γ, and depending on the initial state of the qubit A; the latter is possibly entangled with an ancillary qubit C. The results of the analysis are used for gathering insights on the quantum-information transmission through the chain, so as to characterize the dynamical evolution of the overall system and to maximize the quality of the quantum-state transfer.

Even though the overall scheme could also be used for realizing tasks other than quantum information transfer, via the dynamical correlations that the chain induces between A and B [108], our approach is specifically tailored for studying transfer processes along the chain: the qubit B or the qubit-pair BC are considered as target system, depending on whether the quantum-state of the qubit A or that of the qubit-pair AC are to be transferred, respectively.

5.1 Dynamical evolution

In this section we specifically consider the Hamiltonian (5.1). The system A∪Γ∪B is prepared in the state $\rho^{\mathrm{tot}} = \rho^{\mathrm{A}} \otimes \rho^{\Gamma} \otimes \rho^{\mathrm{B}}$. The Hamiltonian (5.1) is diagonalized as in section 3.2 by using a Jordan-Wigner transformation together with an orthogonal transformation. Without the anisotropy γ the matrix B is null, and the nearest-neighbour interaction between the fermions is described only by the $(N+2)\times(N+2)$ tridiagonal mirror-symmetric matrix A (see C.1.1); an orthogonal transformation O diagonalizes A and hence H [109, 110]. The trivial time-evolution in the Heisenberg picture of the fermion operators entails the time-dependent transformation

$$c_i(t) = \sum_{i=0}^{N+1} U_{ij}(t)\, c_j \,, \tag{5.2}$$

where, as in (B.22),

$$U_{ij}(t) = \sum_{n} O_{ki} O_{kj}\, \mathrm{e}^{-\mathrm{i}E_k t} \,. \tag{5.3}$$

The resulting quantum channel is the same of (3.18), provided that also the state of B has a fixed parity, otherwise there are some further mixed terms (see Section C.4). The difference

is that the parity $(-1)^p$ has to be changed to $-\tilde{p}\langle\sigma^z_{N+1}\rangle$, being $\tilde{p}$ the parity of Γ, in order to consider the structure $\Gamma\cup B$. Following section 3.2, the optimal fidelity of transmission is

$$\mathfrak{F}(t)=\frac{1}{2}+\frac{1}{6}u^2(t)+\frac{1}{3}|\tilde{p}\langle\sigma^z_{N+1}\rangle|\,u(t),$$

while the transmitted entanglement, as measured by the concurrence, is

$$\mathfrak{C}(t)=\max\left\{0,\left|\tilde{p}\langle\sigma^z_{N+1}\rangle\right|u(t)-\sqrt{A(t)[1-u^2(t)-A(t)]}\right\},$$

where, from (3.17),

$$A(t)=|U_{N+1,N+1}(t)|^2\frac{\langle\sigma^z_{N+1}\rangle+1}{2}+C_{N+1}(t)\,, \tag{5.4}$$

$$C_i(t)=\sum_{j,j'=1}^{N}U^*_{ij}(t)U_{ij'}(t)\,\mathrm{Tr}\left[\rho^\Gamma c^\dagger_j c_{j'}\right]\,. \tag{5.5}$$

From the above formulas it appears that the choice of the initial state $\rho^\Gamma\otimes\rho^B$ plays an important role [82]: in particular, in order to get the largest concurrence and fidelity it must be

$$-\tilde{p}\,\langle\sigma^z_{N+1}\rangle=(-1)^p\,, \tag{5.6}$$

meaning that ρ^Γ is an eigenstate of the parity and the state of qubit B is $|\uparrow\rangle$ or $|\downarrow\rangle$. As for the initial state of the data-bus, the choices range, for example, from its ground state to a fully polarized state. Such limitation in the choice of the initial state might be overcome by applying a two-qubit encoding and decoding on states ρ^A and ρ^B, respectively [67, 111]. When (5.6) holds, the state transmission protocol can be simplified if at the arrival time t^*

$$0=\phi_u(t^*)=\arg U_{N+1,0}(t^*)+p\pi. \tag{5.7}$$

Indeed, when condition (5.7) holds, according to (3.20), the state is not rotated around the z-axis during the transmission, and no local unitary protocols for increasing the fidelity are required. Condition (5.7) can be fulfilled by choosing a proper magnetic field [112] or the parity of N, as we will see in the next section.

The above analysis shows that, provided that (5.6) holds, the quality of the state and entanglement transfer

$$\mathfrak{F}(t)=\frac{1}{2}+\frac{1}{6}u^2(t)+\frac{1}{3}\,u(t), \tag{5.8}$$

$$\mathfrak{C}(t)=\max\left\{0,u(t)-\sqrt{A(t)[1-u^2(t)-A(t)]}\right\}, \tag{5.9}$$

mainly depends on $u(t)$ and increases with it.

5.2 Optimal dynamics

We now have the tools for determining the conditions for a dynamical evolution that corresponds to the best quality of the transmission processes. In C.1.1 the algebraic problem of diagonalizing the XX Hamiltonian in the case of nonuniform mirror-symmetric endpoint interactions is analytically solved. The eigenvalues of the matrix Ω can be written as

$$E_k = h + \cos k \,, \tag{5.10}$$

in terms of the pseudo-wavevector k, which takes $N+2$ discrete values k_n in the interval $(0,\pi)$: from (C.20) and (C.13) it follows that these values obey

$$k_n = \frac{\pi\, n + 2\varphi_{k_n}}{N+3} \,, \quad (n = 1, ..., N+2) \,, \tag{5.11}$$

with

$$\varphi_k = k - \cot^{-1}\Big(\frac{\cot k}{\Delta}\Big) \quad \in \big(-\tfrac{\pi}{2}, \tfrac{\pi}{2}\big) \,, \tag{5.12}$$

$$\Delta = \frac{j_0^2}{2 - j_0^2} \,, \tag{5.13}$$

where we have set $h_0 = h$. From the above equations it follows that the k's correspond to the equispaced values $\pi n/(N+3)$, slightly shifted towards $\pi/2$ of a quantity which is smaller than $\pi/(N+3)$, so that their order is preserved: therefore k can be used as an alternative index for n, understanding that it takes the values k_n, as done in (5.10). According to the conclusions of the previous section, we focus on the transition amplitude $u(t)$, as given by (5.3), which explicitly reads:

$$u(t) = \left| \sum_n \rho(k_n)\, \mathrm{e}^{\mathrm{i}(\pi n - E_{k_n} t)} \right| \,, \tag{5.14}$$

where, after (C.21), it is

$$\rho(k) = \frac{1}{N+3-2\varphi'_k} \, \frac{\Delta(1+\Delta)}{\Delta^2 + \cot^2 k} \,, \tag{5.15}$$

and mirror symmetry is exploited according to (C.16): the transition amplitude above is a superposition of phase factors with normalized weights, $\sum_n \rho(k_n) = 1$, entailing $u(t) \leq 1$, with equality holding when all phases are equal. The distribution $\rho(k)$ is peaked at $k = k_0 = \pi/2$ and its width is characterized by the parameter Δ (5.13) so that the smaller j_0 the narrower $\rho(k)$.

As $u(t)$ essentially measures the state-transfer quality, the condition for maximizing it at some time t^*, i.e., $u(t^*) \simeq 1$, is that all phases $\pi n - E_{k_n} t^*$ almost equal each other. Assume for a moment that the k's are equispaced values, as in the uniform case (see appendix C.1), and that the dispersion relation is linear, $E_k = v\,k$: then (5.14) would read

$$u(t) = \left| \sum_n \rho(k_n)\, \mathrm{e}^{\mathrm{i}\pi n(1 - t/t^*)} \right| \,,$$

with $t^*=(N+3)/v$, so that $u(t^*)=\sum_n \rho(k_n)=1$, i.e., all modes give a coherent contribution and entail perfect transfer. On the other hand, in our case E_k is nonlinear in k, and the k_n are not equally spaced due to the phase shifts (5.12) entering (5.11), so generally the different modes undergo dispersion and lose coherence.

5.2.1 Transfer regimes

The dependence of Δ upon j_0 reveals the possibility of identifying different dynamical regimes, characterized by a qualitatively different distribution $\rho(k)$ (5.15) and hence, as for the transfer process, a different behaviour of the transition amplitude $u(t)$. For extremely small j_0 the distribution $\rho(k)$ can be so thin that (for even N) only two opposite small eigenvalues come into play, say differing by $\delta\omega$, and perfect transmission will be attained at a large time $t=\pi(\delta\omega)^{-1}$ (for odd N there is a third vanishing eigenvalue at $k=\pi/2$ and still two identical spacings $\delta\omega$ do matter). This is the Rabi-like regime.

A different regime is observed when j_0 is increased: a few more eigenvalues come into play and it may occur, in a seemingly random way, that their spacings be (almost) commensurate with each other, i.e., they can be approximated as fractions with the same denominator K, yielding phase coherence at $t_K=\pi K$. By recording the maximum of $u(t)$ over a fixed large time interval T, as j_0 is varied (see [97]), a rapid and chaotic variation is observed. This regime is clearly useless for the purpose of quantum communication.

As j_0 further increases, the ballistic regime eventually manifests itself: $\rho(k)$ involves so many modes that commensurability is practically impossible, and a more regular behaviour with short transmission time $t^*\sim N$ sets in. The ballistic regime is characterized by relatively large values of $u(t^*,\Delta)$ which is the quantity plotted in figure 5.2, reporting numerical results for increasing chain lengths. It appears that each curve shows a maximum for a particular *optimal* value of $\Delta=\Delta^{\rm opt}(N)$ or, equivalently, of $j_0=j_0^{\rm opt}(N)$: such maxima are remarkably stable for very high N and yield very high transmission quality. In Table 5.1 we report some of the optimal values $\Delta^{\rm opt}(N)$ and $j_0^{\rm opt}(N)$ for a wide interval of chain lengths. This last 'ballistic-transfer' regime is the one we are interested in, since it has three strong advantages: first, the transmission time $t^*\sim N$ is the shortest attainable; second, the maximum value $u(t^*,\Delta^{\rm opt})$ of $u(t^*,\Delta)$ is such that one can achieve very good state transfer, e.g., the corresponding transmission fidelity is far beyond the classical threshold, even for very long chains; third, it is not necessary to fine-tune j_0 to $j_0^{\rm opt}$, since from the data set reported in figure 5.2 it can be estimated that the relative loss in amplitude is $u^{\rm opt}-u(j_0^{\rm opt}\pm\delta j_0)\simeq 0.8\left(\delta j_0/j_0^{\rm opt}\right)^2$, e.g., a 15% mismatch in j_0 results in a loss of less than 2% in the transition amplitude.

The above analysis gives a physical interpretation of what is observed in figure 3 of [97], where the Rabi-like, intermediate and ballistic regimes emerge.

A qualitative picture of the ballistic regime can be obtained by viewing the transition am-

$N+2$	Δ^{opt}	j_0^{opt}	$u(t^*,\Delta^{\text{opt}})$
25	0.243	0.625	0.968
51	0.181	0.554	0.949
101	0.138	0.493	0.932
251	0.098	0.422	0.913
501	0.075	0.374	0.900
1 001	0.058	0.332	0.890
2 501	0.042	0.284	0.879
5 001	0.033	0.252	0.873
10 001	0.026	0.224	0.868
25 001	0.0188	0.192	0.862
50 001	0.0148	0.171	0.859
100 001	0.0117	0.152	0.857
250 001	0.0086	0.1303	0.854
500 001	0.0068	0.1160	0.853

Table 5.1 – Optimal values Δ^{opt} and the corresponding j_0^{opt} and $u(t^*,\Delta^{\text{opt}})$ for different N.

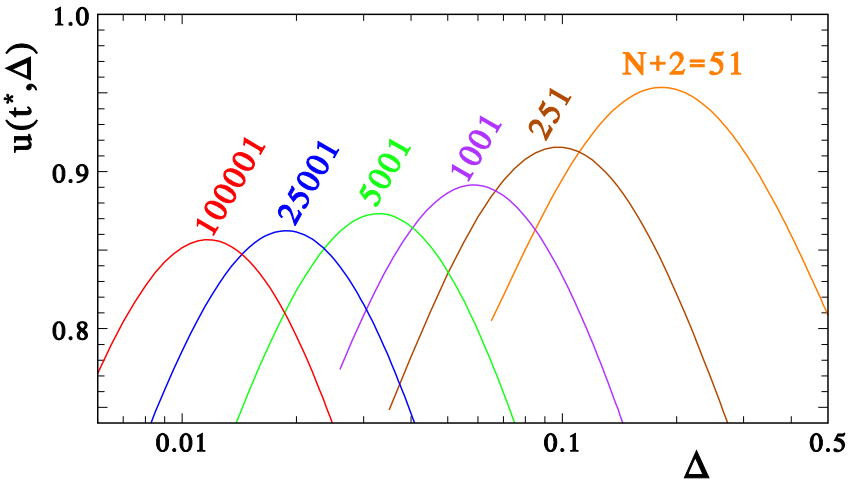

Figure 5.2 – Value of $u(t^*,\Delta)$ as a function of Δ, for different wire lengths N. t^* is obtained numerically by maximizing (5.14) around $t \simeq N+3$. These curves are very well fitted by the function $u(\Delta)=u^{\text{opt}}-c[\ln(\Delta/\Delta^{\text{opt}})]^2$, with c ranging from ∼0.17 (low N) to ∼0.21 (large N).

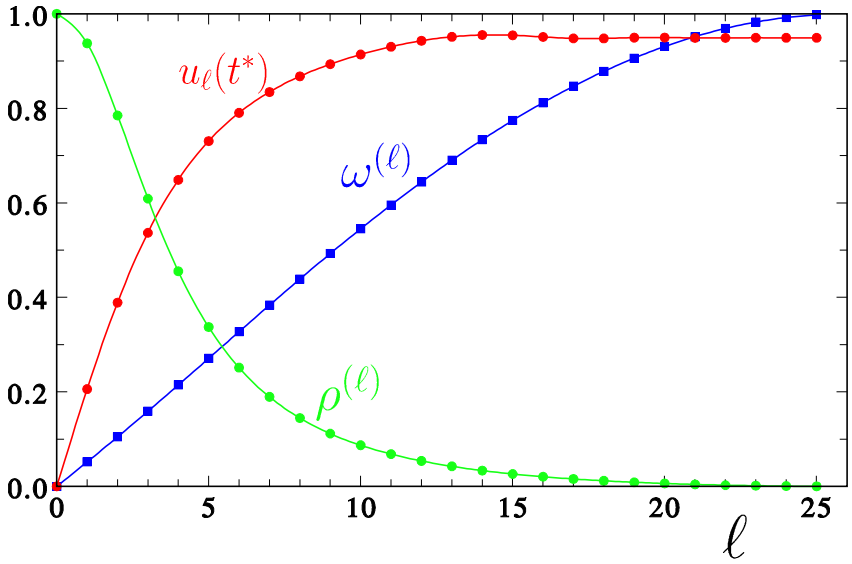

Figure 5.3 – Partial sum of the amplitude $u_\ell(t^*)$ vs ℓ for $N+2=51$ and $j_0=0.58$, together with the corresponding frequency and density.

plitude (5.14) as a wavepacket with $N+2$ components. It can be evaluated by progressively adding the contributions from symmetric eigenvalues, i.e., for odd N summing between $(N+1)/2 \mp \ell$, for $\ell = 0, 1, ..., (N+1)/2$. This yields the partial sum $u_\ell(t^*)$ shown in figure 5.3, together with the corresponding frequency and density. One can see that the amplitude increases only over the modes of the linear-frequency zone, i.e., where frequencies are equally spaced, indicating that only those wavepacket components whose frequency lies in such zone play a role in the transmission process.

5.2.2 Ballistic regime and optimal values

From the above reasoning, since the modes contributing to the amplitude lie in a range of size Δ around k_0, in order to get high-quality transfer processes it is necessary that the corresponding frequencies be almost equally spaced, meaning that E_{k_n} is approximately linear in n. Actually, E_k has an inflection point in k_0: its nonlinearity is of the third order in $k-k_0$ and the modes close to k_0 satisfy the required condition. However, from the phase-shifts (5.12) a further cubic term arises, which depends on Δ. As Δ varies with j_0, the latter can be chosen so as to eliminate the cubic terms, yielding a wide interval with almost constant frequency spacing. The latter can be expressed just as the derivative of E_{k_n} with respect to n,

$\partial_n E_{k_n} = \sin k\ \partial_n k$. The last term is evaluated from (5.11) and (5.12),

$$\partial_n k = \frac{\pi + 2\varphi'_k \partial_n k}{N+3} = \frac{\pi}{N+3-2\varphi'_k}\,, \tag{5.16}$$

$$\varphi'_k = -\frac{1-\Delta}{\Delta} + \frac{(1-\Delta^2)\cos^2 k}{\Delta[\Delta^2 + (1-\Delta^2)\cos^2 k]}\,, \tag{5.17}$$

so that

$$\begin{aligned}\partial_n E_{k_n} &= \frac{\pi \sin k}{N+3-2\varphi'_k} \\ &= \frac{\pi}{t^*}\left[1 + \left(2\,\frac{1-\Delta^2}{t^*\Delta^3} - \frac{1}{2}\right)\cos^2 k + (\cos^4 k)\right],\end{aligned} \tag{5.18}$$

where $t^* = N+3+2(1-\Delta)/\Delta$ is the arrival time. It follows that one can minimize the nonlinearity of E_{k_n} by setting the width to the value Δ_0 satisfying

$$\Delta_0 = \left[\frac{4}{t^*}(1-\Delta_0^2)\right]^{1/3} \underset{N\gg 1}{\longrightarrow} 2^{2/3} N^{-1/3}\,, \tag{5.19}$$

i.e., $j_0 \simeq 2^{5/6} N^{-1/6}$ for large N. Therefore the main mechanism that produces an optimal ballistic transmission is that of varying the endpoint exchange parameter to the value j_0 that 'linearizes' the dispersion relation. Actually, if the corresponding $\Delta_0 = \Delta(j_0)$ is such that $\rho(k)$ exceeds the region of linearity, further gain arises by lowering j_0 so as to tighten the relevant modes towards k_0. However, at the same time E_{k_n} becomes less linear and the trade-off between these two effects explains why a maximum is observed. This is well apparent in Fig 5.4, where for different values of Δ the shapes of $\partial_n E_k$ can be compared with the excitation density $\rho(k)$: for $\Delta = \Delta_0$ the density still has important wings in the nonlinear zone, so the optimal value $\Delta^{\rm opt}$ turns out to be smaller.

The dynamics in the ballistic regime is best illustrated by the time evolution of the magnetization (3.12) along the chain, plotted in figure 5.5 when the initial state is $|\uparrow\rangle \otimes |\downarrow\downarrow\cdots\downarrow\rangle \otimes |\uparrow\rangle$, and in figure 5.6 when the initial state is $|\uparrow\rangle|\Omega_\Gamma\rangle|\downarrow\rangle$, being $|\Omega_\Gamma\rangle$ the ground state of the chain Γ. The initial magnetizations at the endpoints generate two travelling wavepackets: for non-optimal coupling ($j_0 = 1$, upper panel of figure 5.5 and left panel of figure 5.6) they change their shape and quickly straggle along the chain; for optimal coupling ($j_0 = j_0^{\rm opt}$, lower panel of figure 5.5 and right panel of figure 5.6) they travel with minimal dispersion. This confirms that the coherence is best preserved when the optimal ballistic dynamics is induced. In the latter the induced coherent propagation makes $\langle S^z_{\rm B}(t^*)\rangle$, at the arrival time $t^* \simeq N$, an almost perfect reproduction of the initial magnetization $\langle S^z_{\rm A}(0)\rangle$ of the qubit A, while in the non-optimal case the dynamics is apparently more dispersive. In the next section we show that such dynamics does in fact correspond to high values of the quality estimators for the state and entanglement transfer.

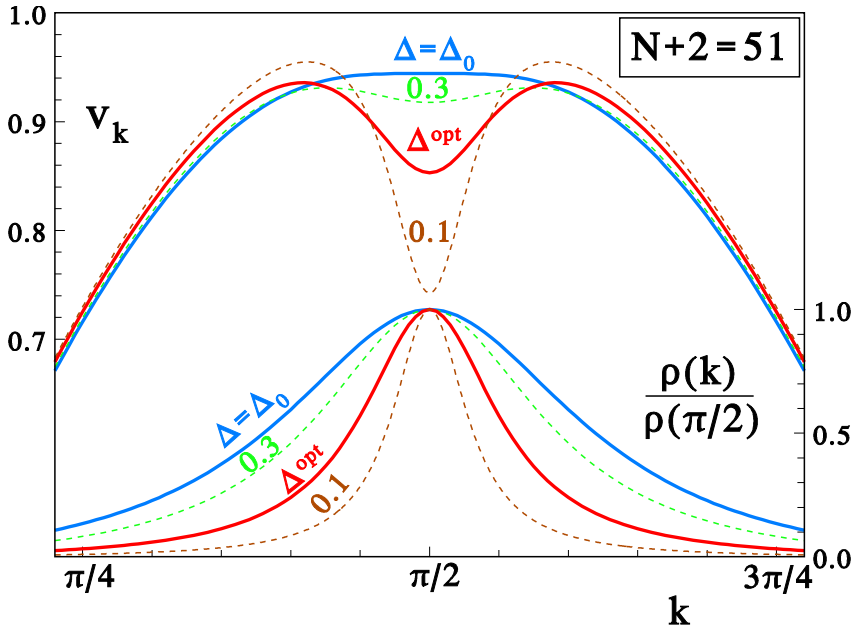

Figure 5.4 – The 'group velocity' $v_k \equiv [(N+3)/\pi]\, \partial_n E_{k_n}$ and $\rho(k)$ vs k for different values of Δ. The thicker curves correspond to $\Delta_0 = 0.3944$ (5.19) that gives the flat behaviour at k_0, and to $\Delta^{\rm opt} \simeq 0.1825$.

5.3 Information transmission exploiting optimal dynamics

The requirement (5.7), means that the state is not rotated by the dynamics when it arrives on site B, though during the evolution it may undergo a rotation around the z axis. In [108] it has been shown that $\phi_u(t^*) = -\frac{\pi}{2}(N+1)$ at the transmission time t^*. Therefore, also without applying a counter-rotation on qubit B [82], condition (5.7) can be fulfilled by choosing $N = 4M \pm 1$ where the sign $\pm$ is given by (5.6) and thus depends on the initial state of the chain. In the following we assume that conditions (5.6) and (5.7) are always satisfied.

Let us consider for the moment that Γ and B are initially in the fully polarized state $|{\downarrow}{\downarrow}\cdots{\downarrow}\rangle \otimes |{\downarrow}\rangle$. In that case $A(t) \equiv 0$ and the transmission fidelity (5.8), as well as the concurrence (5.9), only depend on, and monotonically increase with, $u(t)$. The best attainable information transfer quality corresponds therefore to the maximum amplitude $u_{\rm opt} \equiv u(t^*, \Delta^{\rm opt})$. In Fig. 5.7 and in Table. 5.1 we report these values together with the corresponding optimal $\Delta^{\rm opt}$ as a function of the chain length N in a logarithmic scale; the inset shows that $\Delta^{\rm opt}$ obeys the same power-law behaviour predicted in (5.19) for Δ_0. Fig. 5.7 also shows that for larger and larger N the maximal amplitude $u_{\rm opt}$ does not decrease towards zero, but it rather tends to a constant value of about 0.85, which is surprisingly high, as, e.g., it corresponds to an average fidelity $\mathfrak{F}(t^*) \gtrsim 0.9$ (see Fig. 5.8). This can indeed be proven: we show in C.3 that

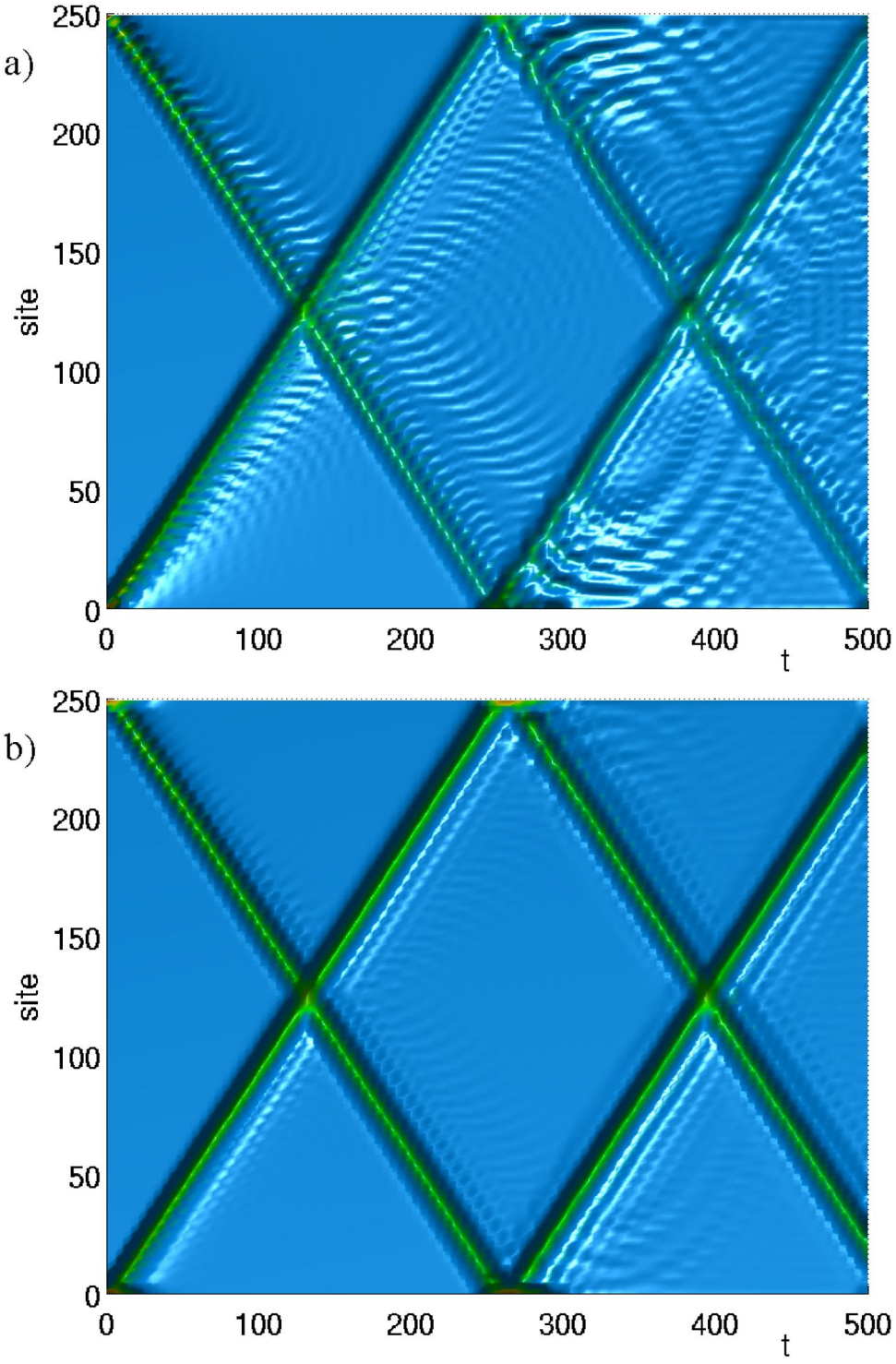

Figure 5.5 – Dynamics of the magnetization $\sigma_i^z(t)$ at time t and site i when a) $j_0 = 1$ and b) $j_0 = j_0^{\text{opt}}$. The initial state of the whole system is $|\uparrow\rangle \otimes |\downarrow\downarrow \cdots \downarrow\rangle \otimes |\uparrow\rangle$ and the length of the chain is $N+2 = 250$.

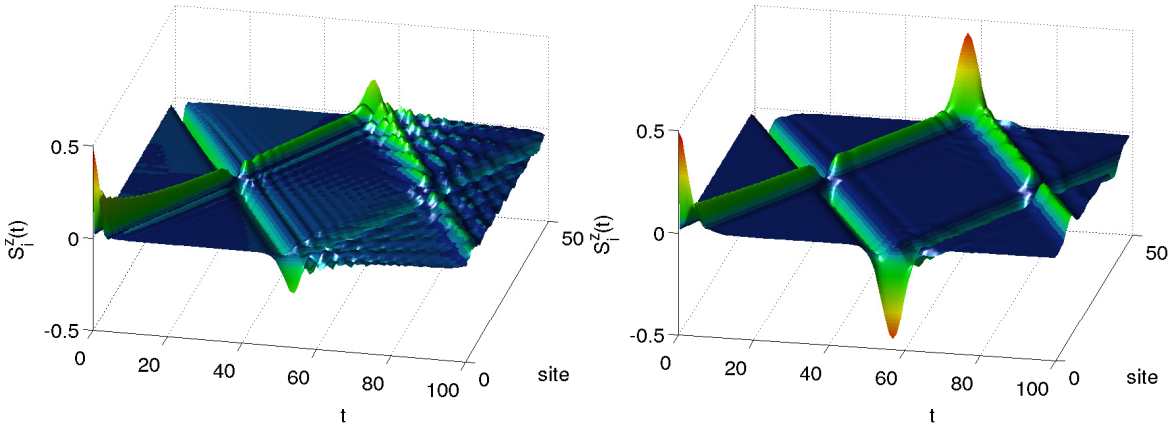

Figure 5.6 – Time evolution of the on-site z-magnetization for $N=50$ and an initial state $|\uparrow\rangle|\Omega_\Gamma\rangle|\downarrow\rangle$; the qubit-wire coupling is $j_0=1$ (left) and $j_0=j_0^{\rm opt}=0.58$ (right).

in the limit of $N\to\infty$ the optimized amplitude tends to $u_{\rm opt}=0.8469$. Basically, this tells us that it is possible to transmit quantum states with very good quality also over macroscopic distances. From (C.36) we can derive the asymptotic behaviour of the optimal coupling

$$j_0^{\rm opt}\simeq 1.030\,N^{-1/6}\,. \tag{5.20}$$

In the optimal ballistic case the bus initialization is not crucial, as different initial states satisfying (5.6) give rise to almost the same dynamics. In fact, the term $C_{N+1}(t)$ entering (5.4) essentially embodies the effect of bus initialization and it is expected to be small at t^*: since $u(t^*)\simeq 1$ in the optimal case, the dynamical prefactors $U_{N+1,j}(t^*)$ in (5.5) are expected to be small for $j\neq N+1$ as the matrix $U(t)$ is unitary. This is apparent in figure 5.9, where for $j_0=j_0^{\rm opt}$, $C_{N+1}(t^*)$ stays well below 0.1 for N as long as 1000.

The transmitted entanglement, as measured by the concurrence (5.9), is shown in Fig. 5.10 as a function of j_0 and t, with the bus initially prepared in its ground state. As expected, the peak of the transmitted concurrence is observed for $j_0=j_0^{\rm opt}$; away from $j_0^{\rm opt}$ the quality of transmission falls down because $u(t^*)$ decreases and, accordingly, $A(t^*)$ is allowed to increase. In fact, in the non-optimal ballistic case the quality of entanglement transfer does depend on the initial state of the bus [113, 82]; for instance, when $j_0=1$ and the chain is initially in its ground state, the contribution of the overlap terms $\mathrm{Tr}[\rho^\Gamma c_j^\dagger c_{j'}]$ in (5.5) is not quenched by the dynamical prefactors, and higher values of $C_{N+1}(t^*)$ (see figure 5.9) inhibit the transmission of entanglement even if $u(t^*)\neq 0$.

The effect of the optimization of j_0 is clearly evident in the time behaviour, reported in figure 5.11, of the minimum fidelity $\mathfrak{F}^{\rm min}(t)$ given by (2.25): its peak for $j_0^{\rm opt}$ occurs at the arrival time $t^*=N+3+s$ with a time delay s that agrees with the asymptotic value $s\simeq 2.29\,N^{1/3}$ derived in C.3. The 'reading time', i.e., the time interval during which the qubit B keeps being in the transferred quantum state, is $t_{\rm R}\simeq\Delta^{-1}$, as the same figure also shows; note that, in

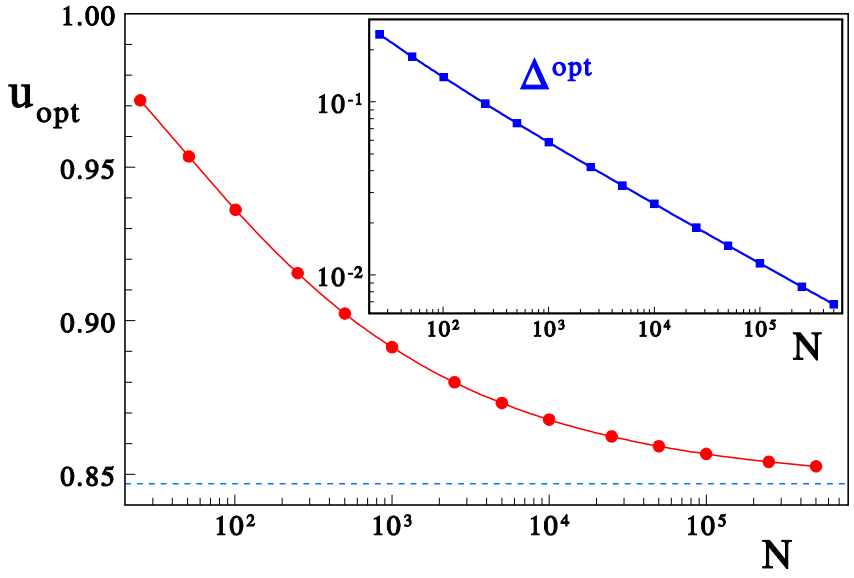

Figure 5.7 – Behaviour of the maximum attainable amplitude u_{opt} and (inset) of the corresponding optimal value of Δ^{opt} vs logarithm of the chain length N. The horizontal dashed line is the infinite N limit of u_{opt}.

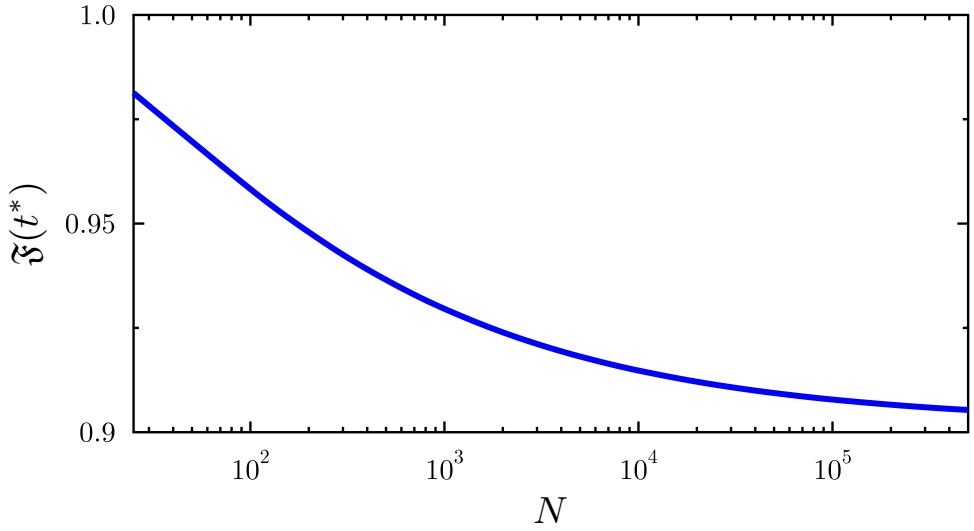

Figure 5.8 – Scaling of the average fidelity at the transmission time and for $j_0 = j_0^{\mathrm{opt}}$ as a function of the length N.

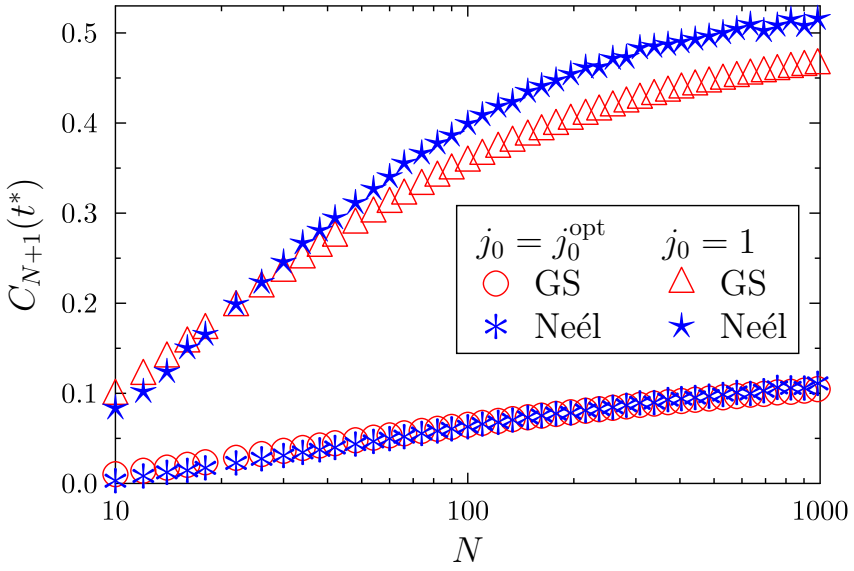

Figure 5.9 – $C_{N+1}(t^*)$ for different initial states of the chain (ground state, anti-ferromagnetic Neél state, and series of singlets [82]) when $j_0 = j_0^{\text{opt}}$ and $j_0 = 1$. The results for a series of singlets are numerically indistinguishable from those with the Neél state.

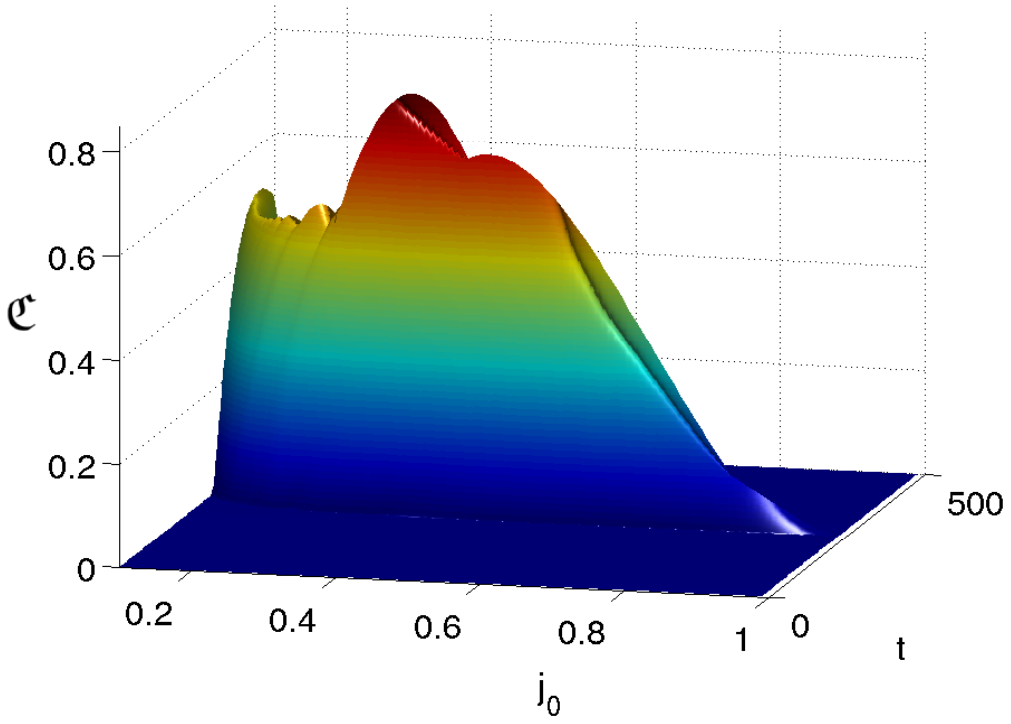

Figure 5.10 – Evolution of the concurrence $\mathfrak{C}$ vs $j0$ and t. The length of the chain is $N+2=250$.

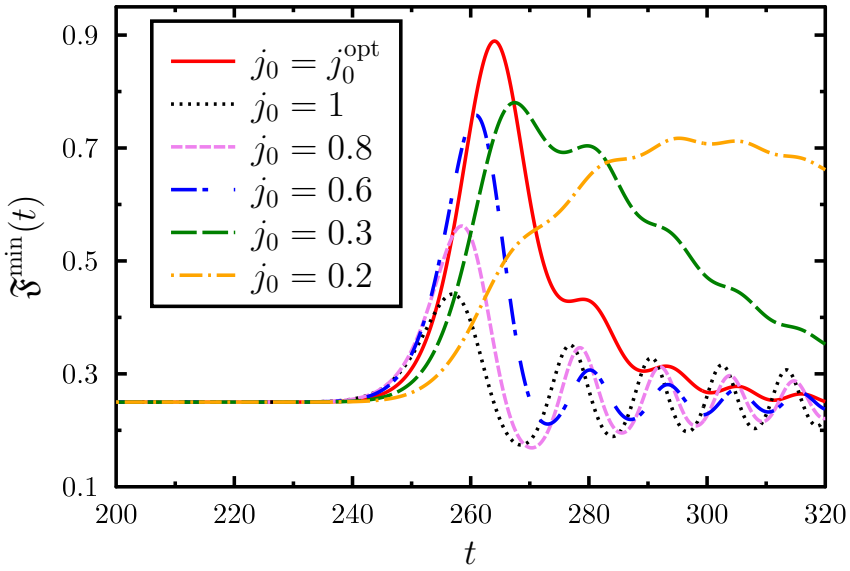

Figure 5.11 – Minimum fidelity vs time for different values of j_0. The length of the chain is $N+2=251$ and $j_0^{\rm opt}=0.422$.

the optimal case, $t_{\rm R}$ increases with N according to the asymptotic behaviour $t_{\rm R}\simeq 1.89\,N^{1/3}$.

5.4 Concluding remarks

In [68, 114] we have shown that high-quality quantum state and entanglement transfer between two qubits A and B is obtained through a uniform XX data-bus of arbitrary length N by a proper choice of the interaction j_0 between the bus and the qubits. The value of such interaction is found to control the transfer regime of the bus, which varies, as j_0 increases, from the Rabi-like one, characterized by very long transmission time, to an intermediate regime, which turns useless for the purpose of quantum communication, and finally becomes ballistic for j_0 of the order of the intra-bus interaction.

In order to get coherent transfer in the ballistic regime, it is desirable that the k-density of the travelling wavepacket generated by Alice's initialized qubit A be narrow and concentrated in the linear zone of the dispersion relation, i.e., with equispaced frequencies. As the parameter j_0 controls both the width of the k-density and the spacings of the frequencies entering the dynamics, one can therefore improve the transmission quality up to a best balance obtained for an optimal value $j_{\rm opt}(N)$ which for large N behaves as $j_{\rm opt}(N)\simeq 1.03\,N^{-1/6}$. Remarkably, we have found that for such a choice the quantum-state-transfer quality indicators are very high and, indeed, have a lower bound for $N\to\infty$ that still allows to efficiently perform quantum-information tasks: e.g., the average fidelity of state transmission is larger than 90 %. Moreover, as remarked in Section 5.2.1, a fine-tuning of j_0 (and/or N) is not required, since even a relatively large mismatch from the optimal value does not affect sig-

nificantly the quality of transmission.

The ballistic regime ensures fast transmission on a time scale of the order of N, at variance with the Rabi-like regime, and in the optimal case the reading time increases as $N^{1/3}$. It is also to be noted that, if experimental settings constrain to a given value $j_0^{\rm exp}$, yet one can optimize the chain length in such a way that $j_0^{\rm exp} = j_0^{\rm opt}(N)$. The only requirement on the initial state of the receiving qubit B and the spin bus is to possess $U(1)$ symmetry, a condition that can be fulfilled by several configurations concerning the spin bus, ranging from the fully polarized state to the highly-entangled ground state. If a large magnetic field can be switched on during the initialization procedure (in order to fully polarize the data-bus), and switched off as soon as the transmission starts, then, from our analytical treatment it emerges that temperature is not a major issue as far as the dynamical evolution of the data-bus is concerned, though low temperatures are obviously necessary to protect the qubits from phase and amplitude damping due to the solid-state environment.

To judge if the proposed scheme identifies a reasonable experimental framework, let us estimate the magnitude of the involved physical quantities. Consider a solid-state implementation with lattice spacing of about 10 Å and intrachain exchange $J \simeq 10^2$ K. A quantum state will then be transferred with fidelity 90 % along a bus of length 1 cm ($N \simeq 10^7$) using $j_0 \simeq 1.03\, N^{-1/6}\, J \simeq 7.0$ K, with transmission time $t = N\hbar/(k_{\rm B}J) \simeq 0.75\,\mu$s and reading time $t_{\rm R} \simeq 1.9\, N^{1/3}\, \hbar/(k_{\rm B}J) \simeq 0.03$ ns.

6

Optimal dynamics with the XY model

In this chapter we study the ballistic regime in more complicated models [115]. As in the previous chapter, the channel (Fig. 5.1) we consider is realized by a *uniform* (i.e., with identical exchange coupling $J=1$ between neighbors) spin chain Γ of length N, to which an external magnetic field h can be applied. In particular, we choose the XY model, which also allows for an anisotropy parameter γ and can be analytically approached as described in section 3.2. The only interactions that can be different are the endpoint exchange coupling j_0 to A and B, and the local magnetic field h_0 on A and B; these parameters are assumed to be identical for A and B, so that the overall system is mirror-symmetric.

Using the labels $i=1,\dots,N$ for the chain and $i=0$ and $i=N+1$ for the endpoint spins A and B, the total Hamiltonian reads

$$H=\sum_{i=1}^{N-1}\left[(1+\gamma)S_i^xS_{i+1}^x+(1-\gamma)S_i^yS_{i+1}^y\right]+h\sum_{i=1}^{N}S_i^z+$$
$$+j_0\sum_{i=0,N}\left[(1+\gamma)S_i^xS_{i+1}^x+(1-\gamma)S_i^yS_{i+1}^y\right]+h_0(S_0^z+S_{N+1}^z)\,.$$

The figures of merit for both state and entanglement transmission can be written using the same language of Section 3.2. Thanks to the mirror-symmetry of the Hamiltonian, the Eqs. (B.24) holds:

$$U_{N+1,0}(t)=\sum_k O_{k,0}O_{k,N+1}\cos(\omega_k t)-i\frac{O_{k,0}^2+O_{k,N+1}^2}{2}s_k\sin(\omega_k t)\,, \tag{6.1}$$

$$V_{N+1,0}(t)=\sum_k \frac{O_{k,0}^2-O_{k,N+1}^2}{2i}s_k\sin(\omega_k t). \tag{6.2}$$

We assume that $s_k\simeq(-1)^k$ and $O_{k,0}\simeq\pm(-1)^kO_{k,N+1}$. These relations are exact in the XX case and are true with some approximation even in the XY case in most practical situations, i.e. when we found that $U_{N+1,0}(t^*)\approx 1$ and $V_{N+1,0}(t^*)\approx 0$ at the transmission time t^*. The approximated evolution operator $u(t)=|U_{N+1,0}(t)|$ is thus

$$u(t)\approx\left|\sum_k\rho(k)e^{i(\pi k\pm\omega_k t)}\right|\,,\qquad\qquad \rho(k)=O_{k,0}^2\,, \tag{6.3}$$

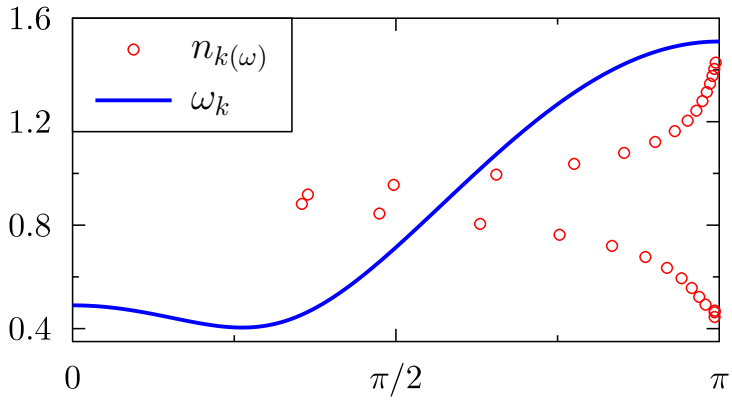

Figure 6.1 – Dispersion relation of the spin-$\frac{1}{2}$ XY chain for $\gamma = 0.5$ and $h = 0.54$. The bell-shaped distribution $n_{\rm opt}(\omega)$ (circles) is the optimized density of excitations vs. ω, corresponding to $h_0 = 0.85$ and $j_0 = 0.48$.

and $\rho(k)$ is the density of excitations in the XY case.

The induction of a coherent dynamics in the XY model begins, as in the XX case, with the analysis of the dispersion relation in the infinite chain limit,

$$\omega_k = \sqrt{(h-\cos k)^2 + \gamma^2 \sin^2 k}\,, \tag{6.4}$$

displayed in Fig. 6.1. One can easily spot the existence of more or less wide regions of linearity in the neighborhood of the inflection point(s) k_0, where $\omega_k \approx \text{const} + v\,k$ holds. By tuning $h_0 \simeq \omega_{k_0}$, the peak of $\rho(k)$ is made to sit at k_0. Indeed, in the weak coupling limit $j_0 \ll 1$, only the modes which are almost resonant with the local energy h_0 of the external qubits are engaged in the dynamics. When j_0 increases more modes are involved and the optimal coupling $j_0^{\rm opt}$ is then numerically determined[1] so as to fulfill Eq. (4.14).

The dispersion relation strongly depends on the parameters of the bus Hamiltonian, γ and h: in particular, the region of linear dispersion sensibly shrinks as the anisotropy γ increases, which might make the bus to be useless; however, the linear region can be extended again by increasing the field h: therefore, one can act on the latter parameter so as to fulfil the conditions for optimal dynamics. For example, in the extreme case of the Ising chain ($\gamma = 1$) for $h = 0$ the dispersion relation becomes flat and does not allow for propagation; however, a wide linear region can yet be obtained by applying a finite h on Γ.

[1] Indeed, in the XY case the analytical expression for the density of excitations is unavailable, with the exception of the Ising ($\gamma = 1$) case which will be analysed in the following, and we can only rely on the simpler condition (4.14), without the analysis of the shifts (5.18).

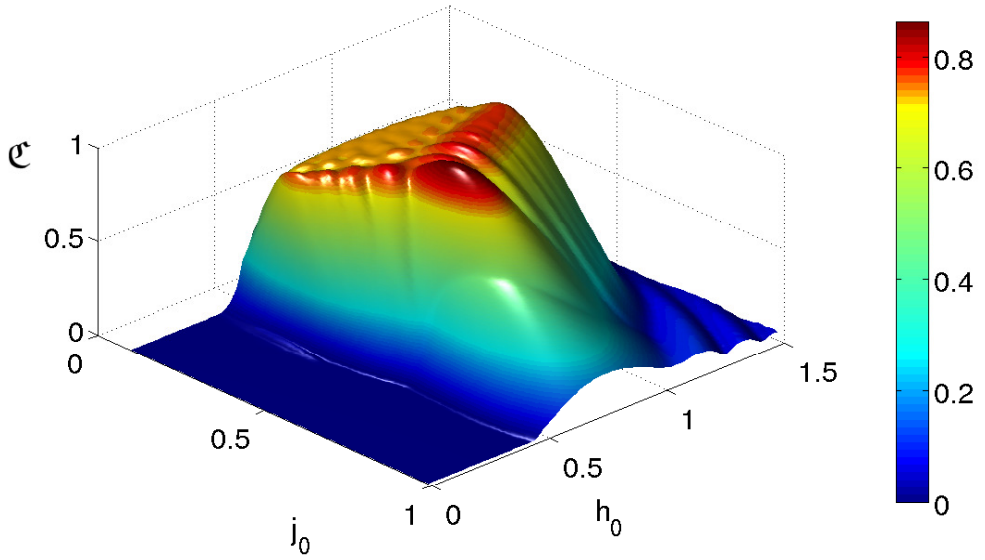

Figure 6.2 – Concurrence vs j_0 and h_0 for $\gamma=0.5$ and $h=0.54$. The chain length is $N=50$.

6.1 Optimal transfer

In the XX case without applied magnetic field we have seen that the inflection point $k_0=\pi/2$ corresponds to $\omega_{k_0}=0$. There is no need for an applied magnetic field because $\rho(k)$ is already peaked around this minimum energy, which is notably also the energy at the center of the linear zone. The width of $\rho(k)$ only depends on the coupling j_0 and reads $\Delta=j_0^2/(2-j_0^2)$. Therefore, Eq. (4.14) ensures the existence of an optimal coupling $j_0^{\rm opt}$ which, at leading order, is $j_0^{\rm opt}\propto N^{-\frac{1}{6}}$. More detailed arguments are given in Chapter 5.

In the XY case the analytical expressions are more complicated and the optimal parameters are found numerically. Here we consider the transmission of entanglement, following the scheme of Fig. 5.1: the state of qubit A, which at $t=0$ is maximally entangled with C, propagates through the bus when j_0 is switched on; if the information were transmitted exactly, at some arrival time t^* the qubit B should be maximally entangled with C. Therefore, the natural estimator of the quality of entanglement transmission is the maximum (reached at t^*) of the transmitted concurrence $\mathfrak{C}(t)$, as given by (3.22).

The dispersion relation of the XY model (6.4) is gapped, making $\omega_{k_0}\neq 0$. Hence, at variance with the XX case, we have to switch on a local magnetic field $h_0\simeq\omega_{k_0}$, in order to increase the average energy of the initial state and make $\rho(k)$ peaked around the linear zone. In Fig. 6.2 we plot $\mathfrak{C}(t^*)$ for different j_0 and h_0, in the XY model with $\gamma=0.5$ and $h=0.54$. It is clear that for fixed j_0 the best transmission is achieved when $h_0\simeq\omega_{k_0}\simeq 0.89$. With decreasing j_0, the distribution $\rho(k)$ shrinks in width and the range of the optimal h_0 extends over the whole linear dispersion zone. On the other hand, decreasing j_0 causes the packet to become delocalized along the chain and the result is that there exists an optimal interme-

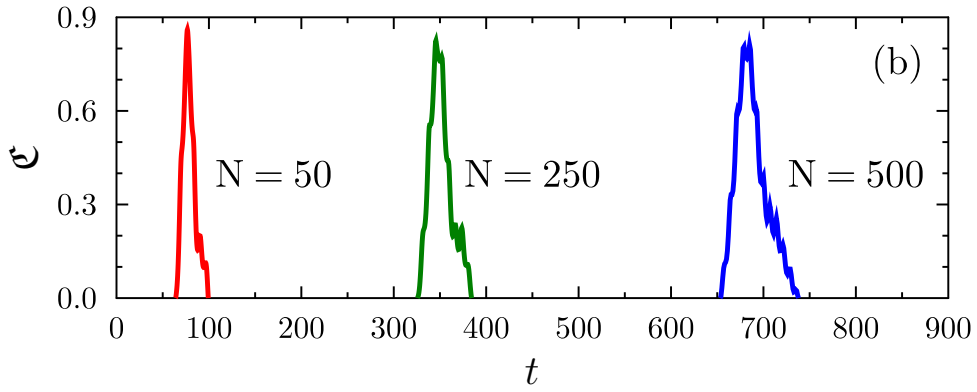

Figure 6.3 – (b) Time evolution of the concurrence for different data-bus lengths; $\gamma=0.5$, $h=0.54$, $h_0=0.85$, and $j_0=0.49$, 0.39, 0.34 for $N=50$, 250, 500, respectively.

diate value, $j_0 = 0.49$, in agreement with Eq. (4.14), for obtaining an almost dispersionless transmission.

Very good transmission is obtained also for considerably large N, as show in Fig. 6.3.

6.1.1 Ising case

The region of linear dispersion shrinks for increasing anisotropy γ, while in the Ising limit ($\gamma=1$) with $h=0$ one has $\omega_k=1$, which does not allow for propagation. This explains the observation [113] that in such limit no entanglement propagation takes place: indeed, a vanishing group velocity means that nothing can be transmitted over the chain. However, applying a finite h on Γ fixes the problem by inducing a finite group velocity.

The Ising model with open ends is diagonalized as explained in Section (C.1.2), and the density of excitations (C.26) is obtained. In particular, we found that $\rho(k)$ is peaked around (C.28)

$$\bar{\omega}=\sqrt{\frac{2h_0^2+(1-h^2)j_0^2}{2-j_0^2}}\,,$$

and the width of this peak is given by (C.23)

$$\Delta=\frac{hj_0^2}{\sqrt{h^2(2-j_0^2)^2-(h_0^2+j_0^2-1-h^2)^2}}\,.$$

For making the optimal dynamics to emerge, the peak must be in the linear zone of the dispersion relation Eq. (6.4) with $\gamma=1$, i.e., $\bar{\omega}=\sqrt{|1-h^2|}$. This condition is satisfied by setting

$$h_0=\begin{cases}\sqrt{(1-j_0^2)(1-h^2)} & \text{for} \quad |h|\leq 1\,,\\ \sqrt{h^2-1} & \text{for} \quad |h|\geq 1\,,\end{cases} \tag{6.5}$$

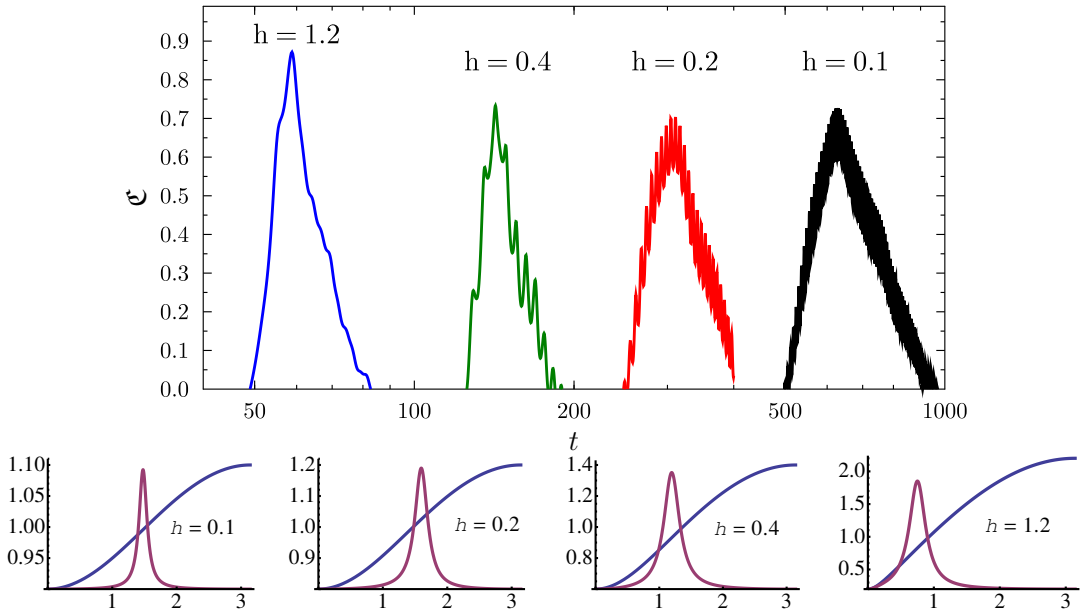

Figure 6.4 – Concurrence (top), dispersion relation and density of excitations (bottom) for the case of the Ising chain ($\gamma=1$) for different fields $h = 0.1$, 0.2, 0.4, 1.2. The corresponding optimized endpoint interactions are $h_0 = 0.94$, 0.93, 0.82, 0.82 and $j_0 = 0.39$, 0.43, 0.48, 0.48. The chain length is $N=50$.

and the corresponding width is

$$\Delta = \frac{\max\{|h|,1\}}{\sqrt{|1-h^2|}}\,\frac{j_0^2}{2-j_0^2}\,, \tag{6.6}$$

while Δ diverges at the critical value $h = 1$. However, as Eq. (6.5) for $h = 1$ forces $h_0 = 0$, and accordingly (C.29) imposes $O_{k,N+1} = 0$, the above analysis, based on (6.3), does not hold at $h = 1$. Indeed when $O_{k,N+1} = 0$ it follows that $U_{N+1,0}(t) = V_{N+1,0}(t)$, and according to (3.22) and (3.19) the corresponding transmission is very bad. Notice that the width Δ has a prefactor, as compared with the XX case, which is greater than 1. The optimal j_0 is then expected to be smaller than the XX counterpart.

In Fig. 6.4 we analyze the entanglement transmission in an Ising chain for various h, with the optimal value for the parameters j_0 and h_0. Raising h the linear zone gets larger in energy, and, furthermore, the group velocity increases, making the transmission faster and better.

6.2 Concluding remarks

We have devised a procedure for achieving high-quality entanglement transmission between distant qubits. The procedure relies on tuning the qubit interaction and the coupling

with a homogeneous quantum data-bus in order to induce a coherent ballistic dynamics. There is no need for a specific design neither of the bus, nor of its initial state. Our approach is then tested with the spin-$\frac{1}{2}$ XY model and extremely good entanglement transfer is obtained. Due to the induced ballistic dynamics, the transfer time scale is considerably shorter than in previous works [116, 97, 117, 107, 118] and essentially depends only on the group velocity of the elementary excitations, which can be increased by varying the parameters of the data-bus. Moreover, the quality of the state and entanglement transfer that we obtain only weakly deteriorates as the length of the bus increases.

7

Entangling gates between distant qubits

Universal quantum computation can be achieved by arbitrary local operations on single qubit and one two-qubit entangling gate [119]. While single qubit operations are easily achieved by local actions, the story is very different for the two qubit gate. In an array of spins an entangling gate between neighboring qubits can be accomplished by letting them interact. However, for non-neighboring qubits, a direct interaction is normally not possible, especially without disturbing the intervening qubits, unless there is a separate common bus mode [120] or flying qubits. In realizations without an additional bus mode, such as with cold atoms in optical lattices, one cannot choose an arbitrary pair of atomic qubits for a gate operation and usually gates parallely occur between all neighboring pairs [121]. Thus, designing bus modes for logic gates between arbitrary and distant pairs of qubits is of utmost importance in any physical realizations and various unconventional examples of buses are continuously being proposed [122, 123, 67]. One possible realization is to have both the qubits and the bus composed of the same physical objects, generally called spin chains. The quality of an unmodulated spin chain, even as a data-bus, is affected by dispersion [112, 113]. Thus, in order to have a quantum gate between two qubits through such buses [124, 125, 126, 67], delocalized encodings over several spins [90], delicately engineered couplings [85] or very weak couplings between qubits and the bus [67] is thought to be necessary. Here we exploit the high quality state transmission assured by the coherent ballistic dynamics described in the previous chapters for achieving an entangling quantum gate between arbitrarily distant qubits. This is a very general mechanism and potentially applicable to a variety of physical systems. In this chapter we will consider also its applicability to one specific setup.

Cold atoms in optical lattices are now an established field for testing many-body physics [54, 55, 56, 57, 58, 59]. In particular, chains of atoms in Mott insulator regime (one atom per site) are being built experimentally [57, 58, 59], paving the way for realizing spin Hamiltonians [60]. With recent progress in cooling methods, the required temperatures for observing correlated magnetic quantum phases has become experimentally reachable [64]. In this framework, series of multiple two-qubit gates, acting globally and simultaneously, have

been proposed [127] and then realized [56]. Could the same framework solve the problem of realizing quantum gates between any two selected neutral atom qubits? This is still an outstanding problem, unless one uses the physical movements of neutral atoms to each other's proximity [128, 129]. While such movements may still have the ability to create a scalable neutral atomic quantum computer [130], alternative methodologies, without the complexity of mechanical processes, are worth pursuing for long range scalable gates, for the sake of simplicity.

Recently, single site addressing in an optical lattice setup has been experimentally achieved [58, 59]. Furthermore, local traps have been proposed for individual atoms using Near Field Fresnel Diffraction (NFFD) light [131]. A new approach for scalable quantum computation has been suggested [132] through a combination of local NFFD traps, for qubits, and an empty optical lattice, for mediating interaction between them. Since the interaction is achieved through controlled collisions between *delocalized* atoms it may suffer a high decoherence when qubits, on which the gate is applied, are far apart [56].

In this chapter we describe our scalable, non-perturbative (i.e. not relying on weak couplings) dynamical scheme [108] for achieving high-quality entangling gates between two arbitrarily distant qubits, suitable for subsequent uses without resetting. Unlike previous proposals, we do not demand encoding, engineering or weak couplings: we only need switchable couplings between qubits and the bus. We have also proposed an application, based on a combination of NFFD traps and optical lattices, which is robust against possible imperfections.

7.1 Introducing the model

Let us describe our bus as a chain of spin 1/2 particles interacting through

$$H_\Gamma = J \sum_{n=1}^{N-1} \left(\sigma_n^x \sigma_{n+1}^x + \sigma_n^y \sigma_{n+1}^y + \lambda \sigma_n^z \sigma_{n+1}^z \right), \tag{7.1}$$

where σ_n^α ($\alpha = x, y, z$) are Pauli operators acting on site n, J is the exchange energy and λ is the anisotropy. The qubits A and B, on which the gate acts, sit at the opposite sides of the bus, labeled by site 0 and $N+1$ respectively. The interaction between the bus and the qubits is

$$H_I = j_0 \sum_{n=0,N} \left(\sigma_n^x \sigma_{n+1}^x + \sigma_n^y \sigma_{n+1}^y + \lambda \sigma_n^z \sigma_{n+1}^z \right), \tag{7.2}$$

where the coupling j_0 can be switched on/off. For the moment the anisotropy λ is set to zero. Initially the qubits are prepared in the states $|\psi_A\rangle$ and $|\psi_B\rangle$ and decoupled from the bus which is in the state $|\psi_\Gamma\rangle$, an eigenstate of H_Γ, for instance the ground state. Since H_Γ commutes with the parity operator $\prod_{n=1}^N (-\sigma_n^z)$, the state $|\psi_\Gamma\rangle$ has a definite parity $(-1)^p$, for some integer p. At time $t = 0$ the coupling j_0 is switched on and the whole system evolves

under the effect of the total Hamiltonian $H = H_\Gamma + H_I$, i.e. $|\Psi(t)\rangle = e^{-iHt}|\psi_A\rangle|\psi_\Gamma\rangle|\psi_B\rangle$. In chapter 5 it was shown that by properly tuning j_0 to an optimal non-perturbative value $j_0^{\rm opt} \simeq 1.03JN^{-1/6}$ one can make the linear part of the dispersion relation to rule the dynamics, thus almost satisfying the mirror-inversion condition [124] and resulting in a fast high-quality transmission. In fact, when $|\psi_B\rangle$ is initialized in either $|0\rangle \equiv |\uparrow\rangle$ or $|1\rangle \equiv |\downarrow\rangle$ an arbitrary quantum state of A is transmitted almost perfectly to B after time $t^* \simeq (0.25N + 0.52N^{1/3})/J$. When $j_0 = j_0^{\rm opt}$ the dynamical amplitude $u(t) = |U_{0,N+1}(t)|$ satisfies $u(t^*) \simeq 1$, and thus we set $U_{0,N+1}(t^*) = e^{i\alpha_N}$.

In any transmission problem there always might be an overall phase which is irrelevant to the quality of transmission. However, exploiting this phase is the heart of our proposal [108] for obtaining an entangling two-qubit gate between A and B. We define $|\Psi_{ab}\rangle = |\Psi(0)\rangle$ with $|\psi_A\rangle = |a\rangle$ and $|\psi_B\rangle = |b\rangle$ where $a, b \in \{0,1\}$. When j_0 is switched on the whole system evolves and at $t = t^*$ the states of A and B are swapped (see Fig. 5.6), while the bus takes its initial state $|\psi_\Gamma\rangle$, as a result of the mirror inverting dynamics. Therefore, an almost perfect transmission is achieved with an overall phase ϕ_{ab}, namely $e^{-iHt^*}|\Psi_{ab}\rangle \approx e^{i\phi_{ab}}|\Psi_{ba}\rangle$. The explicit form of ϕ_{ab} follows from the dynamics depicted above with the freedom of setting $\phi_{00} = 0$. For instance to get ϕ_{10} we have

$$\begin{aligned} e^{-iHt^*}|\Psi_{10}\rangle =& e^{-iHt^*} c_0 \,|\Psi_{00}\rangle \simeq U_{0,N+1}(-t^*)\, c_{N+1}\,|\Psi_{00}\rangle = \\ =& (-1)^{p+1} e^{-i\alpha_N}\,|\Psi_{01}\rangle \equiv e^{i\phi_{10}}\,|\Psi_{01}\rangle. \end{aligned} \tag{7.3}$$

This defines $\phi_{10} = (p+1)\pi - \alpha_N$ while $\phi_{01} = \phi_{10}$ due to the symmetry of the system. With similar argument we get $\phi_{11} = \pi - 2\alpha_N$. Therefore, the ideal mirror-inverting dynamics defines a quantum gate G between A and B, which reads $G|ab\rangle = e^{i\phi_{ab}}|ba\rangle$ in the computational basis. Irrespective of the value of α_N when the pair A, B is initially in the state of $|{+}{+}\rangle$, where $|+\rangle = (|0\rangle + |1\rangle)/\sqrt{2}$, the application of the gate G results in a maximally entangled state between A and B. Furthermore, the phase α_N is found to be equal to $\frac{\pi}{2}(N+1)$.

Since the dynamics is not perfectly dispersionless, $|U_{0,N+1}(t^*)|$ is not exactly 1, meaning that there is some entanglement between the bus and the qubits which prevents the gate G from being a perfect unitary operation. In fact, the dynamics of the qubits is generally described by a completely positive map: $\rho_{AB}(t) = \mathcal{E}_t\left[\rho_{AB}(0)\right]$. To quantify the quality of the gate we calculate average gate fidelity $\mathcal{F}_G(t) = \int d\psi\, \langle\psi|G^\dagger \mathcal{E}_t\left[|\psi\rangle\langle\psi|\right] G|\psi\rangle$ where the integration is over all possible two-qubit pure states. Using (2.9) for $d = 4$ we get

$$\mathcal{F}_G(t) = \frac{1}{5} + \frac{1}{5}\langle\Phi^+|\mathbb{1}\otimes G^\dagger \hat{\mathcal{E}}_t\, \mathbb{1}\otimes G|\Phi^+\rangle \tag{7.4}$$

where $|\Phi^+\rangle$ is defined in (2.4) and $\hat{\mathcal{E}}_t$ is the Choi matrix (1.23) associated to the dynamical map $\mathcal{E}_t$, which is numerically evaluated using the techniques described in section C.4.

In Fig. 7.1(a) we plot the time evolution of the average gate fidelity for a bus of length $N = 100$ initially in its ground state: $\mathcal{F}_G(t)$ displays a marked peak at $t = t^*$. The value at the

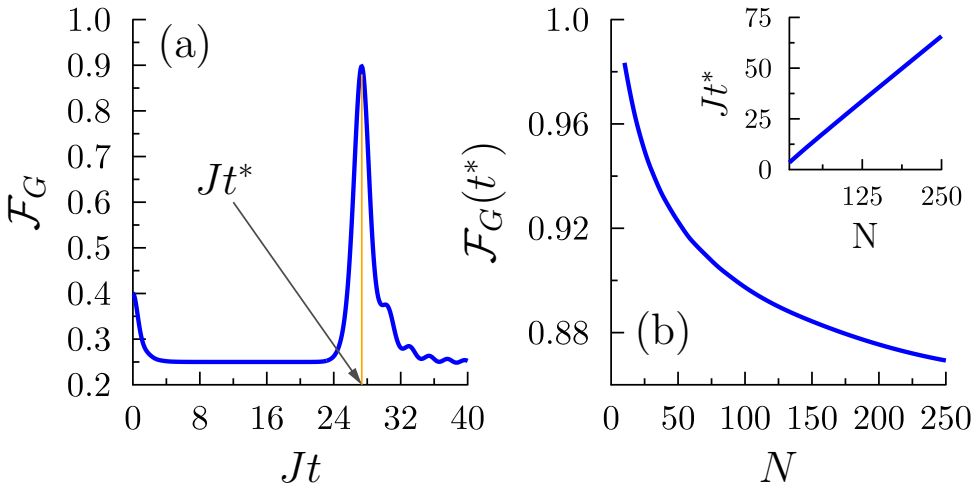

Figure 7.1 – (Color online) (a) Evolution of the average gate fidelity for a chain of $N = 100$ and $j_0 = 0.5J$. (b) $\mathcal{F}_G(t^*)$ as a function of N. Insets show the optimal time versus N.

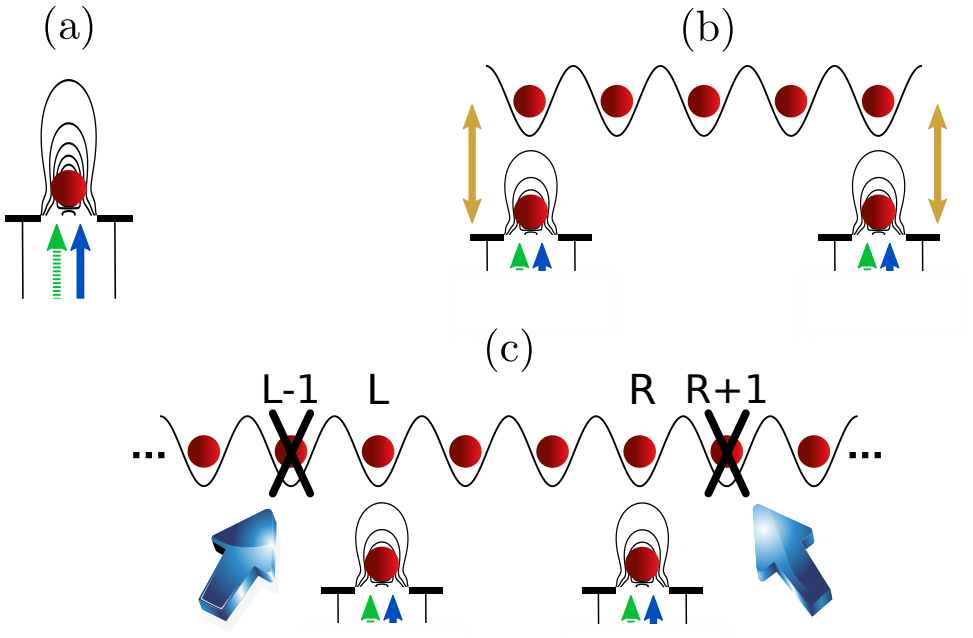

Figure 7.2 – (Color online) (a) Local NFFD trap with two optical fibers, one for trapping (solid blue) and one for unitary single qubit operations (dashed green). (b) Schematic interaction between qubits (local traps) and the ending sites of the bus (optical lattice). (c) Adiabatic cutting of the bus into three parts.

k	1	2	3	4	5	6	7	8
$\mathscr{F}_G(kt^*)$	0.984	0.961	0.939	0.918	0.898	0.879	0.861	0.844
$F_\Gamma(kt^*)$	0.966	0.926	0.884	0.840	0.795	0.748	0.701	0.654

Table 7.1 – $\mathscr{F}_G(kt^*)$ and $F_\Gamma(kt^*)$ for up to 8 subsequent uses of the bus of length $N=8$ without resetting.

peak is plotted as a function of N in Fig. 7.1(b) where we remarkably see that $\mathscr{F}_G(t^*)$ exceed 0.9 even for chains up to $N=100$ and decays very slowly with N. Moreover, as shown in the inset of Fig. 7.1(b) and unlike the perturbative schemes proposed in [97, 67] our dynamics is fast.

Our dynamical gate works properly for arbitrary initial states of the bus with fixed parity. Ideally after each gate application the parity of the bus remains unchanged making it perfect for reusing without resetting. However, initialization in an eigenstate of H_Γ, besides automatically fixing the parity, has the advantage of simplicity for preparation and robustness against disturbance. Let us initially set the bus in its ground state and define $F_\Gamma(t)$ as the fidelity between the ground state of H_Γ and the density matrix of the bus at time t. To see how the quality of the gate operation is affected by k subsequent uses of the bus, we compute $\mathscr{F}_G(kt^*)$ and $F_\Gamma(kt^*)$ which are shown in TABLE I for $k=1,\ldots,8$ subsequent uses.

7.2 Application

We now propose an application of the above gate mechanism for a scalable neutral atom quantum computer with qubits held in static traps. We consider a network of qubits each encoded in two degenerate hyperfine levels of a neutral atom, cooled and localized in a separate NFFD trap [131]. In Fig. 7.2(a) we show a single atom confined in a NFFD trap. The position of the minimum of the trapping potential is controlled by varying the aperture radius [131] through micro electro mechanical system technology, as proposed in [132]. Local unitary operation on each qubit may be applied through an extra fiber, along with the NFFD trapping fiber [132], as show in Fig. 7.2(a). The qubits in the network are connected by a bus realized by cold atoms in an optical lattice, prepared in the Mott insulator regime [57, 58, 59]. The polarization and intensity of lasers are tuned so that one ends up [60] with the effective Hamiltonian of Eq. (7.1). For the moment we assume that the distance between the two qubits, on which we want to apply the gate, is equal to the length of the lattice such that the two qubits interact with the atoms at the ending sites of the lattice, as shown in Fig. 7.2(b). To switch on the interaction H_I between the qubits and the bus we have to move the minimum of NFFD trapping potential slightly higher such that the qubits move upwards and sit at a certain distance from the ends of the lattice. By controlling such distance one can tune

the interaction coupling to be $j_0^{\rm opt}$. In order to simultaneously obtain interactions effectively described by H_Γ and H_I we have to use the same spin dependent trapping laser beams in both NFFD traps and optical lattice.

Now we consider a more general situation in which the optical lattice size is larger than the distance between the two qubits on which we want to apply the gate (see Fig. 7.2(c)). In this case if we simply switch on the interaction between qubits and two intermediate sites (L, R) of the optical lattice, shown in Fig. 7.2(c), the two external parts of the lattice play the role of environment and deteriorate the quality of the gate. To preserve the high quality of our scheme we need to cut the lattice into three parts and separate the bus, extended from L to R, from the rest of the optical lattice. This can be done by adiabatically shining a localized laser beam on the atoms sitting on sites $L-1$ and $R+1$ to drive them off resonance, as shown in Fig. 7.2(c). In this case driving the atom effectively generates a Stark shift between the two degenerate ground state through a highly detuned classical laser beam with strength Ω and detuning $\Delta \gg \Omega$. This provides an energy shift $\delta E = \Omega^2/\Delta$ between the two degenerate ground states, which can be treated as a local magnetic field in the z direction on sites $L-1$ and $R+1$. Keeping Ω/Δ small one can control the strength Ω and detuning Δ such that δE becomes larger than J. When $\delta E \gg J$ the bus is separated from the external parts of the optical lattice. Moreover, as δE adiabatically increases, the bus moves into its ground state, meanwhile splitting up from the rest. Despite the gapless nature of Hamiltonian (7.1) there is always a gap $\propto J/N$ due to the finite size of the bus which guarantee the success of the adiabatic evolution. In Fig. 7.3(a) we plot $F_\Gamma(t)$ over the course of adiabatic cutting when the whole lattice is initially in its ground state. In this adiabatic evolution δE is linearly increased from 0 to $30J$ over the time interval of $100/J$. Once the bus has been prepared in its ground state the gate operation can be accomplished as discussed above. After the operation of the gate one may want to glue the previously split optical lattice and bring it back into its ground state. This can be done easily by adiabatically switching off δE as shown in Fig. 7.3(a) where the fidelity of the state of the whole optical lattice with its ground state is plotted.

7.2.1 Time scale

We now pause to give an estimation of t^* in the *worst* scenario in which N is of the order of whole lattice size ($\simeq 100$), although most gates are much faster due to smaller qubit separations. The typical value for J in optical lattice realization is few hundred Hertz (e.g. $J = 360\,h\,$Hz in [133]). From the inset of Fig. 7.1(b) we get $Jt^* \simeq 30$ for $N = 100$ and thus $t^* \simeq 13\,$ms which is well below the typical decoherence time of the hyperfine levels ($\simeq 10\,$minutes [134]). Though, this is slower than other mechanisms for atomic gates [128, 129] our proposal offers an alternative paradigm without involving physical movement. Note that for static qubits separated by N sites a time $\mathcal{O}(N/J)$ is the best possible in any physical realiza-

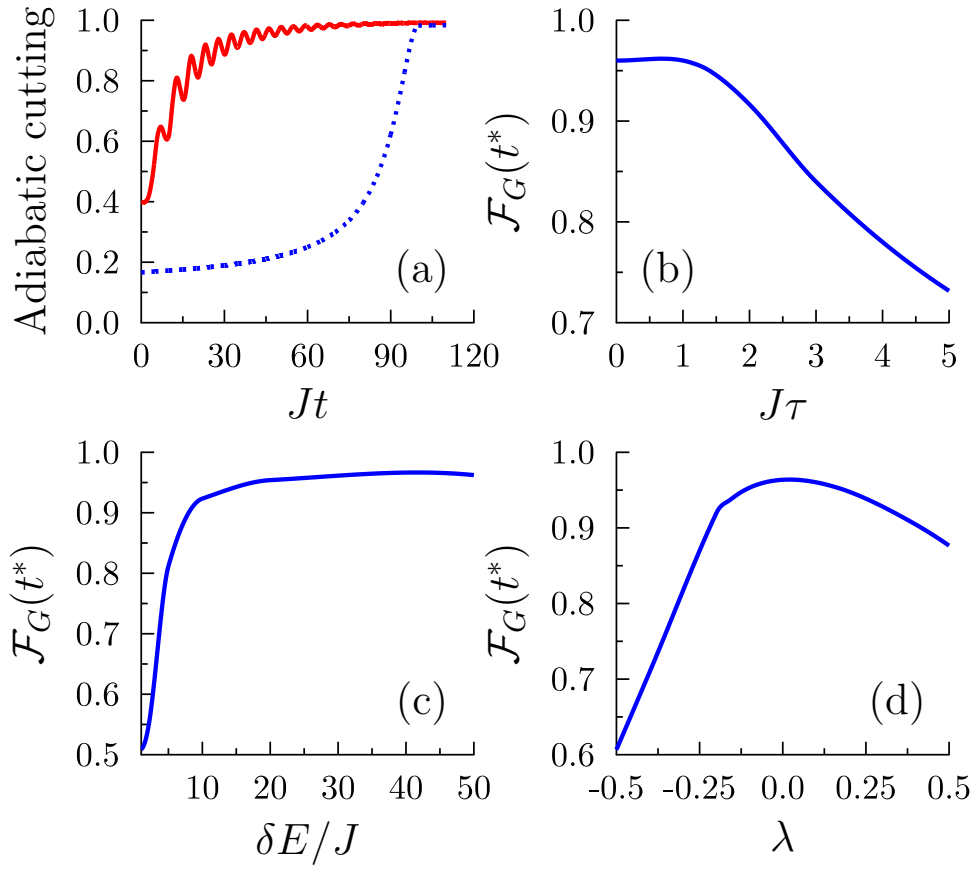

Figure 7.3 – (Color online) (a) Evolution of $F_{\uparrow}(t)$ under the adiabatic cutting (solid red). Evolution of the fidelity between the ground state of the whole optical lattice with the state of the split one under the adiabatic gluing (dashed blue). $\delta E/J$ is linearly varied between 0 and 30 over the time $100/J$. (b) $\mathcal{F}_G(t^*)$ vs. switching time τ over which j_0 is linearly switched on from 0 to j_0^{opt}. (c) $\mathcal{F}_G(t^*)$ vs. $\delta E/J$ after adiabatic cutting of the optical lattice. (d) $\mathcal{F}_G(t^*)$ as a function of anisotropy λ. The length of the bus is set to $N=16$.

tion, e.g. Josephson junction arrays with stronger J.

7.2.2 Imperfections

Cold atom systems are usually clean and almost decoherence free; however, in the above proposed setup there might be some sources of destructive effects which may deteriorate the quality of our scheme. In particular, we consider: (i) gradual switching of j_0; (ii) imperfect cutting of the chain when δE is not large enough; (iii) existence of interaction terms in the Hamiltonian which alter its non-interacting free-fermionic nature. In Fig. 7.3(b) we show $\mathcal{F}_G(t^*)$ when j_0 is gradually switched on from 0 to j_0^{opt} according to $j_0(t)=j_0^{\text{opt}}t/\tau$, as a function of switching time τ. It is indeed of general relevance that a plateau over which $\mathcal{F}_G(t^*)$ remains constant is observed, even for τ as long as $1/j_0$. In Fig. 7.3(c) we plot $\mathcal{F}_G(t^*)$

as a function of the energy splitting δE on which the cutting process is based. As it is clear from Fig. 7.3(c), when $\delta E > 10J$ the bus is well isolated from the external parts, which guarantees the high quality of the gate. We have also studied the effect of the anisotropy λ, possibly entering H_Γ and H_I, due to imperfect tuning of laser parameters [60]. In Fig. 7.3(d) we plot $\mathscr{F}_G(t^*)$ as a function of λ and observe weak deterioration of the gate quality as far as $|\lambda| < 0.2$.

7.3 Concluding remarks

In [108], we have proposed a scalable scheme for realizing a two-qubit entangling gate between arbitrary distant qubits. In our proposal, qubits are made of localized objects which makes single qubit gates affordable. The qubits interact dynamically via an extended unmodulated bus which does not need being specifically engineered and, besides embodying a quantum channel, actively serves to operate the entangling gate. Moreover, thanks to the non-perturbative interaction between the qubits and the bus our dynamics is fast, which minimizes destructive decoherence effects. Provided the coupling between the qubits and the bus is properly tuned, the dynamical evolution of the whole system is essentially dispersionless, thus allowing several subsequent uses of the bus without resetting. Surprisingly, a sudden switching of the coupling is not necessary and our fast dynamical gate mechanism is not altered by a possibly gradual switching: this is of absolute relevance, not only from practical viewpoints but also in a theoretical perspective. Our proposal is general and can be implemented in various physical realizations. Specifically we have proposed an application based on neutral atom qubits in an array of separated NFFD traps connected by an optical lattice spin chain data bus, which are both accessible to the current technology.

Prospects

In this thesis we have theoretically studied the quantum information transmission and exchange between distant parts. Our research has prompted several questions which could be the topic of future examinations. Amongst these, the possible implementation of our scheme using nowadays technology is of particular relevance. Indeed, no experiments have been performed so far on using a spin chain as a quantum data-bus, although this is an active theoretical subject, well motivated from a technological point of view, and there are many experimental candidates for both general purpose quantum computation and quantum information processing [135].

Our scheme has been guided all along by the quest for experimental simplicity, but there are some theoretical simplifications that must be considered in looking for an implementation of the coherent ballistic quantum information transport. The problems that may arise have common factors, which lead to general questions, and specific ones, depending on the particular experimental setup.

Some general problems which can arise irrespective of the specific setup have been investigated in Chapter 7, as the gradual (non-sudden) switching of the coupling between the qubits and the bus, or the role of spurious interactions. In future works other deviations from the ideal case analysed in this thesis will be tackled, notably the role of imperfections, noise and temperature in the quantum transmission capabilities of spin chains. Static imperfections in the couplings between nearest neighbours have been studied in [89], where it is shown that our approach described in Chapter 5, requiring only the ability of controlling the boundaries, is more robust than those requiring the full engineering of the coupling strengths. In Chapter 7 we have also shown that small imperfections in the Hamiltonian do not affect much the dynamics. On the other hand, an exhaustive study of the effects of temperature and system-environment interaction is still missing, even if it is expected that both have negative consequences on the transmission quality [113]. As for the effect of temperature, all the necessary formalism for handling thermal initial states have already been developed (see Appendix B) and we can predict some possible results. For instance, it is clear from (3.15), (5.4), and (5.5) that the dynamics of the magnetization along the z direction is not substantially altered by the temperature, while all the quantities depending on the parity of the initial state do: the average parity of a thermal state (B.20), instead of being an unimportant phase, goes to zero for increasing temperature. Accordingly, a temperature threshold arises, depending on the gap of the Hamiltonian, above which the transmission quality is suppressed [96], though no significant alterations are expected in the dynamics of the z component magnetization. Finally, the study of the possible dynamical interaction with a thermal environment is much more complicated, as the theory needs to be highly expanded; nevertheless in some specific cases the dissipative evolution can be handled using the theory described in [136] or numerically for very small systems.

In addition to the problems described above, whose strength depends on the particular setup, there could be also other specific ones. As a matter of fact, in order to use many-body dynamics for transferring quantum information it is required a long coherence time and the ability of performing single-site addressing and time-dependent measurements. An imperfect implementation of these requisites could introduce further error sources. Understanding whether a current established experimental apparatus can be used as a coherent ballistic quantum data-bus is complicated, as we have to fathom if the various requisites might be somehow achieved in the near future.

Cold atom experiments are now established *quantum simulators*: they can effectively implement a spin chain and seem the most convenient for testing the predictions of this thesis. They have long coherence times, operating practically at zero temperature and without decoherence. For this reason, in [108] and chapter 7 we have put forward a promising possible experimental realization using cold atoms trapped in optical lattices and near field Fresnel trapping potentials, each of which is accessible to current technology. However, there are still no experiments mixing this two trapping techniques, and we are looking for other possibilities.

Nuclear magnetic resonance experiments are now another promising candidate for quantum information transport [137, 138, 139, 140]. However, their highly mixed (high-temperature) initial state prevents the possibility of using such a setup for transferring superposition of quantum states, using our theoretical scheme. Nevertheless our results might be observed in current NMR experiments, as we strongly believe that the coherent dynamics of the z component magnetization survives also for highly mixed initial states. Coherent dynamics of the z component magnetization means that the two *classical* values $|0\rangle$ and $|1\rangle$ of the qubit are faithfully transported, irrespective of what happens to their superposition, making the spin-wire still useful for classical information transfer. Classical transmission over quantum systems is motivated by the current growing interest in finding alternatives to conventional electronics for transmitting signals. To this aim, several proposals are being put forward, ranging from spintronics [141, 142] to quite visionary ones. The leading thread connecting most of these proposals is the need of taking into consideration the quantum character of the dynamical processes underlying the information manipulation, no matter whether the information is classical or quantum. The application of the tools developed for the coherent ballistic dynamics over quantum spin chains to the investigation of classical information transmission along spin wires may thus represent a natural fruitful development of our studies.

A

Some mathematical results

A.1 The Weyl-Schur duality

The Weyl-Schur duality is an important, though simple, result of representation theory for the n-fold tensor product of the Hilbert space $\mathscr{H} = \mathbb{C}^d$, that is the space $\left(\mathbb{C}^d\right)^{\otimes n}$. Consider indeed an n-fold tensor product of rays in $\mathscr{H}$: $|\psi_1\rangle \otimes \cdots \otimes |\psi_n\rangle$. We can let the permutation group S_n act on this space by permuting the factors:

$$P_\pi : |\psi_1\rangle \otimes \cdots \otimes |\psi_n\rangle \quad \longrightarrow \quad |\psi_{\pi^{-1}(1)}\rangle \otimes \cdots \otimes |\psi_{\pi^{-1}(n)}\rangle.$$

This is a representation of S_n in which the permutation π is represented by an index permutation matrix: for any $|\psi^{(n)}\rangle \in \mathscr{H}^{\otimes n}$ expressed in some suitable basis $|\psi^{(n)}\rangle = \sum_{\{i_k\}} \psi^{(n)}_{i_1,i_2,\cdots,i_n} |i_1 i_2 \cdots i_n\rangle$

$$\psi^{(n)}_{i_1,i_2,\cdots,i_n} \quad \longrightarrow \quad \psi^{(n)}_{\pi(i_1),\pi(i_2),\cdots,\pi(i_n)}.$$

The space of rank-n tensors can serve also as a representation space of the unitary group. Let U be an element of SU(d). This unitary matrix induces in the tensor product space the transformation

$$|\psi^{(n)}\rangle \quad \longrightarrow \quad U^{\otimes n} |\psi^{(n)}\rangle.$$

The duality [143, 144, 145] stems from the fact that the two above representations turn out to be commuting with each other. Every operator on $\mathscr{H}^{\otimes n}$ that commutes with $U^{\otimes n}$, for all $U \in \mathrm{SU}(d)$, is a linear combination of index permutation operators P_π. Conversely, any operator commuting with the index permutation operators P_π, for all $\pi \in S_n$, is a linear combination of tensor powers $U^{\otimes n}$.

A.1.1 The *twirling* superoperator

The twirling superoperator is defined by

$$\mathscr{T}_n(A) = \int dU \, U^{\otimes n} A \left(U^\dagger\right)^{\otimes n}, \tag{A.1}$$

where A is an operator in $\mathscr{H}^{\otimes n}$ and dU is the Haar measure over the unitary group, i.e., it satisfies $dU = dUV = dVU$ for each unitary matrix V, and it is normalized such that $\int dU = \mathbb{1}$. The twirling superoperator is an important tool in quantum information as it appears in tons of proofs. Since

$$V^{\otimes n}\,\mathscr{T}_n(A)\left(V^\dagger\right)^{\otimes n} = \int dU\,(VU)^{\otimes n} A \left(U^\dagger V^\dagger\right)^{\otimes n} = \int d(V^\dagger U)\,(U)^{\otimes n} A \left(U^\dagger\right)^{\otimes n}$$
$$= \int dU\,(U)^{\otimes n} A \left(U^\dagger\right)^{\otimes n} = \mathscr{T}_n(A),$$

the twirling operator commutes with each $U^{\otimes n}$ and, accordingly, from the Weyl-Schur duality it is a linear combination of index permuting operators $\mathscr{T}_n(A) = \sum_\pi b_\pi\, P_\pi$. Multiplying the two sides by P_σ, and taking the trace it holds that

$$a_\sigma = \mathrm{Tr}\left[P_\sigma\,\mathscr{T}_n(A)\right] = \mathrm{Tr}\left[P_\sigma\,A\right] = \sum_\pi b_\pi\,\mathrm{Tr}\left[P_\sigma\,P_\pi\right],$$

i.e., a linear system of equations $\sum_\pi M_{\sigma\pi} b_\pi = a_\sigma$ arises, where $M_{\sigma\pi} = \mathrm{Tr}\left[P_\sigma\,P_\pi\right]$. Even if the matrix M is singular we can define M^{-1} as the Moore-Penrose *pseudo-inverse*[1], which is nothing but the standard inverse when M is invertible, and accordingly [147]

$$\mathscr{T}_n(A) = \int dU\,U^{\otimes n} A \left(U^\dagger\right)^{\otimes n} = \sum_{\pi,\sigma}\left(M^{-1}\right)_{\pi\sigma}\,\mathrm{Tr}\left[P_\sigma\,A\right]\,P_\pi. \tag{A.2}$$

Case $n = 2$

When $n = 2$ there are only two index permuting operators: the identity operator $P_0 = \mathbb{1}\otimes\mathbb{1}$ and the swap operator $P_1 = S$ such that $S|ij\rangle = |ji\rangle$. Since $\mathrm{Tr}\,P_0 = d^2$ and $\mathrm{Tr}\,S = \sum_{ij}\delta_{ij} = d$

$$M = \begin{pmatrix} d^2 & d \\ d & d^2 \end{pmatrix}, \qquad \Longrightarrow \qquad M^{-1} = \frac{1}{d(d^2-1)}\begin{pmatrix} d & -1 \\ -1 & d \end{pmatrix},$$

and thus

$$\mathscr{T}_2(A) = \frac{d\,\mathrm{Tr}\,A - \mathrm{Tr}\left[SA\right]}{d(d^2-1)}\,\mathbb{1}\otimes\mathbb{1} + \frac{d\,\mathrm{Tr}\left[SA\right] - \mathrm{Tr}\,A}{d(d^2-1)}\,S. \tag{A.3}$$

A.2 Theorems on tridiagonal matrices

Here we will consider some theorems which simplify considerably the analytic diagonalization of tridiagonal matrices. In a tridiagonal symmetric matrix T the only non-vanishing

[1]The Moore-Penrose pseudo-inverse [146] of a matrix M can be computed from the singular value decomposition (SVD). Indeed, let $M = U\,D\,V^\dagger$ be the SVD of M. Then $M^{-1} = V\,D^{-1}\,U^\dagger$ where the pseudo-inverse of the diagonal matrix D is obtained by taking the reciprocal of each non-zero element on the diagonal, leaving the zeros in place, and transposing the resulting matrix.

terms are $T_{i,i} = a_i$ and $T_{i,i+1} = b_i = T_{i+1,i}$, where the indices range from 1 to n, being T a $n \times n$ matrix. It is useful to introduce the following notation for the submatrices of T

$$T_{\mu:\nu} = \begin{pmatrix} a_\mu & b_\mu & & & & \\ b_\mu & a_{\mu+1} & b_{\mu+1} & & & \\ & b_{\mu+1} & \ddots & \ddots & & \\ & & \ddots & \ddots & & \\ & & & & a_{\nu-1} & b_{\nu-1} \\ & & & & b_{\nu-1} & a_\nu \end{pmatrix}, \tag{A.4}$$

such that $T \equiv T_{1:n}$.

Let $\chi_{\mu:\nu}(\lambda) = \det\left[\lambda \mathbb{1}_{\mu:\nu} - T_{\mu:\nu}\right]$ be the characteristic polynomial of the reduced tridiagonal matrix $T_{\mu:\nu}$. This polynomial satisfies the recurrence relations

$$\chi_{\mu:\nu+1}(\lambda) = (\lambda - a_{\nu+1})\,\chi_{\mu:\nu}(\lambda) - b_\nu^2\,\chi_{\mu:\nu-1}(\lambda), \tag{A.5a}$$

$$\chi_{\mu-1:\nu}(\lambda) = (\lambda - a_{\mu-1})\,\chi_{\mu:\nu}(\lambda) - b_{\mu-1}^2\,\chi_{\mu+1:\nu}(\lambda), \tag{A.5b}$$

which can be derived straightforwardly.

We prove now one of the most important theorems regarding tridiagonal matrices which permits to derive analytically the eigenvectors of T from the characteristic polynomial [88]:

Paige's theorem. *Let $T = O^\dagger \Lambda O$ be the spectral decomposition of the tridiagonal matrix T, where $\Lambda = \mathrm{diag}(\{\lambda_k\})$ and $O_{ki} = O_i^{(k)}$, being $O^{(k)}$ the eigenvector of T with eigenvalue λ_k. Then*

$$\chi'(\lambda_k)\, O_i^{(k)} O_j^{(k)} = \chi_{1:i-1}(\lambda_k)\, b_i \cdots b_{j-1}\, \chi_{j+1:n}(\lambda_k). \tag{A.6}$$

In particular,

$$O_1^{(k)} O_n^{(k)}\, \chi'(\lambda_k) = \prod_{i=1}^{n-1} b_i, \tag{A.7a}$$

$$\left[O_1^{(k)}\right]^2\, \chi'(\lambda_k) = \chi_{2:n}(\lambda_k), \tag{A.7b}$$

$$\left[O_n^{(k)}\right]^2\, \chi'(\lambda_k) = \chi_{1:n-1}(\lambda_k). \tag{A.7c}$$

Proof. The proof is based on a simple property of the adjugate matrix. The adjugate matrix is defined as the matrix of cofactors, i.e. $(-1)^{i+j}(\mathrm{adj}\, T)_{ij}$ is the determinant of the matrix that results from deleting row j and column i of T. The importance of the adjugate stems from the Cauchy-Binet formula $T \cdot \mathrm{adj}\, T = \det T \cdot \mathbb{1}$. Accordingly, being $\lambda\mathbb{1} - T$ invertible for $\lambda \neq \lambda_k$,

$$\mathrm{adj}(\lambda - T) = \det(\lambda - T)(\lambda - T)^{-1} = O^\dagger \frac{\chi(\lambda)}{\lambda - \Lambda} O = O^\dagger\, \mathrm{diag}\{\delta_k(\lambda)\}\, O\,,$$

where $\delta_k(\lambda) = \chi(\lambda)/(\lambda - \lambda_k) = \prod_{j\neq k}(\lambda - \lambda_j)$. Taking the limit $\lambda \to \lambda_k$ on both sides and evaluating the (i, j) element of the matrix it holds that

$$\left[\mathrm{adj}(\lambda_k - T)\right]_{ij} = \chi'(\lambda_k)\, O_i^{(k)} O_j^{(k)}.$$

The above equation is very general and holds for every diagonalizable matrix. Eq. (A.6) comes out by explicitly calculating $\left[\mathrm{adj}(\lambda_k - T)\right]_{ij}$ for the tridiagonal matrix (A.4). □

B

Quadratic Hamiltonians for Fermions

In this chapter we study the out-of-equilibrium dynamics of Hamiltonians that can be written as a quadratic form Fermi operators

$$H=\sum_{i,j=1}^{n}\left[A_{ij}\,a_i^\dagger a_j+\frac{1}{2}\left(B_{ij}\,a_i^\dagger a_j^\dagger+B_{ij}^*a_j a_i\right)\right]\,, \tag{B.1}$$

where $a_i^\dagger$ and a_j are fermion creation and annihilation operators obeying the anti-commutation relations

$$\{a_i,a_j^\dagger\}=\delta_{ij},\qquad\qquad \{a_i,a_j\}=0,\qquad\qquad \{a_i^\dagger,a_j^\dagger\}=0. \tag{B.2}$$

Although this method can be generalized to non-Hermitian matrices, as those occurring in open quantum systems [148, 149, 136, 150], we restrict ourselves to the unitary evolution of the system where the Hamiltonian is Hermitian. Accordingly,

$$A=A^\dagger,\qquad\qquad B^T=-B. \tag{B.3}$$

In the following section we consider the diagonalization of the Hamiltonian (B.1) by means of a canonical transformation, and then we study the time evolution of physical observables.

B.1 Canonical transformation

Canonical (Bogoliubov) transformations [151] are transformations of the creation and annihilation operators which preserve the commutation relations (B.2). In order to describe them let us introduce the following notation

$$\alpha=\begin{pmatrix}a\\a^\dagger\end{pmatrix}\,,\qquad\qquad \alpha_i=a_i,\qquad\qquad \alpha_{n+i}=a_i^\dagger,\qquad\qquad i=1,\dots,n. \tag{B.4}$$

In this notation, the anti-commutation relations (B.2) take the compact form

$$\{\alpha,\alpha^\dagger\}=\mathbb{1}_{2n}\,. \tag{B.5}$$

Let us now define a new set of creation and annihilation operators

$$b = Pa + Qa^\dagger\,, \qquad\qquad b_i = \sum_j P_{ij}\, a_j + Q_{ij} a_j^\dagger\,, \tag{B.6}$$

which can also be written in the form

$$\beta = M\alpha\,, \qquad\qquad M = \begin{pmatrix} P & Q \\ Q^* & P^* \end{pmatrix}\,, \qquad\qquad \beta = \begin{pmatrix} b \\ b^\dagger \end{pmatrix}\,. \tag{B.7}$$

The transformation (B.7) preserves the anti-commutation relations (B.5) if $M M^\dagger = \mathbb{1}_{2n}$. It follows that it is invertible; if also M^{-1} preserves the commutation relations, then it holds that $M^{-1}(M^{-1})^\dagger = \mathbb{1}_{2n}$ and thus $M^\dagger M = \mathbb{1}_{2n}$. A general invertible Bogoliubov transformation is therefore given by (B.6) and (B.7) with a unitary matrix M. Accordingly, the matrices P and Q satisfy

$$P P^\dagger + Q Q^\dagger = \mathbb{1}, \qquad\qquad P^\dagger P + Q^T Q^* = \mathbb{1}, \tag{B.8a}$$

$$P Q^T + Q P^T = \mathbb{O}, \qquad\qquad P^\dagger Q + Q^T P^* = \mathbb{O}. \tag{B.8b}$$

An important result for the characterization of the Bogoliubov transformations is the following theorem [152]:

Bloch-Messiah-Zumino's Theorem. *Every unitary matrix M of the form* (B.7) *can always be decomposed into the form*

$$M = \begin{pmatrix} P & Q \\ Q^* & P^* \end{pmatrix} = \begin{pmatrix} U & 0 \\ 0 & U^* \end{pmatrix} \begin{pmatrix} \bar{P} & \bar{Q} \\ \bar{Q} & \bar{P} \end{pmatrix} \begin{pmatrix} V^\dagger & 0 \\ 0 & V^T \end{pmatrix}\,, \tag{B.9}$$

where

$$\bar{P} = \begin{pmatrix} 1 & & & & & & & & & \\ & \ddots & & & & & & & & \\ & & 1 & & & & & & & \\ & & & p_1 & & & & & & \\ & & & & p_1 & & & & & \\ & & & & & \ddots & & & & \\ & & & & & & p_n & & & \\ & & & & & & & p_n & & \\ & & & & & & & & 0 & \\ & & & & & & & & & \ddots \\ & & & & & & & & & & 0 \end{pmatrix},$$

$$\bar{Q} = \begin{pmatrix} 0 & & & & & & & & & \\ & \ddots & & & & & & & & \\ & & 0 & & & & & & & \\ & & & 0 & q_1 & & & & & \\ & & & -q_1 & 0 & & & & & \\ & & & & & \ddots & & & & \\ & & & & & & 0 & q_n & & \\ & & & & & & -q_n & 0 & & \\ & & & & & & & & 1 & \\ & & & & & & & & & \ddots \\ & & & & & & & & & & 1 \end{pmatrix},$$

and

$$p_k^2 + q_k^2 = 1.$$

Proof. The proof is based on this two properties: (i) a Hermitian matrix H can be diagonalized by a unitary transformation U such that $\bar{H} = U^\dagger H U$ is diagonal with real eigenvalues h_k; (ii) a skew-symmetric matrix S can be brought into a canonical form by a (generally different) unitary matrix U such that $\bar{S} = U^\dagger S U^*$ is decomposed into 2×2 blocks of the form $\begin{pmatrix} 0 & s_k \\ -s_k & 0 \end{pmatrix}$ with real numbers s_k along the diagonal line. In the next step we show that if we have the relation

$$HS = SH^*, \tag{B.10}$$

then we can find a matrix U which diagonalizes H and brings S into the canonical form. For this purpose we first diagonalize H and from (B.10) obtain in this basis $(h_i - h_j)S_{ij} = 0$, that is $S_{ij} = 0$ if $h_i \neq h_j$. We can thus restrict to subspaces of degenerate eigenvalues h_i. In these

subspaces H is proportional to unity. We can therefore bring S into canonical form in each subspace without changing the diagonal character of H.

Let $P = U\bar{P}V^\dagger$ be the singular value decomposition of P. Then, thanks to (B.8), the matrices $H = Q^T Q^* = V(\mathbb{1} - \bar{P}^2)V^\dagger$ and $S = Q^T P^* = -S^T$ satisfy (B.10). Indeed

$$\begin{aligned} HS - SH^* = HS + S^T H^* = Q^T Q^* Q^T P^* + P^\dagger Q Q^\dagger Q = (\mathbb{1} - P^\dagger P)Q^T P^* + P^\dagger(\mathbb{1} - PP^\dagger)Q \\ = -P^\dagger P(Q^T P^* + P^\dagger Q) = 0. \end{aligned}$$

We can chose V such that $V^\dagger S V^* = V^\dagger Q^T U^* \bar{P}$ is in the normal form, i.e. $\bar{Q} = U^\dagger Q V^*$ is in the normal form and accordingly $Q = U\bar{Q}V^T$.

The proof ends by noting that Q is unitary in the subspace where the eigenvalues of P are null, and accordingly this unitary matrix can be shifted both in the definition of U or V. □

B.2 Diagonalization

The Hamiltonian (B.1) can be written in the form

$$H = \frac{1}{2}\alpha^\dagger S\alpha + \frac{1}{2}\mathrm{Tr}A, \qquad S = \begin{pmatrix} A & B \\ -B^* & -A^* \end{pmatrix}, \tag{B.11}$$

thanks to the notation (B.4). We show now that there exists a canonical transformation (B.7) such that the matrix $MSM^\dagger$ is real and diagonal, i.e. $S = M^\dagger \Lambda M$ with Λ real and diagonal. Since $(\sigma^x \otimes \mathbb{1})S(\sigma^x \otimes \mathbb{1}) = -S^*$ if $k = \begin{pmatrix} x_k & y_k \end{pmatrix}^T$ is an eigenvector of S with eigenvalue E_k then $(\sigma^x \otimes \mathbb{1})k^* = \begin{pmatrix} y_k^* & x_k^* \end{pmatrix}^T$ is an eigenvector of S with eigenvalue $-E_k$. This means that by grouping the eigenvalues and the eigenvectors the matrix (B.11) can be diagonalized via a canonical transformation [151] and written in the form

$$\begin{aligned} H &= \frac{1}{2}\alpha^\dagger \begin{pmatrix} P & Q \\ Q^* & P^* \end{pmatrix}^\dagger \begin{pmatrix} E & 0 \\ 0 & -E \end{pmatrix} \begin{pmatrix} P & Q \\ Q^* & P^* \end{pmatrix} \alpha + \frac{1}{2}\mathrm{Tr}A \\ &= \frac{1}{2}\beta^\dagger \begin{pmatrix} E & 0 \\ 0 & -E \end{pmatrix} \beta + \frac{1}{2}\mathrm{Tr}A, \end{aligned} \tag{B.12}$$

where E is diagonal and non-negative. That is, in terms of some diagonal Fermi operators (B.6) the Hamiltonian takes the form

$$H = \sum_k E_k b_k^\dagger b_k + \frac{1}{2}\mathrm{Tr}(A - E). \tag{B.13}$$

B.2.1 Ground state

The ground state $|\Omega\rangle$ of Hamiltonian (B.1), thanks to the diagonal expression (B.13), satisfies $b_k|\Omega\rangle = 0$, for each k. Let us express the ground state in terms of the vacuum of the original

Fermi operators, i.e. the state $|0\rangle$ which is annihilated by all the a_i annihilation operators. Recalling the Bloch-Messiah-Zumino decomposition (B.9) we define the new operators

$$\begin{pmatrix} \tilde{b} \\ \tilde{b}^\dagger \end{pmatrix} = \begin{pmatrix} U & 0 \\ 0 & U^* \end{pmatrix}^\dagger \begin{pmatrix} b \\ b^\dagger \end{pmatrix}, \qquad \begin{pmatrix} \tilde{a} \\ \tilde{a}^\dagger \end{pmatrix} = \begin{pmatrix} V^\dagger & 0 \\ 0 & V^T \end{pmatrix}^\dagger \begin{pmatrix} a \\ a^\dagger \end{pmatrix}.$$

Clearly, the states $|\Omega\rangle$ and $|0\rangle$ are annihilated also by $\tilde{b}_k$ and $\tilde{a}_k$ respectively. For the indices k such that $p_k = 1$, and $q_k = 0$ there is no pairing and $\tilde{b}_k|0\rangle = 0$ as well. On the other hand, for the indices k such that $p_k = 0$ then the $\bar{Q}$ matrix is proportional to the identity and thus $\tilde{b}_k^\dagger|0\rangle = 0$. In the remaining case the operators $\tilde{b}_k$ and $\tilde{a}_k$ are connected

$$\tilde{b}_k = p_k \tilde{a}_k + q_k \tilde{a}_{\bar{k}}^\dagger, \qquad \tilde{b}_{\bar{k}} = p_k \tilde{a}_{\bar{k}} - q_k \tilde{a}_k^\dagger,$$

being $\bar{k}$ the index of the mode paired to the mode k. One can simply prove that

$$\tilde{b}_k(p_k - q_k \tilde{a}_k^\dagger \tilde{a}_{\bar{k}}^\dagger)|0\rangle = p_k q_k (\tilde{a}_{\bar{k}}^\dagger - \tilde{a}_{\bar{k}}^\dagger)|0\rangle = 0.$$

Accordingly, the ground state of the Hamiltonian (B.1) can be written in the so-called BCS form [152]

$$|\Omega\rangle = \prod_{\{p_k=0\}} \tilde{a}_k^\dagger \prod_{\{p_k\neq 0\}} \left(p_k - q_k\, \tilde{a}_k^\dagger \tilde{a}_{\bar{k}}^\dagger\right)|0\rangle\,. \tag{B.14}$$

The parity of this ground state, i.e. the eigenvalue of the operator $\Pi = (-1)^N$ where $N = \sum_i a_i^\dagger a_i$ can be found thanks to Eq. (B.14). As U is unitary, $N = \sum_i \tilde{a}_i^\dagger \tilde{a}_i$ and $\Pi = \prod_i \left(1 - 2\tilde{a}_i^\dagger \tilde{a}_i\right)$. Hence, the parity operator anti-commutes with all the creation (annihilation) operators $\tilde{a}_i^\dagger$ ($\tilde{a}_j$) and, according to (B.14),

$$\Pi\,|\Omega\rangle = \prod_{\{p_k=0\}} (-1)|\Omega\rangle \equiv (-1)^{\dim \mathrm{Ker}\, P}|\Omega\rangle. \tag{B.15}$$

B.2.2 Time evolution

The time evolution of a system governed by Hamiltonian (B.1) can be found straightforwardly in the Heisenberg picture. Indeed, thanks to the diagonal form (B.13), the diagonal Fermi operators evolve as $b_k(t) = e^{iHt}\, b_k\, e^{-iHt} = e^{-iE_k t} b_k$ and similarly $b_k^\dagger(t) = e^{iE_k t} b_k^\dagger$. Accordingly, since $\alpha(t) = M^\dagger \beta(t)$ and $\beta = M\alpha$

$$\begin{aligned} \begin{pmatrix} a(t) \\ a^\dagger(t) \end{pmatrix} &= \begin{pmatrix} P^\dagger & Q^T \\ Q^\dagger & P^T \end{pmatrix} \begin{pmatrix} e^{-iEt} & 0 \\ 0 & e^{iEt} \end{pmatrix} \begin{pmatrix} P & Q \\ Q^* & P^* \end{pmatrix} \begin{pmatrix} a \\ a^\dagger \end{pmatrix} \\ &= \begin{pmatrix} P^\dagger e^{-iEt} P + Q^T e^{iEt} Q^* & P^\dagger e^{-iEt} Q + Q^T e^{iEt} P^* \\ Q^\dagger e^{-iEt} P + P^T e^{iEt} Q^* & Q^\dagger e^{-iEt} Q + P^T e^{iEt} P^* \end{pmatrix} \begin{pmatrix} a \\ a^\dagger \end{pmatrix}. \end{aligned} \tag{B.16}$$

The above transformation which represents the time evolution of the Fermi operators α is a Bogoliubov transformation: it is clearly unitary, being a composition of unitary operations, and it has the form (B.7). In standard notations

$$a_j(t) = \sum_\ell U_{j\ell}(t)\, a_\ell + V_{j\ell}(t)\, a_\ell^\dagger, \tag{B.17}$$

where

$$U(t) = P^\dagger\, e^{\text{-}iEt}\, P + Q^T\, e^{iEt}\, Q^*, \qquad V(t) = P^\dagger\, e^{\text{-}iEt}\, Q + Q^T\, e^{iEt}\, P^*. \tag{B.18}$$

B.2.3 Expectation values

The expectation values of physical quantities with respect to the ground state or to a thermal state can be found straightforwardly. Indeed, in matrix notation

$$\langle\Omega| \begin{pmatrix} b \\ b^\dagger \end{pmatrix} \begin{pmatrix} b \\ b^\dagger \end{pmatrix} |\Omega\rangle \equiv \begin{pmatrix} \langle\Omega|b\, b|\Omega\rangle & \langle\Omega|b\, b^\dagger|\Omega\rangle \\ \langle\Omega|b^\dagger\, b|\Omega\rangle & \langle\Omega|b^\dagger\, b^\dagger|\Omega\rangle \end{pmatrix} = \begin{pmatrix} 0 & \mathbb{1} \\ 0 & 0 \end{pmatrix}.$$

When the temperature is introduced, the ground state expectation value has to be replaced with the thermal averaged state $\langle\cdot\rangle_\beta = \mathrm{Tr}[e^{-\beta H}\,\cdot]/\mathscr{Z}$ where $\mathscr{Z} = \mathrm{Tr}[e^{-\beta H}]$. The trace can be performed in the Fock space spanned by $|\{n_k\}\rangle$, where n_k is the number of diagonal b_k fermions, i.e. $|\{n_k\}\rangle = \prod_k \left(b_k^\dagger\right)^{n_k} |\Omega\rangle$. The thermal averages are found straightforwardly as usual thanks to the partition function $\mathscr{Z} = \sum_{\{n_k\}} \prod_k e^{-\beta E_k n_k} = \prod_k (1 + e^{-\beta E_k})$: $\langle b_k^\dagger b_k\rangle_\beta = -\frac{1}{\beta\mathscr{Z}} \frac{\partial \mathscr{Z}}{\partial E_k} = \frac{1}{1+e^{\beta E_k}}$, and $\langle b_k b_k^\dagger\rangle_\beta = \frac{1}{1+e^{-\beta E_k}}$. In matrix notation

$$\langle \begin{pmatrix} b \\ b^\dagger \end{pmatrix} \begin{pmatrix} b \\ b^\dagger \end{pmatrix} \rangle_\beta = \begin{pmatrix} 0 & \frac{\mathbb{1}}{\mathbb{1}+e^{-\beta E}} \\ \frac{\mathbb{1}}{\mathbb{1}+e^{\beta E}} & 0 \end{pmatrix}.$$

Since $\langle\alpha_i \alpha_j\rangle = \sum_{kh} M^*_{ki} M^*_{hj} \langle\beta_k \beta_h\rangle$ the two-point correlation function matrices are

$$\begin{aligned} \Xi = \langle\Omega|\alpha\ \alpha|\Omega\rangle &= \begin{pmatrix} P^\dagger & Q^T \\ Q^\dagger & P^T \end{pmatrix} \begin{pmatrix} 0 & \mathbb{1} \\ 0 & 0 \end{pmatrix} \begin{pmatrix} P^* & Q^* \\ Q & P \end{pmatrix} \\ &= \begin{pmatrix} P^\dagger Q & P^\dagger P \\ Q^\dagger Q & Q^\dagger P \end{pmatrix}, \end{aligned} \tag{B.19a}$$

$$\begin{aligned} \Xi^\beta = \langle\alpha\ \alpha\rangle_\beta &= \begin{pmatrix} P^\dagger & Q^T \\ Q^\dagger & P^T \end{pmatrix} \begin{pmatrix} 0 & \frac{\mathbb{1}}{\mathbb{1}+e^{-\beta E}} \\ \frac{\mathbb{1}}{\mathbb{1}+e^{\beta E}} & 0 \end{pmatrix} \begin{pmatrix} P^* & Q^* \\ Q & P \end{pmatrix} \\ &= \begin{pmatrix} P^\dagger \frac{\mathbb{1}}{\mathbb{1}+e^{-\beta E}} Q + Q^T \frac{\mathbb{1}}{\mathbb{1}+e^{\beta E}} P^* & P^\dagger \frac{\mathbb{1}}{\mathbb{1}+e^{-\beta E}} P + Q^T \frac{\mathbb{1}}{\mathbb{1}+e^{\beta E}} Q^* \\ Q^\dagger \frac{\mathbb{1}}{\mathbb{1}+e^{-\beta E}} Q + P^T \frac{\mathbb{1}}{\mathbb{1}+e^{\beta E}} P^* & Q^\dagger \frac{\mathbb{1}}{\mathbb{1}+e^{-\beta E}} P + P^T \frac{\mathbb{1}}{\mathbb{1}+e^{\beta E}} Q^*. \end{pmatrix}. \end{aligned} \tag{B.19b}$$

All other correlation functions can be be obtained using the Wick theorem [151] from *contractions* of the basic matrices (B.19).

Another important quantity is the parity of the thermal state, i.e. the expectation value $\langle\Pi\rangle_\beta$. As Π anti-commutes with the Fermi operators a_i and $a_j^\dagger$, it anti-commutes also with the diagonal operators $b_k^\dagger$. As $|\{n_k\}\rangle \propto \prod_k (b_k^\dagger)^{n_k}|\Omega\rangle$, it holds $\Pi|\{n_k\}\rangle = (-1)^p \prod_k (-1)^{n_k}|\{n_k\}\rangle$, where $(-1)^p$ is the parity of the ground state (B.15). Then

$$\langle\Pi\rangle_\beta = \frac{(-1)^p}{\mathscr{Z}} \sum_{\{n_k\}} \prod_k e^{-\beta E_k n_k}(-1)^{n_k} = (-1)^p \prod_k \left(\frac{1-e^{-\beta E_k}}{1+e^{-\beta E_k}}\right) = (-1)^p \prod_k \tanh\left(\frac{\beta E_k}{2}\right) . \quad \text{(B.20)}$$

B.3 Particular cases

When the Hamiltonian matrix S is real the diagonalization procedure can be cast in a simpler form. In such a case the matrices P and Q are real as well, and defining $P = \frac{\Phi+\Psi}{2}$ and $Q = \frac{\Phi-\Psi}{2}$ the conditions (B.8) simplify to the requirement that the matrices Φ and Ψ are orthogonal. Moreover, the eigenvalue equation becomes

$$A(\Phi+\Psi) + B(\Phi-\Psi) = (\Phi+\Psi)E\,, \qquad -A(\Phi-\Psi) - B(\Phi+\Psi) = (\Phi-\Psi)E\,,$$

i.e. $(A-B)\Psi = \Phi E$. The orthogonal matrices Φ, Ψ and the diagonal non-negative matrix E can be obtained thus by means of the singular value decomposition of the matrix $A-B$:

$$A - B = \Phi^T E \Psi. \quad \text{(B.21)}$$

In particular, as $(A-B)^T = A+B$ we have also the eigenvalue equations [109]

$$(A+B)(A-B) = \Psi^T E^2 \Psi\,, \qquad (A-B)(A+B) = \Phi^T E^2 \Phi\,.$$

In the rest of the section the Hamiltonian matrix S is assumed to be real.

B.3.1 Conserved number of particles

When the pairing term is null, a lot of simplifications occur: the only need is to diagonalize the matrix A, as $B = 0$. Eq. (B.21) can be cast in the standard eigenvalue decomposition $A = O^T \Omega O$. However, in order to use the results of the previous section the eigenvalues E need to be positive. This can be accomplished by going back to Eq. (B.21) and setting $\Phi = O$, $E = |\Omega|$ and $\Psi = s\,O$, where O and Ω are obtained from the eigenvalue decomposition and $s = \text{sign}(\Omega)$ is the diagonal matrix whose diagonal entries are the signs of the eigenvalues. Hence, $P = \frac{1+s}{2}O$, $Q = \frac{1-s}{2}O$ and accordingly

$$U(t) = O^T \frac{1+s}{2} e^{-iEt} \frac{1+s}{2} O + O^T \frac{1-s}{2} e^{iEt} \frac{1-s}{2} O = O^T e^{-i\Omega t} O \quad \text{(B.22)}$$

and similarly $V(t) = 0$. Moreover, the eigenvalues of P can be only 0 or 1. The zero eigenvalues correspond to the subspace of negative energy states and, according to (B.14), the ground state is the Dirac see, where all the negative energy states are filled.

B.3.2 Reflection symmetry (Mirror symmetry)

The reflection symmetry occurs when the system is invariant under reflection, i.e. when the Hamiltonian does not change by exchanging the sites i and $n-i+1$, being n the number of sites. Formally this means that $A_{i,j} = A_{n-j+1,n-i+1}$ and $B_{i,j} = B_{n-j+1,n-i+1}$, i.e.,

$$XAX = A^T = A, \qquad XBX = B^T = -B, \tag{B.23}$$

being X the exchange matrix defined in (4.5). Matrices P satisfying the condition $XPX = P^T$ are also called persymmetric. One important property of persymmetric matrices is that PX and XP are symmetric, and thus can be diagonalized by standard eigenvalue decomposition. Let

$$(A-B)X = O^T \Omega O\,,$$

be the eigenvalue decomposition of $(A-B)X$. Eq .(B.21) is obtained by setting $O = \Phi$, $E = |\Omega|$ and $\Psi = s\,O\,X$, where $s = \operatorname{sign}\Omega$. Moreover, the commutation relations (4.10) impose that

$$\begin{pmatrix} P & Q \\ Q^* & P^* \end{pmatrix} \begin{pmatrix} X & 0 \\ 0 & -X \end{pmatrix} \begin{pmatrix} P & Q \\ Q^* & P^* \end{pmatrix}^\dagger = \begin{pmatrix} x^+ & 0 \\ 0 & x^- \end{pmatrix},$$

is diagonal, with diagonal x^+ and x^-. Explicit calculations show that $x^+ = -x^- = s$ and accordingly

$$U(t) = \frac{O^T + X\,O^T\,s}{2}\, e^{-iEt}\, \frac{O + s\,O\,X}{2} + \frac{O^T - X\,O^T\,s}{2}\, e^{iEt}\, \frac{O - s\,O\,X}{2} \tag{B.24a}$$

$$= \frac{1}{2}\left(O^T \cos(Et) O + X O^T \cos(Et) O X - i X O^T\, s \sin(Et) O - i O^T\, s \sin(Et) O X\right),$$

$$V(t) = \frac{O^T + X\,O^T\,s}{2}\, e^{-iEt}\, \frac{O - s\,O\,X}{2} + \frac{O^T + X\,O^T\,s}{2}\, e^{iEt}\, \frac{O - s\,O\,X}{2} \tag{B.24b}$$

$$= \frac{1}{2}\left(O^T \cos(Et) O - X O^T \cos(Et) O X - i X O^T\, s \sin(Et) O + i O^T\, s \sin(Et) O X\right).$$

C

Some explicit formulas

C.1 Quasi-uniform tridiagonal matrices

In this section we cope with the analytical diagonalization of quasi-uniform tridiagonal matrices, as those tackled in Chapter 5 and 6. Special emphasis is given to the spectrum and to the density of excitations. The notations of Section (A.2) are assumed.

Let's start with the diagonalization of $n \times n$ uniform tridiagonal matrices (A.4), where without loss of generality, we can set $a_\mu \equiv a$ and $b_\mu \equiv -1$. Setting also $(\lambda - a)/2 \to \lambda$ the characteristic polynomial takes the form

$$\mathbb{U}_n(\lambda) = \det \begin{pmatrix} 2\lambda & 1 & & \\ 1 & 2\lambda & 1 & \\ & 1 & 2\lambda & \ddots \\ & & \ddots & \ddots \end{pmatrix}_{n\times n} . \tag{C.1}$$

The recurrence relations (A.5) read $\mathbb{U}_{n+2} = 2\lambda\mathbb{U}_{n+1} - \mathbb{U}_n$ whose analytical solution can be found using the unilateral Z-transform [153]. Applying the unilateral Z-transform to the recurrence relation we find $z^2\mathbb{U}(\lambda,z) - 2\lambda z - z^2 = 2\lambda z\mathbb{U}(\lambda,z) - 2\lambda z - \mathbb{U}(\lambda,z)$ where $\mathbb{U}(\lambda,z) = \sum_{n=0}^{\infty} \mathbb{U}_n(\lambda)\, z^{-n}$, and we used the explicit results $\mathbb{U}_0(\lambda) = 0$ and $\mathbb{U}_1(\lambda) = 2\lambda$. From the above expressions we find $\mathbb{U}(\lambda,z) = \frac{z^2}{z^2 - 2\lambda z + 1}$. The solution $\mathbb{U}_n(\lambda)$ of the recurrence equation is then given by the inverse Z-transform $\mathbb{U}_n(\lambda) = \frac{1}{2\pi i} \oint \mathbb{U}(\lambda,z)\, z^{n-1}\, dz$, where the closed contour encircles all the poles of $\mathbb{U}(\lambda,z)$. Using standard residue calculus we find

$$\mathbb{U}_n(\lambda) = \frac{\left(\lambda + \sqrt{\lambda^2-1}\right)^{n+1} - \left(\lambda - \sqrt{\lambda^2-1}\right)^{n+1}}{2\sqrt{\lambda^2-1}} , \tag{C.2}$$

i.e. $\mathbb{U}_n(\lambda)$ is the Chebyshev polynomial of the second kind [80] of order n.

Setting $\lambda = \pm\cos(k)$ and using the known property of Chebyshev polynomials $\mathbb{U}_n(\pm\cos(k)) = (\pm 1)^n \frac{\sin[(n+1)k]}{\sin(k)}$ the secular equation $\mathbb{U}_n = 0$ defines $k \equiv k_j = \frac{\pi j}{n+1}$ while the eigenvectors are $O_{kj} = \sqrt{\frac{2}{n+1}} \sin\left(\frac{\pi j k}{n+1}\right)$.

APPENDIX C. SOME EXPLICIT FORMULAS

In the following sections we deal with quasi-uniform $\ell \times \ell$ tridiagonal matrices, i.e. tridiagonal matrices composed of a uniform $n \times n$ block, as that of Eq.(C.1), and different "edges". In the following $P(\lambda)$ is the characteristic polynomial of the complete matrix up to a convenient 2 factor, i.e. $\mathbb{P}(\lambda) = \chi_{1:\ell}(2\lambda)$, while the symbols $\ulcorner$ and $\lrcorner$ are added respectively for the characteristic polynomials of the reduced matrices obtained by removing the leftmost (rightmost) edge. For instance $\chi_{2:\ell}(2\lambda) \equiv \mathbb{P}^{\ulcorner}(\lambda)$ and $\chi_{1:\ell-1}(2\lambda) \equiv \mathbb{P}_{\lrcorner}(\lambda)$. The final goal is to obtain an analytical expression of O_{k1} and $O_{k\ell}$, which characterize the distribution of excitations, as seen in (5.14) and (6.3). Thanks to (A.7)

$$O_{k1}^2 = 2\frac{\mathbb{P}^{\ulcorner}}{\mathbb{P}'}\,, \qquad\qquad O_{k\ell}^2 = 2\frac{\mathbb{P}_{\lrcorner}}{\mathbb{P}'}\,. \tag{C.3}$$

The above expressions are fractions of complicated polynomials of degree $\ell - 1$. In order to simplify them we exploit the homogeneous $n \times n$ part and write the polynomials as a combination of $\mathbb{U}_n$ and $\mathbb{T}_{n+1}$,

$$\mathbb{P}(\lambda) = u(\lambda)\,\mathbb{U}_n(\lambda) + t(\lambda)\,\mathbb{T}_{n+1}(\lambda)\,, \tag{C.4}$$

where $\mathbb{U}_n$ are the Chebyshev polynomials of the second kind, Eq. (C.2), while $\mathbb{T}_n$ are the Chebyshev polynomials of the first kind [80]. These polynomials satisfy the following important relations

$$\mathbb{U}_{n-1}(\lambda) = \lambda\,\mathbb{U}_n(\lambda) - \mathbb{T}_{n+1}(\lambda)\,, \tag{C.5a}$$

$$\mathbb{U}_{n-2}(\lambda) = (2\lambda^2 - 1)\,\mathbb{U}_n(\lambda) - 2\lambda\,\mathbb{T}_{n+1}(\lambda)\,, \tag{C.5b}$$

$$\mathbb{T}'_{n+1}(\lambda) = (n+1)\,\mathbb{U}_n(\lambda)\,, \tag{C.5c}$$

$$\mathbb{U}'_n(\lambda) = \frac{n+1}{\lambda^2-1}\,\mathbb{T}_{n+1}(\lambda) - \frac{\lambda}{\lambda^2-1}\,\mathbb{U}_n(\lambda)\,. \tag{C.5d}$$

that will be used in the following. Accordingly, the first equation of Eq. (C.3) can be written as

$$O_{1k}^2 = 2\frac{u^{\ulcorner}(\lambda_k)\,\mathbb{U}_n(\lambda_k) + t^{\ulcorner}(\lambda_k)\,\mathbb{T}_{n+1}(\lambda_k)}{u_n^{\star}(\lambda_k)\,\mathbb{U}_n(\lambda_k) + t_n^{\star}(\lambda_k)\,\mathbb{T}_{n+1}(\lambda_k)}\,, \tag{C.6}$$

where $u^{\ulcorner}$ and $t^{\ulcorner}$ (respectively $u_n^{\star}(\lambda)$ and $t_n^{\star}(\lambda)$) are the coeffients of $\mathbb{P}^{\ulcorner}$ (respectively $\mathbb{P}'(\lambda)$) when expressed in the form (C.4). Thanks to (C.5)

$$u_n^{\star}(\lambda) = u'(\lambda) - \frac{\lambda}{\lambda^2-1}\,u(\lambda) + (n+1)\,t(\lambda), \tag{C.7a}$$

$$t_n^{\star}(\lambda) = t'(\lambda) + \frac{n+1}{\lambda^2-1}\,u(\lambda). \tag{C.7b}$$

The eigenvalues λ_k are the solutions of the secular equation $\mathbb{P}(\lambda) = 0$, i.e

$$0 = u(\lambda_k)\,\mathbb{U}_n(\lambda_k) + t(\lambda_k)\,\mathbb{T}_{n+1}(\lambda_k)\,. \tag{C.8}$$

Thanks to the above secular equation, the high-degree polynomials $\mathbb{U}_n(\lambda_k)$ and $\mathbb{T}_{n+1}(\lambda_k)$ can be removed from (C.7) and accordingly

$$O^2_{k1} = 2\frac{u^{\ulcorner}(\lambda_k)\,t(\lambda_k) - t^{\ulcorner}(\lambda_k)\,u(\lambda_k)}{u^\star_n(\lambda_k)\,t(\lambda_k) - t^\star_n(\lambda_k)\,u(\lambda_k)}\,, \qquad O^2_{k\ell} = 2\frac{u_{\lrcorner}(\lambda_k)\,t(\lambda_k) - t_{\lrcorner}(\lambda_k)\,u(\lambda_k)}{u^\star_n(\lambda_k)\,t(\lambda_k) - t^\star_n(\lambda_k)\,u(\lambda_k)}\,. \tag{C.9}$$

Further simplifications can be obtained by using the ansatz $\lambda_k = \pm\cos k$. As $\mathbb{U}_n(\pm\cos k) = (\pm)^n \frac{\sin[(n+1)k]}{\sin k}$ and $\mathbb{T}_{n+1}(\pm\cos k) = (\pm)^{n+1}\cos[(n+1)k]$ the secular equation (C.8) can be written

$$\sin\big[(n+1)k - 2\phi_k\big] = 0\,, \tag{C.10}$$

where the *shifts* are defined by

$$\tan 2\phi_k = \mp\frac{t(\pm\cos k)\,\sin k}{u(\pm\cos k)}\,. \tag{C.11}$$

In the following for convenience we will use slightly modified versions of Eqs. (C.10) and (C.11):

$$\sin\big[(\ell+1)k - 2\varphi_k\big] = 0\,, \qquad\qquad \varphi_k = \frac{\ell - n}{2}k + \phi_k\,. \tag{C.12}$$

So the ℓ eigenvalues correspond to

$$k_j = \frac{\pi j + 2\varphi_{k_j}}{\ell+1}\,, \quad (j = 1,\ldots,\ell)\,. \tag{C.13}$$

Moreover, since $2\phi'_k = \frac{\mp t\,u\,\cos k + (t'u - u't)\sin^2 k}{u^2 + t^2\sin^2 k}$, the eigenvector elements (C.9) read

$$O^2_{k1} = \frac{2\sin^2 k}{(\ell + 1 - 2\varphi'_k)}\,\frac{u^{\ulcorner}(\lambda_k)\,t(\lambda_k) - t^{\ulcorner}(\lambda_k)\,u(\lambda_k)}{u(\lambda_k)^2 + t(\lambda_k)^2\,\sin^2 k}\,, \tag{C.14a}$$

$$O^2_{k\ell} = \frac{2\sin^2 k}{(\ell + 1 - 2\varphi'_k)}\,\frac{u_{\lrcorner}(\lambda_k)\,t(\lambda_k) - t_{\lrcorner}(\lambda_k)\,u(\lambda_k)}{u(\lambda_k)^2 + t(\lambda_k)^2\,\sin^2 k}\,, \tag{C.14b}$$

where $\lambda_k = \pm\cos k$.

C.1.1 Mirror symmetric quasi-uniform matrix

Here we consider the matrix

$$\begin{pmatrix}
a_0 & b_0 & & & & & \\
b_0 & a & b & & & & \\
 & b & a & b & & & \\
 & & b & \ddots & \ddots & & \\
 & & & \ddots & & b & \\
 & & & & b & a & b_0 \\
 & & & & & b_0 & a_0
\end{pmatrix}_{(N+2)\times(N+2)}\,. \tag{C.15}$$

It is known that (*i*) if $b_0 \neq 0$ the eigenvalues are nondegenerate [88], (*ii*) the eigenvectors corresponding to the eigenvalues ordered in descending order are alternately symmetric and skew symmetric [87], i.e.,

$$O_{ki} = \pm\, O_{k,M+1-i}\,, \tag{C.16}$$

where $M = N+2$. Setting $\lambda = \frac{a-\omega}{2b}$, $y = \frac{b_0}{b}$ and $x = \frac{a_0-a}{b}$ the characteristic polynomial $\mathbb{P}(\lambda)$ is, up to unimportant constants,

$$\mathbb{P}(\lambda) = \det \begin{pmatrix} x+2\lambda & y & & & & & \\ y & 2\lambda & 1 & & & & \\ & 1 & \ddots & \ddots & & & \\ & & \ddots & & 1 & & \\ & & & 1 & 2\lambda & y & \\ & & & & y & x+2\lambda \end{pmatrix}_{M\times M} .$$

Thanks to the recursion relations (A.5) it holds

$$\mathbb{P}_{1:j}(\lambda) = (x+2\lambda)\,\mathbb{U}_{j-1}(\lambda) - y^2\,\mathbb{U}_{j-2}(\lambda) \tag{C.17}$$

$$\mathbb{P}_{1:N+2}(\lambda) = (x+2\lambda)^2\,\mathbb{U}_N(x) - 2y^2(x+2\lambda)\,\mathbb{U}_{N-1}(\lambda) + y^4\,\mathbb{U}_{N-2}(\lambda)\,, \tag{C.18}$$

where $2 \le j \le N+1$. In the notation of the previous section ($n \equiv N, \ell \equiv M$), thanks to (C.5), it holds

$$u(\lambda) = \left(x+(2-y^2)\lambda\right)^2 - (1-\lambda^2)y^4\,, \qquad t(\lambda) = 2y^2\left(x+(2-y^2)\lambda\right)\,, \tag{C.19a}$$

$$u^{\ulcorner}(\lambda) = u_{\lrcorner}(\lambda) = x+(2-y^2)\lambda\,, \qquad t^{\ulcorner}(\lambda) = t_{\lrcorner}(\lambda) = y^2\,. \tag{C.19b}$$

As in the thermodynamic limit in the uniform case the dispersion relation is $\omega_k = a + 2b\cos(k)$, the rescaled eigenvalues are $\lambda \equiv \lambda_k = -\cos(k)$. Accordingly, the secular equation is given by (C.12) with shifts

$$\varphi_k = k - \tan^{-1}\frac{y^2\sin k}{(2-y^2)\cos k - x}\,. \tag{C.20}$$

As for (C.14),

$$O^2_{k1} = O^2_{k\ell} = \frac{2}{M+1-2\varphi'_k}\,\frac{y^2\sin^2 k}{[(2-y^2)\cos k - x]^2 + y^4\sin^2 k}\,. \tag{C.21}$$

Note that for $x=0$ this expression is in agreement with [97] and that the term with φ'_k becomes irrelevant for large M. In the most common case $x<2-y^2$ the maximum k_0 of O^2_{k1} is located at

$$k_0 = \cos^{-1}\frac{x}{2-y^2}\,. \tag{C.22}$$

Expanding O^2_{k1} around k_0, the leading behaviour is found to be a Lorentzian,

$$O^2_{k1} \simeq \frac{2}{M+1}\,\frac{y^2}{y^4 + [(2-y^2)^2 - x^2](k-k_0)^2}\,,$$

whose width (HWHM) is given by

$$\Delta \simeq \frac{y^2}{\sqrt{(2-y^2)^2-x^2}}\,. \tag{C.23}$$

When x and y are small, $k_0 \simeq (\pi - x)/2$ and $\Delta \simeq y^2/2$, so x rules the position of the peak, while y determines its width.

C.1.2 More elements on the edges

Here we consider the matrix

$$\begin{pmatrix}
a_0 & b_0 & & & & & & \\
b_0 & a_1 & b & & & & & \\
 & b & a & b & & & & \\
 & & b & a & b & & & \\
 & & & b & \ddots & \ddots & & \\
 & & & & \ddots & & b & \\
 & & & & & b & a & b_2 \\
 & & & & & & b_2 & a_2
\end{pmatrix}_{(n+3)\times(n+3)} . \tag{C.24}$$

As in the previous section, setting $\lambda = \frac{a-\omega}{2b}$, $y_i = \frac{b_i}{b}$ and $x_i = \frac{a_i - a}{b}$ the characteristic polynomial $\mathbb{P}(\lambda)$ is, up to unimportant constants,

$$\mathbb{P}(\lambda) = \begin{pmatrix}
2\lambda+x_0 & y_0 & & & & & & & \\
y_0 & 2\lambda+x_1 & 1 & & & & & & \\
 & 1 & 2\lambda & 1 & & & & & \\
 & & 1 & 2\lambda & 1 & & & & \\
 & & & 1 & \ddots & \ddots & & & \\
 & & & & \ddots & & 1 & & \\
 & & & & & 1 & 2\lambda & y_2 & \\
 & & & & & & y_2 & 2\lambda+x_2
\end{pmatrix}_{M\times M} , \tag{C.25}$$

where $M = N+3$. Using straightforward algebra we find that

$$\begin{aligned}
t^{\ulcorner}(\lambda) &= 2\lambda + x_2 + x_1 y_2^2 \\
u^{\ulcorner}(\lambda) &= (\lambda+x_1)(2\lambda+x_2) - (1+\lambda x_1) y_2^2 \\
t_{\lrcorner}(\lambda) &= 2\lambda + x_0 \\
u_{\lrcorner}(\lambda) &= (2\lambda+x_0)(\lambda+x_1) - y_0^2 \\
t(\lambda) &= (2\lambda+x_0)(2\lambda+x_2) + \left((2\lambda+x_0)x_1 - y_0^2\right) y_2^2 \\
u(\lambda) &= (2\lambda+x_2)\left((2\lambda+x_0)(\lambda+x_1) - y_0^2\right) - \left((2\lambda+x_0)(1+\lambda x_1) - \lambda y_0^2\right) y_2^2
\end{aligned}$$

A matrix in the form (C.24) comes out in the Ising model. Indeed, the matrix Z^TZ, being $Z = A - B$ (see appendix B.3.2), takes the form (C.24). After a proper rescaling we can consider (C.25) with $x_0 = (h_0^2 - 1 - h^2)/h$, $x_1 = (j_0^2 - 1)/h$, $x_2 = (h_0^2 + j_0^2 - 1 - h^2)/h$, $y_0 = h_0 j_0/h$, $y_2 = j_0$. In the thermodynamic limit, the eigenvalues of Z^TZ are ω_k^2, being $\omega_k^2 = 1 + h^2 - 2h\cos k$ the square of the dispersion relation (6.4). The rescaled eigenvalues are thus $\lambda_k = \cos k$ and we can use (C.14). Indeed,

$$O_{k1}^2 \propto \frac{y^2 \sin^2 k}{[(2-y^2)\cos k - x]^2 + y^4 \sin^2 k}\,, \tag{C.26}$$

where $y = j_0$ and

$$x = \frac{1 + h^2 - h_0^2 - j_0^2}{h}. \tag{C.27}$$

The peak of (C.26) is given by Eq. (C.22), and accordingly the energy of k_0 mode is

$$\omega_{k_0} = \sqrt{1 + h^2 - 2h\cos k_0} = \sqrt{\frac{2h_0^2 + (1-h^2)j_0^2}{2 - j_0^2}}\,. \tag{C.28}$$

Therefore, in the limit $j_0 \to 0$ the resonant mode is the one with energy $|h_0|$, as expected, but for finite j_0 there is a shift.

Moreover, we find that

$$|O_{kM}| = \frac{h_0}{\omega_k}|O_{k1}|\,. \tag{C.29}$$

Hence, when $h_0 \simeq \omega_{k_0}$, as we are interested in the neighbourhood of the resonant mode, we can neglect the prefactor and consider $|O_{k1}| \simeq |O_{kM}|$, as in chapter 6.

C.2 Analytical evaluation of $U_{N+1,0}(t)$ in the uniform XX model

In the XX model the time evolution is given by Eq. (B.22) where, as we have seen in Section C.1, in the uniform case $\omega_k = j\cos\left(\frac{\pi(k+1)}{N+3}\right) + h$ and $O_{kn} = \sqrt{\frac{2}{N+3}}\sin\left(\frac{\pi(k+1)(n+1)}{N+3}\right)$, for $k, n = 0, \ldots, N+1$. Since the magnetic field causes only a constant shift in the dispersion relation, in the following we set $h = 0$. In this case

$$\begin{aligned} U_{N+1,0}(t) &= \sum_{k=0}^{N+1} e^{-it\omega_k} O_{k0} O_{kN+1} = \sum_{m=1}^{\infty} i^{-m} \mathcal{J}_m(jt) \sum_{k=0}^{N+1} \cos\left(\frac{\pi m(k+1)}{N+3}\right) O_{k0} O_{kN+1} \\ &\simeq i^{-N+1}\left(\mathcal{J}_{N+1}(jt) + 2\mathcal{J}_{N+3}(jt) + \mathcal{J}_{N+5}(jt)\right) \\ &= \frac{4}{i^{N+1}}\left[\left(\frac{N+3}{jt}\right)^2 \mathcal{J}_{N+3}(jt) - \frac{\mathcal{J}'_{N+3}(jt)}{jt}\right], \end{aligned} \tag{C.30}$$

where we used the Jacobi-Anger expansion and some properties of the Bessel functions $\mathcal{J}_n$ [80]. The approximation consists in neglecting the Bessel functions of order $m(N+3)$, with

$m \geq 2$, since they contribute only after times of order $\frac{mN}{j}$. In fact, one can show that at the transmission time t^*, i.e., the time when $U_{N+1,0}(t)$ takes its first peak, $j t^* \simeq N - \xi (N/2)^{\frac{1}{3}}$. Using the properties of Bessel functions [80]

$$u(t^*) \simeq \frac{2^{\frac{7}{3}}}{N^{\frac{1}{3}}} \mathrm{Ai}(\xi) + \frac{2\xi}{5N} \left(3\xi \, \mathrm{Ai}'(\xi) + 22 \, \mathrm{Ai}(\xi) \right) , \tag{C.31}$$

where $\mathrm{Ai}(\xi)$ is the Airy function. It can be proved [81] that the maximum of $u(t^*)$ is reached for $\xi = -1.019$ and thus

$$u(t^*) = \frac{2.700}{N^{\frac{1}{3}}} - \frac{4.804}{N} . \tag{C.32}$$

C.3 Large-N limit of the amplitude in the ballistic XX model

The transition amplitude (5.14) in the case of odd $N = 2M-1$ reads

$$u(t) = \sum_{m=-M}^{M} \frac{\Delta(1+\Delta)}{N+3+2\varphi'_q} \frac{\mathrm{e}^{\mathrm{i}(\pi m - t \sin q_m)}}{\Delta^2 + \tan^2 q_m} ,$$

where the summation has been made symmetric through the change of variable $q = \pi/2 - k$. The shift equation (5.11) turns into

$$\pi \, m = (N+3) \, q_m + 2\varphi_{q_m} ,$$

with

$$\varphi_q = \tan^{-1} \frac{\tan q}{\Delta} - q .$$

In the limit $N \to \infty$ one can write the sum as an integral setting

$$\sum_m \frac{1}{N+3+2\varphi'_q} (\cdots) \longrightarrow \int \frac{\mathrm{d}q}{\pi} (\cdots) .$$

As we are interested in the region of the optimal value of $\Delta \sim N^{-1/3} \to 0$, we have

$$u_\infty(t) = \lim_{N\to\infty} \Delta \int_{-\frac{\pi}{2}}^{\frac{\pi}{2}} \frac{dq}{\pi} \frac{\mathrm{e}^{\mathrm{i}[(N+3)q + 2\varphi_q - t \sin q]}}{\Delta^2 + \tan^2 q} .$$

Writing the arrival time as $t = N+3+s$, where s is the arrival delay, one has then

$$u_\infty(t) = \lim_{t\to\infty} \Delta \int_{-\frac{\pi}{2}}^{\frac{\pi}{2}} \frac{dq}{\pi} \frac{\mathrm{e}^{\mathrm{i}[t(q-\sin q) - sq + 2\varphi_q]}}{\Delta^2 + \tan^2 q} .$$

The relevant q's are of the order of $\Delta \sim N^{-1/3} \to 0$, so we change to $q = \Delta x$, with x of the order of 1; keeping the leading terms for $\Delta \to 0$,

$$\begin{aligned} t\,(q - \sin q) &\longrightarrow \frac{t\Delta^3}{6}\, x^3\,, \\ \varphi_q &\longrightarrow \tan^{-1} x\,, \\ \frac{\Delta\, dq}{\Delta^2 + \tan^2 q} &\longrightarrow \frac{dx}{1+x^2}\,, \end{aligned}$$

and defining the rescaled counterparts of the arrival time $t \simeq N$ and of the delay $s \sim N^{1/3}$,

$$\tau \equiv \frac{\Delta^3}{6}\, t\,, \qquad \sigma \equiv \Delta\, s\,; \tag{C.33}$$

the final asymptotic expression results

$$u_\infty(\tau,\sigma) = \int_{-\infty}^{\infty} \frac{dx}{\pi}\, \frac{\mathrm{e}^{\mathrm{i}(\tau x^3 - \sigma x + 2\tan^{-1} x)}}{1+x^2}\,, \tag{C.34}$$

that can also be rewritten in the form of a simple summation of phases by introducing the variable $z = \tan^{-1} x$,

$$u_\infty(\tau,\sigma) = \frac{2}{\pi} \int_0^{\frac{\pi}{2}} dz\, \cos(\tau \tan^3 z - \sigma \tan z + 2z)\,. \tag{C.35}$$

As in the finite-N case, one has to maximize $u_\infty(\tau,\sigma)$ by finding the optimal values of σ and τ. For $\tau = 0$ it is easy to evaluate (C.34) analytically,

$$u_\infty(0,\sigma) = 2\,\mathrm{e}^{-\sigma}\, \sigma\,;$$

it is maximal for $\sigma = 1$, giving $u(0,1) = 2\,\mathrm{e}^{-1} \simeq 0.736$, to be regarded as a lower bound to the overall maximum of $u_\infty(\tau,\sigma)$. The overall maximization has been performed numerically using (C.35). It turns out that the maximum corresponds to $\sigma = 1.2152$ and $\tau = 0.02483$, and amounts to $u_\infty(0.02483, 1.2152) = 0.84690$, in agreement with the behaviour shown in figure 5.7. The resulting scaling, from (C.33), tells that asymptotically

$$\Delta \simeq 0.530\, N^{-1/3}\,, \qquad s \simeq 2.29\, N^{1/3}\,. \tag{C.36}$$

C.4 Evolution of the boundary spins: algorithms

Referring to Fig. 5.1, in this section we derive the explicit formulas for evaluating the time evolution of the two boundary qubits $Q = A \cup B$, with the assumption that before $t = 0$ both A and B do not interact with the internal chain Γ: $\rho(0) = \rho_Q \otimes \rho_\Gamma(0)$. The state of Q at time t is

given by the dynamical correlation functions according to $\rho_Q(t) = \frac{1}{4}\sum_{\alpha,\beta=0,x,y,z}\langle\sigma_0^\alpha(t)\sigma_N^\beta(t)\rangle\,\sigma_0^\alpha\sigma_N^\beta$, where $\sigma_n^\alpha = 2S_n^\alpha$ for $\alpha = x,y,z$ are the Pauli matrices and $\sigma_n^0 = \mathbb{1}$. Thanks to (3.13)

$$\rho_Q(t) = \begin{pmatrix} \langle c_0^\dagger(t)c_0(t)c_N^\dagger(t)c_N(t)\rangle & \langle c_0^\dagger(t)c_0(t)\Pi c_N(t)\rangle & \langle c_0(t)c_N^\dagger(t)c_N(t)\rangle & \langle c_0(t)\Pi c_N(t)\rangle \\ \langle c_0^\dagger(t)c_0(t)c_N^\dagger(t)\Pi\rangle & \langle c_0^\dagger(t)c_0(t)c_N(t)c_N^\dagger(t)\rangle & \langle c_0(t)c_N^\dagger(t)\Pi\rangle & \langle c_0(t)c_N(t)c_N^\dagger(t)\rangle \\ \langle c_0^\dagger(t)c_N^\dagger(t)c_N(t)\rangle & \langle c_0^\dagger(t)\Pi c_N(t)\rangle & \langle c_0(t)c_0^\dagger(t)c_N^\dagger(t)c_N(t)\rangle & \langle c_0(t)c_0^\dagger(t)\Pi c_N(t)\rangle \\ \langle c_0^\dagger(t)c_N^\dagger(t)\Pi\rangle & \langle c_0^\dagger(t)c_N(t)c_N^\dagger(t)\rangle & \langle c_0(t)c_0^\dagger(t)c_N^\dagger(t)\Pi\rangle & \langle c_0(t)c_0^\dagger(t)c_N(t)c_N^\dagger(t)\rangle \end{pmatrix},$$

while for each boundary qubit we have

$$\rho_A(t) = \begin{pmatrix} \langle c_0^\dagger(t)c_0(t)\rangle & \langle c_0(t)\rangle \\ \langle c_0^\dagger(t)\rangle & \langle c_0(t)c_0^\dagger(t)\rangle \end{pmatrix}, \qquad \rho_B(t) = \begin{pmatrix} \langle c_N^\dagger(t)c_N(t)\rangle & \langle \Pi c_N(t)\rangle \\ \langle c_N^\dagger(t)\Pi\rangle & \langle c_N(t)c_N^\dagger(t)\rangle \end{pmatrix}.$$

The Heisenberg evolution of the Fermi operators for quadratic Hamiltonians has been already discussed in Section (B.2.2), so the final step is the calculation of the expectation values with respect to the non-equilibrium initial state $\rho_Q \otimes \rho_\Gamma(0)$. We define new Fermi operators acting only on the bus Γ: $\tilde{c}_n = \prod_{j=1}^{n-1}\left(-\sigma_n^z\right)\sigma_n^-$. In the compact notation (B.4)

$$\alpha = \begin{pmatrix} c_0 \\ c_1 \\ \vdots \\ c_N \\ c_{N+1} \\ c_0^\dagger \\ c_1^\dagger \\ \vdots \\ c_N^\dagger \\ c_{N+1}^\dagger \end{pmatrix} = \begin{pmatrix} \sigma_0^- \\ -\sigma_0^z \\ -\sigma_0^z \\ \vdots \\ -\sigma_0^z \\ \sigma_0^z\sigma_{N+1}^z\sigma_{N+1}^- \\ \sigma_0^+ \\ -\sigma_0^z \\ \vdots \\ -\sigma_0^z \\ -\sigma_0^z\sigma_{N+1}^z\sigma_{N+1}^+ \end{pmatrix} \otimes \begin{pmatrix} 1 \\ \tilde{c}_1^\dagger \\ \tilde{c}_2^\dagger \\ \vdots \\ \tilde{c}_N^\dagger \\ \tilde{\Pi} \\ 1 \\ \tilde{c}_1 \\ \tilde{c}_2 \\ \vdots \\ \tilde{c}_N \\ \tilde{\Pi} \end{pmatrix} \equiv \mathscr{Q} \otimes \mathscr{C}\,. \tag{C.37}$$

where $\tilde{\Pi}$ is the parity of Γ, $\tilde{\Pi} = \sigma_0^z\sigma_{N+1}^z\Pi$. The operators $\mathscr{Q}_j$ act on the Hilbert space of the boundary spins while the operators $\mathscr{C}_j$ act on the Hilbert space of the bus Γ. Calling $M(t)$ the time evolution matrix of (B.16) we find thus

$$\langle\alpha_a(t)\alpha_b(t)\cdots\rangle = \sum_{a',b',\cdots}(M_{aa'}(t)M_{bb'}(t)\cdots)\times\mathrm{Tr}\left[\rho_Q\mathscr{Q}_{a'}\mathscr{Q}_{b'}\cdots\right]\mathrm{Tr}\left[\rho_\Gamma\mathscr{C}_{a'}\mathscr{C}_{b'}\cdots\right], \tag{C.38}$$

while

$$\langle\Pi\alpha_a(t)\alpha_b(t)\cdots\rangle = \tilde{p}\sum_{a',b',\cdots}(M_{aa'}(t)M_{bb'}(t)\cdots)\times\mathrm{Tr}\left[\rho_Q\sigma_0^z\sigma_N^z\mathscr{Q}_{a'}\mathscr{Q}_{b'}\cdots\right]\mathrm{Tr}\left[\rho_\Gamma\mathscr{C}_{a'}\mathscr{C}_{b'}\cdots\right]. \tag{C.39}$$

Thanks to (C.38) and (C.39) all the expressions in the density matrix $\rho_Q(t)$ can be obtained. For example,

$$\langle\sigma_0^-(t)\rangle = U_{0,0}(t)\langle\sigma_0^-\rangle + V_{0,0}(t)\langle\sigma_0^+\rangle - U_{0,N+1}(t)\langle\sigma_{N+1}^-\Pi\rangle + V_{0,N+1}(t)\langle\sigma_{N+1}^+\Pi\rangle\,, \tag{C.40a}$$

$$\langle\sigma_0^+(t)\rangle = U_{0,0}^*(t)\langle\sigma_0^+\rangle + V_{0,0}^*(t)\langle\sigma_0^-\rangle - U_{0,N+1}^*(t)\langle\Pi\sigma_{N+1}^+\rangle + V_{0,N+1}^*(t)\langle\Pi\sigma_{N+1}^-\rangle\,, \tag{C.40b}$$

$$\begin{aligned}\langle\sigma_{N+1}^-(t)\rangle =& - U_{N+1,0}(t)\langle\sigma_0^-\Pi\rangle - V_{N+1,0}(t)\langle\sigma_0^+\Pi\rangle + \\ &+ U_{N+1,N+1}(t)\langle\sigma_{N+1}^-\rangle - V_{N+1,N+1}(t)\langle\sigma_{N+1}^+\rangle\,,\end{aligned} \tag{C.40c}$$

$$\begin{aligned}\langle\sigma_{N+1}^+(t)\rangle =& - U_{N+1,0}^*(t)\langle\Pi\sigma_0^+\rangle - V_{N+1,0}^*(t)\langle\Pi\sigma_0^-\rangle + \\ &+ U_{N+1,N+1}^*(t)\langle\sigma_{N+1}^+\rangle - V_{N+1,N+1}^*(t)\langle\sigma_{N+1}^-\rangle\,,\end{aligned} \tag{C.40d}$$

and

$$\begin{aligned}\langle\sigma_n^z(t)\rangle =& -1 + U_{n,0}^*(t)U_{n,0}(t)\left(1+\langle\sigma_0^z\rangle\right) + V_{n,0}^*(t)V_{n,0}(t)\left(1-\langle\sigma_0^z\rangle\right) \\ &+ U_{n,N+1}^*(t)U_{n,N+1}(t)\left(1+\langle\sigma_{N+1}^z\rangle\right) + V_{n,N+1}^*(t)V_{n,N+1}(t)\left(1-\langle\sigma_{N+1}^z\rangle\right) \\ &- U_{n,0}^*(t)U_{n,N+1}(t)\langle\sigma_0^+\sigma_{N+1}^-\Pi\rangle + U_{n,0}^*(t)V_{n,N+1}(t)\langle\sigma_0^+\sigma_{N+1}^+\Pi\rangle \\ &- U_{n,N+1}^*(t)U_{n,0}(t)\langle\Pi\sigma_{N+1}^+\sigma_0^-\rangle - U_{n,N+1}^*(t)V_{n,0}(t)\langle\Pi\sigma_{N+1}^+\sigma_0^+\rangle \\ &- V_{n,0}^*(t)U_{n,N+1}(t)\langle\sigma_0^-\sigma_{N+1}^-\Pi\rangle + V_{n,0}^*(t)V_{n,N+1}(t)\langle\sigma_0^-\sigma_{N+1}^+\Pi\rangle \\ &- V_{n,N+1}^*(t)U_{n,0}(t)\langle\Pi\sigma_{N+1}^-\sigma_0^-\rangle - V_{n,N+1}^*(t)V_{n,0}(t)\langle\Pi\sigma_{N+1}^-\sigma_0^+\rangle \\ &+ \sum_{kh}\Big(U_{n,k}^*(t)U_{n,h}(t)\langle\tilde{c}_k^\dagger\tilde{c}_h\rangle + U_{n,k}^*(t)V_{n,h}(t)\langle\tilde{c}_k^\dagger\tilde{c}_h^\dagger\rangle + \\ &\qquad V_{n,k}^*(t)U_{n,h}(t)\langle\tilde{c}_k\tilde{c}_h^\dagger\rangle + V_{n,k}^*(t)V_{n,h}(t)\langle\tilde{c}_k\tilde{c}_h^\dagger\rangle\Big)\,.\end{aligned} \tag{C.41}$$

When Γ is initially in its ground state $|\tilde{\Omega}\rangle$, more complicated expressions can be written in terms of contractions of the the basic correlation matrix $\Xi_{ab} = \langle\tilde{\Omega}|\mathscr{C}_a\mathscr{C}_b|\tilde{\Omega}\rangle$:

$$\Xi = \left(\begin{array}{ccccc|ccccc} 1 & 0 & 0 & \cdots & \tilde{p} & 1 & 0 & 0 & \cdots & \tilde{p} \\ \hline 0 & & & & 0 & 0 & & & & 0 \\ 0 & & \tilde{P}^T\tilde{Q} & & 0 & 0 & & \tilde{P}^T\tilde{P} & & 0 \\ \vdots & & & & \vdots & \vdots & & & & \vdots \\ \hline \tilde{p} & 0 & 0 & \cdots & 1 & \tilde{p} & 0 & 0 & \cdots & 1 \\ \hline\hline 1 & 0 & 0 & \cdots & \tilde{p} & 1 & 0 & 0 & \cdots & \tilde{p} \\ \hline 0 & & & & 0 & 0 & & & & 0 \\ 0 & & \tilde{Q}^T\tilde{Q} & & 0 & 0 & & \tilde{Q}^T\tilde{P} & & 0 \\ \vdots & & & & \vdots & \vdots & & & & \vdots \\ \hline \tilde{p} & 0 & 0 & \cdots & 1 & \tilde{p} & 0 & 0 & \cdots & 1 \end{array}\right)\,, \tag{C.42}$$

where $\tilde{p}$ is the parity of $|\tilde{\Omega}\rangle$, as given by (B.15), and we have used the expressions (B.19), where the tilde means that all the operations are done only on the bus Γ. These results can

be also trivially extended for including the temperature, following secion B.2.3. It should be noted that we can not use the Wick theorem for evaluating $\langle\tilde{\Omega}|\mathscr{C}_{a'}\mathscr{C}_{b'}\cdots|\tilde{\Omega}\rangle$ in (C.38) because the $\mathscr{C}_j$, due to the identity and the parity operators, do not depend linearly on c_n and $c_m^\dagger$. For example the most complicated quantity to calculate is $\langle c_0^\dagger(t)c_0(t)c_N^\dagger(t)c_N(t)\rangle = \langle\alpha_0(t)\alpha_{N+2}(t)\alpha_{N+1}(t)\alpha_{2N+3}(t)\rangle$. In general the four-points correrlation functions is

$$\begin{aligned}
\langle\alpha_{j_1}(t)\alpha_{j_2}(t)\alpha_{j_3}(t)\alpha_{j_4}(t)\rangle = & \\
& \sum_{c_1,c_2,c_3,c_4} M_{j_1c_1}(t)M_{j_2c_2}(t)M_{j_3c_3}(t)M_{j_4c_4}(t)\Big[\Xi_{c_1c_2}\Xi_{c_3c_4}-\Xi_{c_1c_3}\Xi_{c_2c_4}+\Xi_{c_1c_4}\Xi_{c_2c_3}\Big]+ \\
& \sum_{s_1,s_2,s_3,s_4} E_{j_1s_1}(t)E_{j_2s_2}(t)E_{j_3s_3}(t)E_{j_4s_4}(t)\,\mathrm{Tr}\left[\rho_Q\mathscr{Q}_{s_1}\mathscr{Q}_{s_2}\mathscr{Q}_{s_3}\mathscr{Q}_{s_4}\right]\Xi_{0s_1}\Xi_{0s_2}\Xi_{0s_3}\Xi_{0s_4}+ \\
& \sum_{s_1,s_2}\sum_{c_1,c_2}\Xi_{0s_1}\Xi_{0s_2}\Xi_{c_1c_2}\Big[M_{j_1s_1}(t)M_{j_2s_2}(t)M_{j_3c_1}(t)M_{j_4c_2}(t)\,\mathrm{Tr}\left[\rho_Q\mathscr{Q}_{s_1}\mathscr{Q}_{s_2}\right]+ \\
& \qquad M_{j_1s_1}(t)M_{j_2c_1}(t)M_{j_3s_2}(t)M_{j_4c_2}(t)\,\mathrm{Tr}\left[\rho_Q\mathscr{Q}_{s_1}\sigma_0^z\mathscr{Q}_{s_2}\sigma_0^z\right]\zeta_{s_2}+ \\
& \qquad M_{j_1s_1}(t)M_{j_2c_1}(t)M_{j_3c_2}(t)M_{j_4s_2}(t)\,\mathrm{Tr}\left[\rho_Q\mathscr{Q}_{s_1}\mathscr{Q}_{s_2}\right]+ \\
& \qquad M_{j_1c_1}(t)M_{j_2s_1}(t)M_{j_3c_2}(t)M_{j_4s_2}(t)\,\mathrm{Tr}\left[\rho_Q\sigma_0^z\mathscr{Q}_{s_1}\sigma_0^z\mathscr{Q}_{s_2}\right]\zeta_{s_1}+ \\
& \qquad M_{j_1c_1}(t)M_{j_2c_2}(t)M_{j_3s_1}(t)M_{j_4s_2}(t)\,\mathrm{Tr}\left[\rho_Q\mathscr{Q}_{s_1}\mathscr{Q}_{s_2}\right]+ \\
& \qquad M_{j_1c_1}(t)M_{j_2s_1}(t)M_{j_3s_2}(t)M_{j_4c_2}(t)\,\mathrm{Tr}\left[\rho_Q\sigma_0^z\mathscr{Q}_{s_1}\mathscr{Q}_{s_2}\sigma_0^z\right]\zeta_{s_1}\zeta_{s_2}\Big]
\end{aligned} \tag{C.43}$$

where $s_n\in\{0,N+1,N+2,2N+3\}$ are the boundary spin indices, $c_n\in\{1,2,\ldots N,N+3,N+4,\ldots,2N+2\}$ are the internal chain indices, and $j_n\in\{1,2,\ldots,2N+3\}$ are generic indices. The extra term $\zeta_n=(-1)^{\delta_{n,N}+\delta n,(2N+1)}$ is due to the anti-commutation of the parity operator $\tilde{\Pi}$ with the reduced fermi operatos $\tilde{c}_n$ and $\tilde{c}_n^\dagger$. Other important correlation functions are

$$\langle\alpha_{j_1}(t)\alpha_{j_2}(t)\rangle = \sum_{c_1,c_2} M_{j_1c_1}(t)M_{j_2c_2}(t)\Xi_{c_1c_2}+\sum_{s_1,s_2} M_{j_1s_1}(t)M_{j_2s_2}(t)\,\mathrm{Tr}\left[\rho_Q\mathscr{Q}_{s_1}\mathscr{Q}_{s_2}\right]\Xi_{0s_1}\Xi_{0s_2}\,, \tag{C.44}$$

and

$$\langle\alpha_j(t)\Pi\rangle = \tilde{p}\sum_s M_{js}(t)\,\mathrm{Tr}\left[\rho_Q\sigma_0^z\sigma_N^z\mathscr{Q}_s\right]\Xi_{0s_1}\Xi_{0s_2}\,. \tag{C.45}$$

Bibliography

[1] M. A. Nielsen and I. L. Chuang, *Quantum Computation and Quantum Information*. Cambridge University Press, 2000.

[2] J. Preskill, *Lecture Notes for Physics 229: Quantum Information and Computation*. California Institute of Technology, 1998.

[3] M. Schlosshauer, *Decoherence and the quantum-to-classical transition*. Springer Verlag, 2007.

[4] J. Sakurai and J. Napolitano, *Modern Quantum Mechanics*. Addison-Wesley, 2010.

[5] K. Życzkowski, P. Horodecki, A. Sanpera, and M. Lewenstein, "Volume of the set of separable states", *Phys. Rev. A*, vol. 58, pp. 883–892, Aug 1998.

[6] E. Schmidt, "Zur theorie der linearen und nichtlinearen integralgleichungen", *Mathematische Annalen*, vol. 63, no. 4, pp. 433–476, 1907.

[7] E. Schrödinger, "Probability relations between separated systems", in *Mathematical Proceedings of the Cambridge Philosophical Society*, vol. 32, p. 446, Cambridge Univ Press, 1936.

[8] M. Horodecki, "Entanglement measures", *Quantum Information and Computation*, vol. 1, no. 1, pp. 3–26, 2001.

[9] M. A. Nielsen, "Conditions for a class of entanglement transformations", *Phys. Rev. Lett.*, vol. 83, pp. 436–439, Jul 1999.

[10] F. Brandao and M. Plenio, "Entanglement theory and the second law of thermodynamics", *Arxiv preprint arXiv:0810.2319*, 2008.

[11] M. Horodecki, "Quantum entanglement: Reversible path to thermodynamics", *Nature Physics*, vol. 4, pp. 833–834, 2008.

[12] S. Popescu, A. Short, and A. Winter, "Entanglement and the foundations of statistical mechanics", *Nature Physics*, vol. 2, no. 11, pp. 754–758, 2006.

[13] V. Paulsen, *Completely bounded maps and operator algebras*. Cambridge studies in advanced mathematics, Cambridge University Press, 2002.

[14] K. Kraus, "General state changes in quantum theory", *Annals of Physics*, vol. 64, no. 2, pp. 311 – 335, 1971.

[15] W. Stinespring, "Positive functions on c*-algebras", in *Proc. Amer. Math. Soc*, vol. 6, pp. 211–216, 1955.

[16] C. Man-Duen, "Completely positive linear maps on complex matrices", *Linear Algebra and its Applications*, vol. 10, pp. 285–290, June 1975.

[17] A. Fujiwara and P. Algoet, "One-to-one parametrization of quantum channels", *Phys. Rev. A*, vol. 59, pp. 3290–3294, May 1999.

[18] R. Horodecki and M. Horodecki, "Information-theoretic aspects of inseparability of mixed states", *Phys. Rev. A*, vol. 54, pp. 1838–1843, Sep 1996.

[19] R. Srikanth and S. Banerjee, "Squeezed generalized amplitude damping channel", *Phys. Rev. A*, vol. 77, p. 012318, Jan 2008.

[20] P. W. Shor, "Polynomial-time algorithms for prime factorization and discrete logarithms on a quantum computer", *SIAM J. Comput.*, vol. 26, pp. 1484–1509, October 1997.

[21] R. Feynman, "Simulating physics with computers", *International journal of theoretical physics*, vol. 21, no. 6, pp. 467–488, 1982.

[22] B. Lanyon, J. Whitfield, G. Gillett, M. Goggin, M. Almeida, I. Kassal, J. Biamonte, M. Mohseni, B. Powell, M. Barbieri, *et al.*, "Towards quantum chemistry on a quantum computer", *Nature Chemistry*, vol. 2, no. 2, pp. 106–111, 2010.

[23] M. A. Nielsen and C. M. Caves, "Reversible quantum operations and their application to teleportation", *Phys. Rev. A*, vol. 55, pp. 2547–2556, Apr 1997.

[24] G. Bowen and S. Bose, "Teleportation as a depolarizing quantum channel, relative entropy, and classical capacity", *Phys. Rev. Lett.*, vol. 87, p. 267901, Dec 2001.

[25] S. Albeverio, S.-M. Fei, and W.-L. Yang, "Optimal teleportation based on bell measurements", *Phys. Rev. A*, vol. 66, p. 012301, Jul 2002.

[26] R. Werner, "All teleportation and dense coding schemes", *Journal of Physics A: Mathematical and General*, vol. 34, p. 7081, 2001.

[27] W. Wootters and W. Zurek, "A single quantum cannot be cloned", *Nature*, vol. 299, no. 5886, pp. 802–803, 1982.

[28] M. Horodecki, P. Horodecki, and R. Horodecki, "General teleportation channel, singlet fraction, and quasidistillation", *Phys. Rev. A*, vol. 60, pp. 1888–1898, Sep 1999.

[29] S. Popescu, "Bell's inequalities versus teleportation: What is nonlocality?", *Phys. Rev. Lett.*, vol. 72, pp. 797–799, Feb 1994.

[30] M. Horodecki and P. Horodecki, "Reduction criterion of separability and limits for a class of distillation protocols", *Phys. Rev. A*, vol. 59, pp. 4206–4216, Jun 1999.

[31] R. F. Werner, "Quantum states with einstein-podolsky-rosen correlations admitting a hidden-variable model", *Phys. Rev. A*, vol. 40, pp. 4277–4281, Oct 1989.

[32] P. Badziag, M. Horodecki, P. Horodecki, and R. Horodecki, "Local environment can enhance fidelity of quantum teleportation", *Phys. Rev. A*, vol. 62, p. 012311, Jun 2000.

[33] N. Johnston and D. Kribs, "Quantum gate fidelity in terms of choi matrices", *Arxiv preprint arXiv:1102.0948*, 2011.

[34] I. Bengtsson and K. Życzkowski, *Geometry of quantum states: an introduction to quantum entanglement*. Cambridge Univ Pr, 2006.

[35] C. H. Bennett, D. P. DiVincenzo, J. A. Smolin, and W. K. Wootters, "Mixed-state entanglement and quantum error correction", *Physical Review A*, vol. 54, no. 5, pp. 3824–3851, 1996.

[36] S. Hill and W. K. Wootters, "Entanglement of a pair of quantum bits", *Physical Review Letters*, vol. 78, no. 26, pp. 5022–5025, 1997.

[37] W. K. Wootters, "Entanglement of formation of an arbitrary state of two qubits", *Physical Review Letters*, vol. 80, no. 10, pp. 2245–2248, 1998.

[38] W. K. Wootters, "Entanglement of formation and concurrence", *Quantum Information and Computation*, vol. 1, no. 1, pp. 27–44, 2001.

[39] Syljuåsen, "Entanglement and spontaneous symmetry breaking in quantum spin models", *Physical Review A*, vol. 68, no. 6, p. 60301, 2003.

[40] T. Konrad, F. De Melo, M. Tiersch, C. Kasztelan, A. Aragão, and A. Buchleitner, "Evolution equation for quantum entanglement", *Nature physics*, vol. 4, no. 2, pp. 99–102, 2007.

[41] D. Deutsch and R. Jozsa, "Rapid solution of problems by quantum computation", *Proceedings: Mathematical and Physical Sciences*, pp. 553–558, 1992.

[42] L. Grover, "Quantum computers can search arbitrarily large databases by a single query", *Physical review letters*, vol. 79, no. 23, pp. 4709–4712, 1997.

[43] D. Kielpinski, C. Monroe, and D. Wineland, "Architecture for a large-scale ion-trap quantum computer", 2002.

[44] A. Skinner, M. Davenport, and B. Kane, "Hydrogenic spin quantum computing in silicon: a digital approach", *Physical review letters*, vol. 90, no. 8, p. 87901, 2003.

[45] R. Vrijen and E. Yablonovitch, "A spin-coherent semiconductor photo-detector for quantum communication", *Physica E: Low-dimensional Systems and Nanostructures*, vol. 10, no. 4, pp. 569–575, 2001.

[46] A. Costa Jr and S. Bose, "Impurity scattering induced entanglement of ballistic electrons", *Physical review letters*, vol. 87, no. 27, p. 277901, 2001.

[47] M. Oskin, F. Chong, I. Chuang, and J. Kubiatowicz, "Building quantum wires: the long and the short of it", in *Computer Architecture, 2003. Proceedings. 30th Annual International Symposium on*, pp. 374–385, IEEE, 2003.

[48] P. Hammar, M. Stone, D. Reich, C. Broholm, P. Gibson, M. Turnbull, C. Landee, and M. Oshikawa, "Characterization of a quasi-one-dimensional spin-1/2 magnet which is gapless and paramagnetic for $g\mu_b h \leq j$ and $k_b t \ll j$", *Physical Review B*, vol. 59, no. 2, p. 1008, 1999.

[49] A. Romito, R. Fazio, and C. Bruder, "Solid-state quantum communication with josephson arrays", *Phys. Rev. B*, vol. 71, p. 100501, Mar 2005.

[50] A. O. Lyakhov and C. Bruder, "Use of dynamical coupling for improved quantum state transfer", *Phys. Rev. B*, vol. 74, p. 235303, Dec 2006.

[51] A. Lyakhov and C. Bruder, "Quantum state transfer in arrays of flux qubits", *New Journal of Physics*, vol. 7, p. 181, 2005.

[52] M. Steiner, J. Villain, and C. Windsor, "Theoretical and experimental studies on one-dimensional magnetic systems", *Advances in Physics*, vol. 25, pp. 87–209, Mar. 1976.

[53] H. Mikeska and A. Kolezhuk, "Quantum magnetism", *Lecture Notes in Physics*, vol. 645, pp. 1–83, 2004.

[54] W. S. Bakr, J. I. Gillen, A. Peng, S. Fölling, and M. Greiner, "A quantum gas microscope for detecting single atoms in a Hubbard-regime optical lattice", *Nature*, vol. 462, pp. 74–77, 2009.

[55] G. K. Brennen, C. M. Caves, P. S. Jessen, and I. H. Deutsch, "Quantum Logic Gates in Optical Lattices", *Phys. Rev. Lett.*, vol. 82, pp. 1060–1063, 1999.

[56] O. Mandel, M. Greiner, A. Widera, T. Rom, T. W. Hänsch, and I. Bloch, "Controlled collisions for multi-particle entanglement of optically trapped atoms", *Nature*, vol. 425, pp. 937–940, 2003.

[57] M. Greiner, O. Mandel, T. Esslinger, T. W. Hänsch, and I. Bloch, "Quantum phase transition from a superfluid to a Mott insulator in a gas of ultracold atoms", *Nature*, vol. 415, pp. 39–44, 2002.

[58] J. F. Sherson, C. Weitenberg, M. Endres, M. Cheneau, I. Bloch, and S. Kuhr, "Single-atom-resolved fluorescence imaging of an atomic Mott insulator", *Nature*, vol. 467, pp. 68–72, 2010.

[59] W. S. Bakr, A. Peng, M. E. Tai, R. Ma, J. Simon, J. I. Gillen, S. Fölling, L. Pollet, and M. Greiner, "Probing the Superfluid-to-Mott Insulator Transition at the Single-Atom Level", *Science*, vol. 329, pp. 547–, 2010.

[60] L. Duan, E. Demler, and M. D. Lukin, "Controlling Spin Exchange Interactions of Ultracold Atoms in Optical Lattices", *Phys. Rev. Lett.*, vol. 91, no. 9, pp. 090402–+, 2003.

[61] C. Weitenberg, M. Endres, J. Sherson, M. Cheneau, P. Schauß, T. Fukuhara, I. Bloch, and S. Kuhr, "Single-spin addressing in an atomic mott insulator", *Nature*, vol. 471, no. 7338, pp. 319–324, 2011.

[62] A. Koetsier, R. A. Duine, I. Bloch, and H. T. C. Stoof, "Achieving the Néel state in an optical lattice", *Phys. Rev. A*, vol. 77, no. 2, pp. 023623–+, 2008.

[63] P. Barmettler, A. M. Rey, E. Demler, M. D. Lukin, I. Bloch, and V. Gritsev, "Quantum many-body dynamics of coupled double-well superlattices", *Phys. Rev. A*, vol. 78, no. 1, pp. 012330–+, 2008.

[64] P. Medley, D. M. Weld, H. Miyake, D. E. Pritchard, and W. Ketterle, "Spin gradient demagnetization cooling of ultracold atoms", *Phys. Rev. Lett.*, vol. 106, p. 195301, May 2011.

[65] M. Christandl, N. Datta, T. Dorlas, A. Ekert, A. Kay, and A. Landahl, "Perfect transfer of arbitrary states in quantum spin networks", *Physical Review A*, vol. 71, no. 3, p. 032312, 2005.

[66] C. Di Franco, M. Paternostro, and M. S. Kim, "Perfect State Transfer on a Spin Chain without State Initialization", *Phys. Rev. Lett.*, vol. 101, no. 23, pp. 230502–+, 2008.

[67] N. Y. Yao, L. Jiang, A. V. Gorshkov, Z.-X. Gong, A. Zhai, L. M. Duan, and M. D. Lukin, "Robust quantum state transfer in random unpolarized spin chains", Nov. 2010, arXiv:1011.2762.

[68] L. Banchi, T. J. G. Apollaro, A. Cuccoli, R. Vaia, and P. Verrucchi, "Optimal dynamics for quantum-state and entanglement transfer through homogeneous quantum systems", *Phys. Rev. A*, vol. 82, no. 5, p. 052321, 2010.

[69] C. Di Franco, M. Paternostro, D. I. Tsomokos, and S. F. Huelga, "Control-limited perfect state transfer, quantum stochastic resonance, and many-body entangling gate in imperfect qubit registers", *Physical Review A*, vol. 77, p. 062337, June 2008.

[70] S. Sachdev, *Quantum Phase Transitions*. Cambridge University Press, 2011.

[71] T. Roscilde, P. Verrucchi, A. Fubini, S. Haas, and V. Tognetti, "Studying quantum spin systems through entanglement estimators", *Physical Review Letters*, vol. 93, p. 167203, Oct. 2004.

[72] L. Amico, F. Baroni, A. Fubini, D. Patanè, V. Tognetti, and P. Verrucchi, "Divergence of the entanglement range in low-dimensional quantum systems", *Physical Review A*, vol. 74, no. 2, p. 022322, 2006.

[73] F. Baroni, A. Fubini, V. Tognetti, and P. Verrucchi, "Two-spin entanglement distribution near factorized states", *Journal of Physics A: Mathematical and Theoretical*, vol. 40, pp. 9845–9857, Aug. 2007.

[74] L. Amico, A. Osterloh, F. Plastina, R. Fazio, and G. Massimo Palma, "Dynamics of entanglement in one-dimensional spin systems", *Physical Review A*, vol. 69, p. 022304, Feb. 2004.

[75] A. V. Loginov, "Classification of states and macroscopic degeneracy in an open XY-chain in transverse field", *Low Temperature Physics*, vol. 23, p. 534, July 1997.

[76] J. Cullum and R. Willoughby, *Lanczos Algorithms for Large Symmetric Eigenvalue Computations: Theory*. Classics in applied mathematics, Society for Industrial and Applied Mathematics, 2002.

[77] R. Chen and H. Guo, "The chebyshev propagator for quantum systems", *Computer physics communications*, vol. 119, no. 1, pp. 19–31, 1999.

[78] A. Weiße and H. Fehske, "Chebyshev expansion techniques", *Computational Many-Particle Physics*, pp. 545–577, 2008.

[79] H. Tal-Ezer and R. Kosloff, "An accurate and efficient scheme for propagating the time dependent schrödinger equation", *The Journal of chemical physics*, vol. 81, p. 3967, 1984.

[80] M. Abramowitz and I. Stegun, *Handbook of mathematical functions with formulas, graphs, and mathematical tables*, vol. 55. Dover publications, 1964.

[81] S. Bose, "Quantum communication through an unmodulated spin chain", *Physical review letters*, vol. 91, no. 20, p. 207901, 2003.

[82] A. Bayat, L. Banchi, S. Bose, and P. Verrucchi, "Initializing an unmodulated spin chain to operate as a high-quality quantum data bus", *Phys. Rev. A*, vol. 83, p. 062328, Jun 2011.

[83] C. H. Bennett, G. Brassard, S. Popescu, B. Schumacher, J. A. Smolin, and W. K. Wootters, "Purification of noisy entanglement and faithful teleportation via noisy channels", *Physical Review Letters*, vol. 76, pp. 722–725, Jan. 1996.

[84] M. Christandl, N. Datta, T. C. Dorlas, A. Ekert, A. Kay, and A. J. Landahl, "Perfect transfer of arbitrary states in quantum spin networks", *Phys. Rev. A*, vol. 71, no. 3, pp. 032312–+, 2005.

[85] C. Albanese, M. Christandl, N. Datta, and A. Ekert, "Mirror Inversion of Quantum States in Linear Registers", *Phys. Rev. Lett.*, vol. 93, no. 23, pp. 230502–+, 2004.

[86] A. Kay, "A review of perfect state transfer and its application as a constructive tool", *Arxiv preprint arXiv:0903.4274*, 2009.

[87] A. Cantoni and P. Butler, "Eigenvalues and eigenvectors of symmetric centrosymmetric matrices", *Linear Algebra Appl.*, vol. 13, pp. 275–288, 1976.

[88] B. N. Parlett, *The Symmetric Eigenvalue Problem*. SIAM, Philadelphia, 1998.

[89] A. Zwick, G. Álvarez, J. Stolze, and O. Osenda, "Boundary-controlled spin chains for robust quantum state transfer", *Arxiv preprint arXiv:1111.2238*, 2011.

[90] T. J. Osborne and N. Linden, "Propagation of quantum information through a spin system", *Phys. Rev. A*, vol. 69, no. 5, pp. 052315–+, 2004.

[91] H. L. Haselgrove, "Optimal state encoding for quantum walks and quantum communication over spin systems", *Phys. Rev. A*, vol. 72, no. 6, pp. 062326–+, 2005.

[92] M. Miyagi and S. Nishida, "Pulse spreading in a single-mode fiber due to third-order dispersion", *Appl. Opt.*, vol. 18, pp. 678–682, 1979.

[93] M. Miyagi and S. Nishida, "Pulse spreading in a single-mode optical fiber due to third-order dispersion - Effect of optical source bandwidth", *Appl. Opt.*, vol. 18, pp. 2237–2240, 1979.

[94] G. Agrawal, *Fiber-optic communication systems*. No. v. 1 in Wiley series in microwave and optical engineering, Wiley-Interscience, 2002.

[95] A. Wójcik, T. Łuczak, P. Kurzyński, A. Grudka, T. Gdala, and M. Bednarska, "Multiuser quantum communication networks", *Phys. Rev. A*, vol. 75, p. 022330, Feb 2007.

[96] L. Campos Venuti, C. Degli Esposti Boschi, and M. Roncaglia, "Qubit Teleportation and Transfer across Antiferromagnetic Spin Chains", *Phys. Rev. Lett.*, vol. 99, no. 6, pp. 060401–+, 2007.

[97] A. Wójcik, T. Łuczak, P. Kurzyński, A. Grudka, T. Gdala, and M. Bednarska, "Unmodulated spin chains as universal quantum wires", *Phys. Rev. A*, vol. 72, no. 3, pp. 034303–+, 2005.

[98] M. B. Plenio and F. L. Semiao, "High efficiency transfer of quantum information and multiparticle entanglement generation in translation-invariant quantum chains", *New Journal of Physics*, vol. 7, no. 1, p. 73, 2005.

[99] M. J. Hartmann, F. G. S. L. Brandao, and M. B. Plenio, "Effective spin systems in coupled microcavities", *Physical Review Letters*, vol. 99, no. 16, p. 160501, 2007.

[100] R. Bhatia, *Matrix analysis*. Graduate texts in mathematics, Springer, 1997.

[101] S. Oh, M. Friesen, and X. Hu, "Even-odd effects of heisenberg chains on long-range interaction and entanglement", *Phys. Rev. B*, vol. 82, p. 140403, Oct 2010.

[102] T. Osborne and H. Yadsan-Appleby, "Achievable qubit rates for quantum information wires", *Arxiv preprint arXiv:1102.2427*, 2011.

[103] P. Karbach and J. Stolze, "Spin chains as perfect quantum state mirrors", *Phys. Rev. A*, vol. 72, p. 030301, Sep 2005.

[104] M. Yung and S. Bose, "Perfect state transfer, effective gates, and entanglement generation in engineered bosonic and fermionic networks", *Physical Review A*, vol. 71, no. 3, p. 032310, 2005.

[105] L. Campos Venuti, S. M. Giampaolo, F. Illuminati, and P. Zanardi, "Long-distance entanglement and quantum teleportation in xx spin chains", *Phys. Rev. A*, vol. 76, no. 5, p. 052328, 2007.

[106] S. M. Giampaolo and F. Illuminati, "Long-distance entanglement in many-body atomic and optical systems", *New Journal of Physics*, vol. 12, no. 2, p. 025019, 2010.

[107] G. Gualdi, V. Kostak, I. Marzoli, and P. Tombesi, "Perfect state transfer in long-range interacting spin chains", *Phys. Rev. A*, vol. 78, no. 2, pp. 022325–+, 2008.

[108] L. Banchi, A. Bayat, P. Verrucchi, and S. Bose, "Nonperturbative entangling gates between distant qubits using uniform cold atom chains", *Phys. Rev. Lett.*, vol. 106, p. 140501, Apr 2011.

[109] E. Lieb, T. Schultz, and D. Mattis, "Two soluble models of an antiferromagnetic chain", *Ann. Phys.*, vol. 16, pp. 407–466, 1961.

[110] M. Cozzini, P. Giorda, and P. Zanardi, "Quantum phase transitions and quantum fidelity in free fermion graphs", *Phys. Rev. B*, vol. 75, no. 1, pp. 014439–+, 2007.

[111] M. Markiewicz and M. Wieśniak, "Perfect state transfer without state initialization and remote collaboration", *Phys. Rev. A*, vol. 79, p. 054304, May 2009.

[112] S. Bose, "Quantum Communication through an Unmodulated Spin Chain", *Phys. Rev. Lett.*, vol. 91, no. 20, pp. 207901–+, 2003.

[113] A. Bayat and S. Bose, "Information transferring ability of the different phases of a finite xxz spin chain", *Phys. Rev. A*, vol. 81, p. 012304, 2010.

[114] L. Banchi, T. Apollaro, A. Cuccoli, R. Vaia, and P. Verrucchi, "Long quantum channels for high-quality entanglement transfer", *New Journal of Physics*, vol. 13, no. 12, p. 123006, 2011.

[115] L. Banchi, T. Apollaro, A. Cuccoli, R. Vaia, and P. Verrucchi, "Efficient quantum information transfer through a uniform channel", *Nanomaterials and Nanotechnology*, vol. 1, no. 1, pp. 24–28, 2011.

[116] S. Bose, "Quantum Communication Through Spin Chain Dynamics: An Introductory Overview", *Contemp. Phys.*, vol. 48, p. 13, 2007.

[117] F. Plastina and T. J. G. Apollaro, "Local Control of Entanglement in a Spin Chain", *Phys. Rev. Lett.*, vol. 99, no. 17, pp. 177210–+, 2007.

[118] S. I. Doronin and A. I. Zenchuk, "High-probability state transfers and entanglements between different nodes of the homogeneous spin-(1)/(2) chain in an inhomogeneous external magnetic field", *Phys. Rev. A*, vol. 81, no. 2, pp. 022321–+, 2010.

[119] M. J. Bremner, C. M. Dawson, J. L. Dodd, A. Gilchrist, A. W. Harrow, D. Mortimer, M. A. Nielsen, and T. J. Osborne, "Practical Scheme for Quantum Computation with Any Two-Qubit Entangling Gate", *Physical Review Letters*, vol. 89, pp. 247902–+, Nov. 2002, arXiv:arXiv:quant-ph/0207072.

[120] J. I. Cirac and P. Zoller, "Quantum Computations with Cold Trapped Ions", *Physical Review Letters*, vol. 74, pp. 4091–4094, May 1995.

[121] D. Jaksch, H. Briegel, J. I. Cirac, C. W. Gardiner, and P. Zoller, "Entanglement of Atoms via Cold Controlled Collisions", *Physical Review Letters*, vol. 82, pp. 1975–1978, Mar. 1999, arXiv:arXiv:quant-ph/9810087.

[122] K. Stannigel, P. Rabl, A. S. Sørensen, P. Zoller, and M. D. Lukin, "Optomechanical transducers for long-distance quantum communication", *Phys. Rev. Lett.*, vol. 105, p. 220501, Nov 2010.

[123] G. Burkard and A. Imamoglu, "Ultra-long-distance interaction between spin qubits", *Phys. Rev. B*, vol. 74, p. 041307, Jul 2006.

[124] M. Yung and S. Bose, "Perfect state transfer, effective gates, and entanglement generation in engineered bosonic and fermionic networks", *Phys. Rev. A*, vol. 71, no. 3, pp. 032310–+, 2005.

[125] S. R. Clark, C. Moura Alves, and D. Jaksch, "Efficient generation of graph states for quantum computation", *New Journal of Physics*, vol. 7, pp. 124–+, May 2005, arXiv:arXiv:quant-ph/0406150.

[126] A. V. Gorshkov, J. Otterbach, E. Demler, M. Fleischhauer, and M. D. Lukin, "Photonic phase gate via an exchange of fermionic spin waves in a spin chain", *Phys. Rev. Lett.*, vol. 105, p. 060502, Aug 2010.

[127] H. Briegel, T. Calarco, D. Jaksch, J. I. Cirac, and P. Zoller, "Quantum computing with neutral atoms", *Journal of Modern Optics*, vol. 47, pp. 415–451, 2000.

[128] T. Wilk, A. Gaëtan, C. Evellin, J. Wolters, Y. Miroshnychenko, P. Grangier, and A. Browaeys, "Entanglement of Two Individual Neutral Atoms Using Rydberg Blockade", *Physical Review Letters*, vol. 104, pp. 010502–+, Jan. 2010, arXiv:0908.0454.

[129] L. Isenhower, E. Urban, X. L. Zhang, A. T. Gill, T. Henage, T. A. Johnson, T. G. Walker, and M. Saffman, "Demonstration of a neutral atom controlled-not quantum gate", *Phys. Rev. Lett.*, vol. 104, p. 010503, Jan 2010.

[130] J. Cirac and P. Zoller, "A scalable quantum computer with ions in an array of microtraps", *Nature*, vol. 404, no. 6778, pp. 579–581, 2000.

[131] T. N. Bandi, V. G. Minogin, and S. N. Chormaic, "Atom microtraps based on near-field Fresnel diffraction", *Phys. Rev. A*, vol. 78, no. 1, pp. 013410–+, 2008.

[132] M. Nakahara, T. Ohmi, and Y. Kondo, "Scalable neutral atom quantum computer with interaction on demand", 2010, arXiv:arXiv:1009.4426.

[133] S. Trotzky, Y.-A. Chen, U. Schnorrberger, P. Cheinet, and I. Bloch, "Controlling and detecting spin correlations of ultracold atoms in optical lattices", Sept. 2010, arXiv:1009.2415.

[134] J. Bollinger, D. Heinzen, W. Itano, S. Gilbert, and D. Wineland, "A 303-MHz frequency standard based on trapped Be+ ions", *IEEE Trans. on Instrum. and Measurement*, vol. 40, no. 2, pp. 126–128, 1991.

[135] H. Everitt, *Experimental aspects of quantum computing*. Springer, 2005.

[136] T. Prosen and B. Žunkovič, "Exact solution of markovian master equations for quadratic fermi systems: thermal baths, open xy spin chains and non-equilibrium phase transition", *New Journal of Physics*, vol. 12, p. 025016, 2010.

[137] P. Cappellaro, L. Viola, and C. Ramanathan, "Coherent-state transfer via highly mixed quantum spin chains", *Physical Review A*, vol. 83, no. 3, p. 032304, 2011.

[138] P. Cappellaro, C. Ramanathan, and D. Cory, "Simulations of information transport in spin chains", *Physical review letters*, vol. 99, no. 25, p. 250506, 2007.

[139] C. Ramanathan, P. Cappellaro, L. Viola, and D. Cory, "Experimental characterization of coherent magnetization transport in a one-dimensional spin system", *New Journal of Physics*, vol. 13, p. 103015, 2011.

[140] C. Ramanathan, P. Cappellaro, L. Viola, and D. Cory, "Dynamics of magnetization transport in a one-dimensional spin system", *Arxiv preprint arXiv:1102.3400*, 2011.

[141] S. Wolf, D. Awschalom, R. Buhrman, J. Daughton, S. Von Molnar, M. Roukes, A. Chtchelkanova, and D. Treger, "Spintronics: A spin-based electronics vision for the future", *Science*, vol. 294, no. 5546, p. 1488, 2001.

[142] D. Awschalom, D. Loss, and N. Samarth, *Semiconductor spintronics and quantum computation*. Nanoscience and technology, Springer, 2002.

[143] H. Boerner, *Representations of groups: with special consideration for the needs of modern physics*. North-Holland Pub. Co., 1970.

[144] M. Christandl, "The structure of bipartite quantum states-insights from group theory and cryptography", *Arxiv preprint quant-ph/0604183*, 2006.

[145] K. M. R. Audenaert, "A digest on representation theory of the symmetric group", `http://personal.rhul.ac.uk/usah/080/QITNotes_files/Irreps_v06.pdf`.

[146] A. Ben-Israel and T. Greville, *Generalized inverses: theory and applications*. CMS books in mathematics, Springer, 2003.

[147] F. Brandão, P. Ćwikliński, M. Horodecki, P. Horodecki, J. Korbicz, and M. Mozrzymas, "Convergence to equilibrium under a random hamiltonian", *Arxiv preprint arXiv:1108.2985*, 2011.

[148] H. Breuer and F. Petruccione, *The Theory of Open Quantum Systems*. Oxford University Press, 2007.

[149] T. Prosen, "Third quantization: a general method to solve master equations for quadratic open fermi systems", *New Journal of Physics*, vol. 10, p. 043026, 2008.

[150] T. Prosen and E. Ilievski, "Nonequilibrium phase transition in a periodically driven xy spin chain", *Phys. Rev. Lett.*, vol. 107, p. 060403, Aug 2011.

[151] J. Blaizot and G. Ripka, *Quantum theory of finite systems*. MIT Press, 1986.

[152] P. Ring and P. Schuck, *The nuclear many-body problem*. Springer Verlag, 2004.

[153] R. Attar, *Lecture Notes on Z-Transform*. Lulu Press, 2006.